ELECTROSPUN NANOFIBER COMPOSITE PROTON EXCHANGE MEMBRANES

By

Jason Bryan Ballengee

Dissertation

Submitted to the Faculty of the

Graduate School of Vanderbilt University

in partial fulfillment of the requirements

for the degree of

DOCTOR OF PHILOSOPHY

in

Chemical Engineering

May, 2013

Nashville, Tennessee

Approved:

Professor Peter N. Pintauro

Professor G. Kane Jennings

Professor Scott Guelcher

Professor Charles Lukehart

To my family.

ACKNOWLEDGEMENTS

I would like to thank my research advisor, Professor Peter Pintauro, for the opportunity to be apart of this laboratory and his support of this dissertation research. Thanks also to my committee members Professors Kane Jennings, Scott Guelcher, and Charles Lukehart for their encouragement and suggestions.

External collaborators, including 3M Company, General Motors, Florida Solar Energy Center, and Scribner Associates made contributions to this work. In particular, Dr. Steve Hamrock and Dr. Greg Haugen provided polymer and MEA fabrication assistance with 3M's 660 equivalent weight polymer.

Many members of the Vanderbilt community provided invaluable support for this project. Mark Holmes gave frequent and friendly assistance with all matters mechanical. Mary Gilleran and Rae Uson provided administrative help and always saved me from my paperwork errors. John Fellenstein advised-on and manufactured several important pieces of laboratory equipment. Robin Midgett helped with electronics and Dr. Tony Hmelo tirelessly supported usage of VINSE facilities. Thanks to all of you.

Thanks to all my research colleagues for their company and assistance. In particular I would like to thank Dr. Jonghyun Choi for teaching me many of the experimental techniques foundational to my dissertation. Special thanks also to Dr. Jun Lin and Dr. Angela Zhang for their support, guidance, and training.

Anton Cottrill, Andrew Couch, and Daniel Kish were undergraduate researchers who made contributions to this dissertation. In particular I would like to acknowledge Anton Cottrill's substantial efforts on direct methanol fuel cells.

I have been fortunate to find many great, steadfast friends who have made Nashville feel like home. Thank you for being there.

Most importantly, I want to thank my family. This dissertation would not have been completed without their presence. In particular, my parents, sister, and brother gave support, encouragement, and advice. My cousin, Blake Branson, was invaluable in helping me navigate the Ph.D. process, beginning before I even arrived at Vanderbilt. I am very grateful to my future wife, Margarita Prieto Chacon, for her love, counsel, and ever-constant support.

This research was funded by the U.S. Department of Energy Hydrogen Program (Award DE-FG36-06GO16030) and the National Science Foundation (grant CBET-1032948).

TABLE OF CONTENTS

Page

LIST OF TABLES

LIST OF FIGURES

CHAPTER I

INTRODUCTION

Technological innovation is required to alleviate sky-rocketing energy demand without contributing to the environmental and political ramifications of fossil fuel use. As petroleum reserves shrink and air pollutant levels rise, proton exchange membrane fuel cells (PEMFCs) present an attractive and clean alternative to internal combustion engines. Thus, their widespread use could have a significant impact on the transportation sector, responsible for 28% of U.S. energy consumption.[1] However PEMFCs still need improvement, particularly of the membrane at the heart of the fuel cell assembly.[2]

Broader application of hydrogen-fueled PEMFCs is restricted by the proton exchange membrane (PEM) in two ways: i) the PEM has limited proton conductivity at high temperature (90-120^{o}C), low relative humidity (10-50% RH) conditions, and ii) the PEM exhibits poor durability in an automotive environment due to inadequate mechanical stability upon swelling with water and shrinking when dry.[3,4] Direct methanol fuel cells (DMFCs), a methanol-fueled subclass of PEMFCs, are limited by the high methanol permeability in a PEM.[5]

Many approaches have been pursued to address the limitations of PEM performance in hydrogen/air fuel cells and DMFCs. Avenues of research include the synthesis of new ionomeric materials and the development of a wide variety of composite membranes, which are discussed in more detail in Chapter II. Unfortunately, each membrane has not met expectations for various reasons. In summary, no hydrogen/air

fuel cell membrane has achieved the necessary proton conductivity at high temperature, low humidity conditions without sacrificing mechanical and/or chemical stability. While some positive progress has been made on the development of DMFC membranes, there is still a need for membrane materials with high conductivity, low methanol permeability, low cost, and good electrode compatibility.

A new class of PEM membranes, known as nanofiber network membranes (NNMs), was introduced by Choi et al.[5] in 2008 to address the problems with hydrogen/air PEM performance. NNMs are composed of a charged ionomer and an uncharged polymer, where the latter imparts mechanical strength and dimensional stability to the membrane. The ionomer is electrospun into nanofibers with diameters ranging from 150-1000 nm. In Choi's work the uncharged polymer was impregnated into the fiber mat, thus filling the interfiber void space. In a NNM, the polymer for ion conduction is decoupled from the polymer for mechanical strength/stability, permitting the use of high-conductivity materials (which swell greatly in water) while maintaining sufficient membrane strength for fuel cell operation. Preliminary conductivity results with Choi's NNMs were encouraging, but further development was required to meet the U.S. Department of Energy's fuel cell requirements.[6]

This dissertation builds on previous NNM work. Here, a new dual-fiber electrospinning manufacturing method was introduced as a technique for the fabrication of PEMs. Two polymers, an ionomer and an uncharged material, are electrospun from separate syringes onto a common collecting surface. Follow-on processing allows for the fabrication of two distinct structures, either i) an ionomer film reinforced by uncharged fibers or ii) ionomer fibers encapsulated in uncharged polymer. This "forced-assembly"

approach provides i) ease of fabrication, in particular through the elimination of a separate polymer impregnation step often required for other composite membrane systems, ii) versatility of membrane composition, i.e., normally immiscible/incompatible polymers can be blended together on a sub-micron scale, and iii) a high degree of morphological control, where two distinct structures are fabricated from the same dual-fiber mat and where the nanofiber diameter and volume fraction can be independently controlled. This dissertation describes the fabrication, material properties, and fuel cell performance of these nanofiber composite membranes. Each chapter stands alone, however, when taken together they tell a compelling story of nanofiber composite membranes' current performance and future promise.

The first step to produce nanofiber PEMs is electrospinning. Chapter III describes the first comprehensive electrospinning study of a common fuel cell membrane ionomer, DuPont's perfluorosulfonic acid (PFSA) known as Nafion®. The effects of a number of electrospinning properties were investigated including: air humidity, voltage, solution flow rate, solvent type, and carrier polymer molecular weight. Furthermore, electrospinning conditions are identified for the preparation of well-formed nanofiber mats with a tunable average fiber diameter.

Chapter IV builds on Nafion electrospinning to describe the first dual-fiber electrospun PEMs, composed of Nafion as the ionomer and polyphenylsulfone (PPSU) as the uncharged polymer. A membrane fabrication scheme is described for the preparation of two structures: i) a Nafion film reinforced by PPSU fibers, and ii) Nafion fibers encapsulated in PPSU polymer. A variety of membrane properties are reported as a function of membrane structure and Nafion volume fraction, including in-plane proton conductivity, water swelling, and mechanical properties. Additionally, membrane-

electrode-assemblies (MEAs) were prepared from the nanofiber membranes. Fuel cell power output and durability of the MEAs are presented and discussed.

Chapter V further investigates the Nafion/PPSU dual-fiber system. The focus here is on the effect of various post-electrospinning processing steps on membrane properties while also seeking to reduce the overall mat processing time, thus providing a more practical set of conditions for possible industrial scale-up. In particular, interfiber void-filling, Nafion annealing, and acid/water washing are investigated for their effects on membrane conductivity, swelling, and mechanical properties.

Chapters IV and V describe nanofiber composite membranes ideally suited for operation at moderate temperatures, ~80^{o}C. However, higher temperature (90-120^{o}C) operation is also desirable for automotive applications. Toward this end, Chapter VI extends the dual-fiber technique to the preparation of membranes with 3M Company's 660 equivalent weight PFSA ionomer (3M660) while retaining PPSU as the uncharged polymer. 3M660's higher fixed-charge concentration and higher conductivity makes it more suitable for high temperature operation. This study focuses on preparing membranes with 3M660 films reinforced by PPSU fibers. Material properties and fuel cell performance of reinforced 3M660 nanofiber membranes are presented and discussed.

The dual-fiber electrospinning technique is a robust platform for the fabrication of membranes with different structure and polymer compositions. Chapter VII highlights this point by using the dual-fiber process to fabricate multi-layered membranes. In this particular case, three-layered membranes are prepared where the middle layer serves as a methanol blocking layer for use in direct methanol fuel cells (DMFCs). Three-layer fiber mats are prepared by varying the relative flow rates of Nafion and PPSU during

electrospinning. The mats are then processed into dense membranes using the same techniques as for a non-layered composite. Material properties relevant to DMFC operation are presented, including both in-plane and through-plane conductivity, methanol permeability, and selectivity. Fuel cell performance is also shown as a function of methanol fuel concentration.

1.1 References

(1) Whitesides, G. M.; Crabtree, G. W., *Science* **2007** 315 (5813), 796-798.

(2) Buxton, G. A.; Balazs, A. C., *Physical Review E* **2003,** 67, (3), 12.

(3) Hamrock, S. J., Yandrastis, Michael A., *Polymer Reviews* **2006,** 46, 219-244.

(4) Mathias, M. F. M., Rohit, Gasteiger, Hubert A.; Conley, Jason J.;Fuller, Timothy J.; Gittlman, Craig J.; Kocha, Shaya S.; Miller, Daniel P.; Mittelsteadt, Corky K.; Xie, Tao; Yan, Susan G.; Yu, Paul T., *Interface* **2005,** 15, (3), 24-35.

(5) Choi, J.; Lee, K. M.; Wycisk, R.; Pintauro, P. N.; Mather, P. T., *Macromolecules* **2008,** 41, (13), 4569-4572.

(6) Kleen, G. J.; Kopasz, J. P.; Peterson, D. R.; Garland, N. L.; D. L. Ho, K. E. M.; Marcinkoski, J.; Podolski, W.; Benjamin, T.; Papageorgopoulos, D. C., Membrane Development in the U. S. DOE Fuel Cell Technologies Program. In *Fuel Cell Seminar and Exhibition*, Orlando, Florida, 2011. Available at http://www.fuelcellseminar.com/media/9072/lrd34-1%20kopasz.pdf

CHAPTER II

BACKGROUND

2.1 Principles of hydrogen/air and direct methanol fuel cells

Fuel cells are electrochemical devices that directly convert the chemical energy in a fuel and an oxidant to electrical energy. Fuel cells are not subject to the same thermodynamic limitations (i.e., Carnot cycle) as a heat engine, thus allowing operation at higher efficiencies than typical internal combustion engines (~55% vs. ~20% operating efficiencies).[1] One of the most widely studied fuel cells is the hydrogen/air fuel cell, shown schematically in Figure 2.1a. The proton exchange membrane (PEM) is at the heart of the fuel cell assembly. Catalytic powder electrodes are directly attached to both membrane faces to form a membrane-electrode-assembly (MEA).[2] The electrodes are usually composed of platinum dispersed on carbon powder with an ionomeric binder. Gas diffusion layers (GDL), typically carbon paper or carbon cloth are attached to the electrodes and permit hydrogen and air transport to the electrodes. GDLs also minimize the condensation of liquid water on the electrode surface.

During hydrogen/air fuel cell operation, hydrogen gas (the fuel) is supplied to the anode and oxygen (the oxidant) to the cathode. Hydrogen undergoes oxidation at the anode to form protons and electrons. The electrons provide electrical energy and the protons migrate through the PEM toward the cathode where they react with oxygen and electrons to form water.

Direct methanol fuel cells are a subclass of PEMFCs. DMFCs have the advantage of using a liquid fuel, but generally require higher catalyst loadings, operate at lower thermodynamic efficiencies, and produce carbon dioxide (a greenhouse gas). The fundamental principles of operation are similar to a hydrogen/air fuel cell, but the fuel and associated electrode reactions differ. See Fig. 2.1b for a schematic representation of a DMFC.

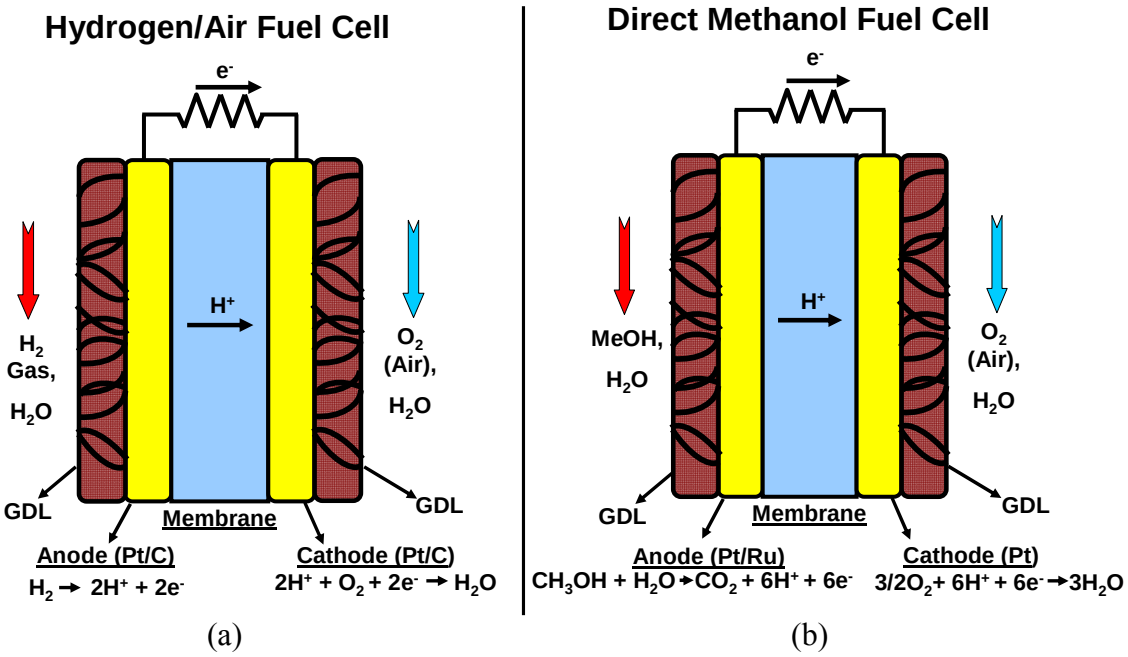

Figure 2.1. Schematic representation of a) hydrogen/air fuel cell and b) direct methanol fuel cell.

A fuel cell's power output is quantified by a polarization curve (see Figure 2.2) which graphs the relationship between voltage and current density, the product of which being power density. A polarization curve has three distinct regions: a kinetically-controlled region associated with activation losses at the electrode, an ohmic region where the membrane's area-specific resistance dictates performance, and a transport-

controlled region in which gas diffusion to the electrode surface limits the overall reaction rates and power output.[3, 4]

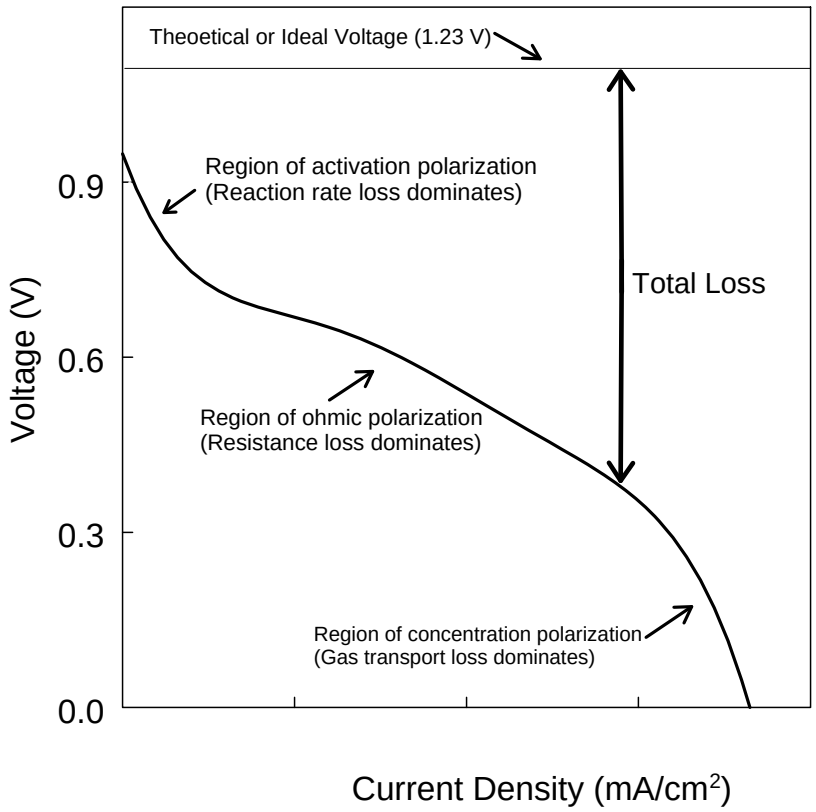

Figure 2.2. Representative polarization curve, adapted from reference (4).

2.2 Membrane performance

The proton exchange membrane is the central component of the fuel cell's membrane-electrode-assembly. A PEM's required properties include: i) zero electronic conductivity, preventing a short circuit between the anode and cathode, ii) high proton conductivity, minimizing ohmic losses during current flow for high power production, iii) low fuel/oxidant permeability, ensuring high thermodynamic efficiency, iv) chemical,

thermal, and mechanical stability in both the dry and wet states, v) low cost, and vi) compatibility with electrodes.[5]

The benchmark PEM for moderate temperature (~80^{o}C) hydrogen/air fuel cells is Nafion®, a perfluorosulfonic acid (PFSA) polymer membrane developed by DuPont in the 1960s.[5] Nafion ionomer has had commercial success for chlor-alkali processes and remains the focus of much academic research.[5-8] Unfortunately, it has very low conductivity in the dry state and has suspect durability for automotive applications.[7, 9-13] Nafion's structure is shown in Figure 2.3. The Teflon backbone imparts crystallinity and mechanical rigidity, while the sulfonic acid groups permit proton conductivity when the Nafion is sorbed with water. The acid sites also create a large osmotic driving force for water to enter the membrane and dilute the acid groups – resulting in dimensional swelling upon exposure to liquid water or a high relative humidity gas stream. Most PEMs, whether PFSA or an alternative ionomer, rely on covalently bound sulfonic acid groups for proton conduction. The concentration of acid groups in a PEM is typically expressed in terms of equivalent weight (EW) or ion-exchange-capacity (IEC), as defined by Equation 2.1[7] and Equation 2.2[7]. Generally a higher concentration of acid groups, or higher IEC, results in higher proton conductivity, lower area specific resistance (Equation 2.3) for a given membrane thickness, and greater water swelling (Equation 2.4). These properties are used for preliminary screening of PEMs. For use in a DMFC, an additional membrane property is of critical importance: selectivity (Equation 2.5). Relative selectivity (Equation 2.6)[14] is often used for comparison of PEM materials for DMFC applications.

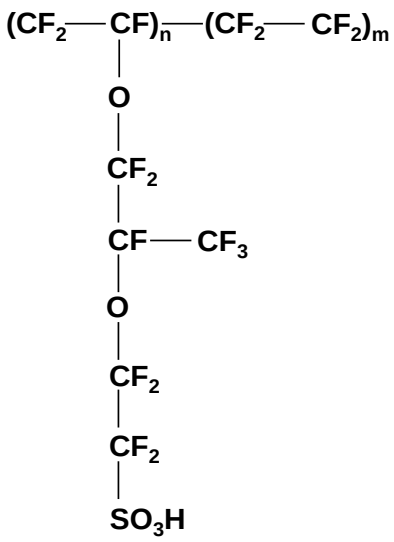

Figure 2.3. Nafion's repeat unit. n=1 and m=6.5 for 1100 EW.

$$EW = \frac{grams\ of\ dry\ ionomer}{moles\ of\ sulfonic\ acid\ groups} \tag{2.1}$$

$$IEC = \frac{milliequivalents\ of\ acid\ group}{gram\ dry\ Ionomer} = 1000 / EW \tag{2.2}$$

$$Area\ Specific\ \mathrm{Re}sis\tan ce = \frac{\delta}{\sigma} \tag{2.3}$$

$$Water\ Swelling = \frac{m_{Wet} - m_{Dry}}{m_{Dry}} \tag{2.4}$$

$$Selectivity = \frac{\sigma}{P} \tag{2.5}$$

$$\mathrm{Re}lative\ Selectivity = \frac{\left[\frac{\sigma}{P}\right]}{\left[\frac{\sigma}{P}\right]_{Nafion}} \tag{2.6}$$

where m is mass [g]; σ is proton conductivity [S/cm], δ is membrane thickness [cm], and P is methanol permeability [cm^2/s].

2.3 Alternative approaches to proton exchange membranes

Several possibilities have been explored to allow PEMs to operate at high temperature and low humidity, improve durability, and improve selectivity (Equation 2.5). The approaches can be divided into two broad categories: the synthesis of new ionomeric materials and the modification of existing materials via the fabrication of composite membranes. Here, research in these areas is generally described.

2.3.1 High IEC perfluoro- polymers

Perfluorosulfonic acid (PFSA) materials such as DuPont's Nafion are synthesized by copolymerization of perfluoroalkyl sulfonyl fluoride and tetrafluoroethylene into a PFSA precursor.[15, 16] These monomers are hazardous and require special safety precautions, limiting work on PFSA synthesis primarily to the industrial sector.[5, 10] The polymerized precursor can be extruded and converted to the acidic form (PFSA) by reaction with an aqueous KOH solution and subsequent acid treatment.[7] Producing thin membranes (<50 μm) by extrusion is difficult. Thin films, such as the popular Nafion 212, are solution-cast in the acid form.

PFSA's fluorocarbon backbone imparts chemical stability and crystallinity, while the sulfonic acid terminated side chains allow for ionic conductivity in the hydrated state. 900-1200 EW PFSAs are the most widely studied because they provide an appropriate balance between proton conductivity, mechanical performance, and water swelling.[5]

However, the IEC of PFSA materials can be increased by shortening the side chain or by decreasing the backbone ($-CF_2-$) segment length between side chains. A higher concentration of acidic sites improves water retention at low humidity and provides additional acidic moieties for proton conduction. Thus, high IEC PFSAs have improved conductivity at low humidity, as clearly shown by 3M Company (3M).[2, 17] For example, 3M's 580 EW PFSA has a conductivity of 0.146 S/cm at 120°C, 50% RH (compared to 0.039 S/cm for Nafion). Unfortunately, high IEC materials swell excessively upon exposure to liquid water, have poor mechanical properties in the wet-state, and in some cases are liquid water soluble.[18, 19] These drawbacks make neat films of these materials unsuitable for PEMFC applications requiring high durability (e.g., automotive applications).[19]

Recently 3M has developed a synthesis route for perfluoro polymers with more than one sulfonic acid group per side chain.[20] These polymers, referred to as perfluoro-imide acids (PFIA), are based on a PFSA polymer structure, but have an additional sulfonoimide acid group as shown in Figure 2.4. PFIA's additional acid groups permit very low EWs. Furthermore, the ($-CF_2-$) repeat between chains is longer for PFIA than PFSA when EW is held constant. Thus, PFIA materials have higher crystallinity than PFSA polymers of similar EW.[19, 21] One 650 EW PFIA had slightly higher conductivity the 3M's 700 EW PFSA material at 80°C, where RH ranged from 20% - 90%.[20] Also, since the 650 EW PFIA was more crystalline, it had lower water swelling than the 700 EW PFSA (~50% linear swelling in boiling water for the PFIA as opposed to ~100% linear swelling for the PFSA)[19] and is expected to have better mechanical properties.[19] Initial fuel cell studies suggest that MEAs with 650 EW PFIA outperform MEAs with

3M's 825 EW PFSA. A MEA with the PFIA membrane produced twice as much power as the PFSA membrane at 105°C, 45% RH and lasted nearly twice as long in a fuel cell humidity cycling/durability study at 80°C.[21] Unfortunately, these materials are not yet commercially available.

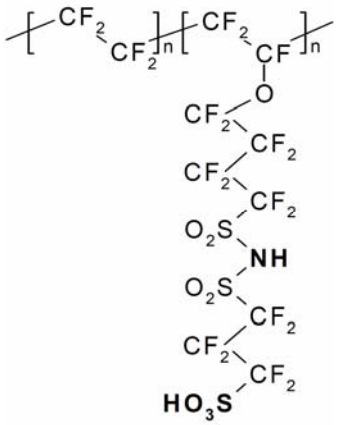

Figure 2.4 Chemical structure of 3M Company's PFIA. Image from Reference (21).

2.3.2 Sulfonated hydrocarbons

As an alternative to perfluorosulfonic acids, the development of sulfonated hydrocarbon membranes has been explored. Sulfonated hydrocarbon synthesis is not subject to the same safety concerns as PFSA synthesis, and thus has been studied in many academic laboratories (unlike PFSA). There are two general synthetic strategies[5] for the preparation of sulfonated hydrocarbon-based membranes, i) post-sulfonation of an aromatic polymer using concentrated sulfuric acid, fuming sulfuric acid, chlorosulfonic acid, or sulfur trioxide[22] or ii) direct copolymerization of sulfonated and uncharged monomers. Direct copolymerization provides more control over the degree and location of sulfonation/functionalization than post-sulfonation.[5] However, the synthesis of copolymers tends to be more complex than the post-sulfonation route.

Examples of hydrocarbon ionomers include sulfonated polyether ether ketone[23, 24], sulfonated polyarylene ether sulfone[25], sulfonated polytriflourostyrene,[26] sulfonated polyphenylene[27], and sulfonated polyimides.[28] One class of hydrocarbon-based ionomers that has received recent attention is sulfonated polyphenylenes, with notable work coming from the groups of Litt and Kreuer.[27, 29-31] Litt's approach takes advantage of the high rigidity of polyphenylene's polymer chains to generate long nanopores that, when lined with sulfonic acid groups, hold water tightly and thus improve conductivity.[29, 31] One membrane prepared by Litt and co-workers had an IEC of 8 meq/g and achieved a high conductivity of 0.10 S/cm at 120^{o}C and 30% RH. However, the fuel cell power output of a MEA containing this membrane did not improve relative to a MEA with a Nafion 212 membrane. Kreuer and co-workers prepared sulfonated polyphenylene films with an IEC of 4.5 meq/g and a conductivity seven-times higher than that of Nafion at 135^{o}C and 35% RH.[30] Unfortunately these high IEC polyphenylenes are typically brittle in the dry state and some are water soluble.[30, 32]

Another well-known example of hydrocarbon based ionomers (sulfonated polyarylene ether sulfone) was developed by Professor McGrath's group at Virginia Tech in the early 2000's.[33] The ionomer, commonly called BPSH, was prepared by copolymerization, as shown in Figure 2.5. This material was reported to have lower proton conductivity than Nafion (0.08 S/cm compared to 0.12 S/cm, in water at 30^{o}C) and also had higher liquid water swelling than Nafion (70 wt% vs. 37 wt%). Still, this was an important step forward from the standpoint of synthetic strategies for PEM materials.

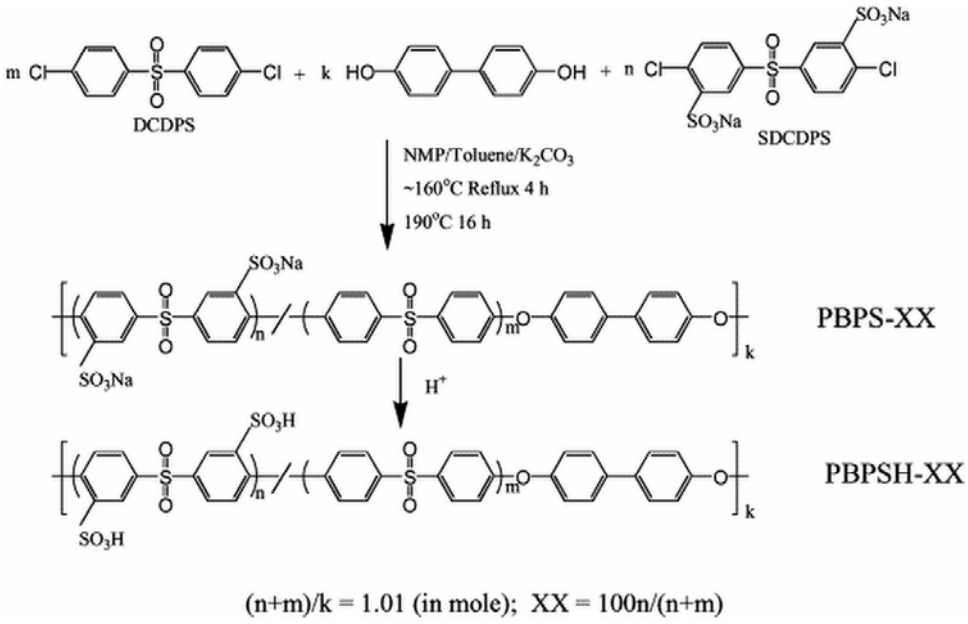

Figure 2.5. Synthesis route for the preparation of BPSH. Reprinted *Journal of Membrane Science*, 197, Wang, F.; Hickner, M.; Kim, Y. S.; Zawodzinski, T. A.; McGrath, J. E, Direct polymerization of sulfonated poly(arylene ether sulfone) random (statistical) copolymers: candidates for new proton exchange membranes, with permission from Elsevier.[33]

.

McGrath and co-workers later pioneered the development of block copolymers to improve the microstructure and control of hydrocarbon ionomers.[34-38] One block is composed of hydrophobic, unsulfonated mer units and the other is sulfonated and proton conducting. The copolymers are typically solution cast into thin films where the hydrophobic and hydrophilic components self-assemble into separate domains. An example of the well-defined microstructure in block copolymers relative to a random copolymer is shown in Figure 2.6. One of McGrath's copolymers, which contains blocks of perfluorinated poly(arylene ether) and sulfonated poly(arylene ether sulfone), has a higher conductivity than Nafion at low humidity (~10 mS/cm vs. 2 mS/cm at 30°C and 20% RH).[34] The increased conductivity was attributed to the material's high IEC (1.55 meq/g) and its well-defined hydrophilic/hydrophobic domains. However, the polymer

swelled excessively in liquid water (138 wt% as compared to 38 wt% for Nafion) and thus is not ideal for fuel cell applications.

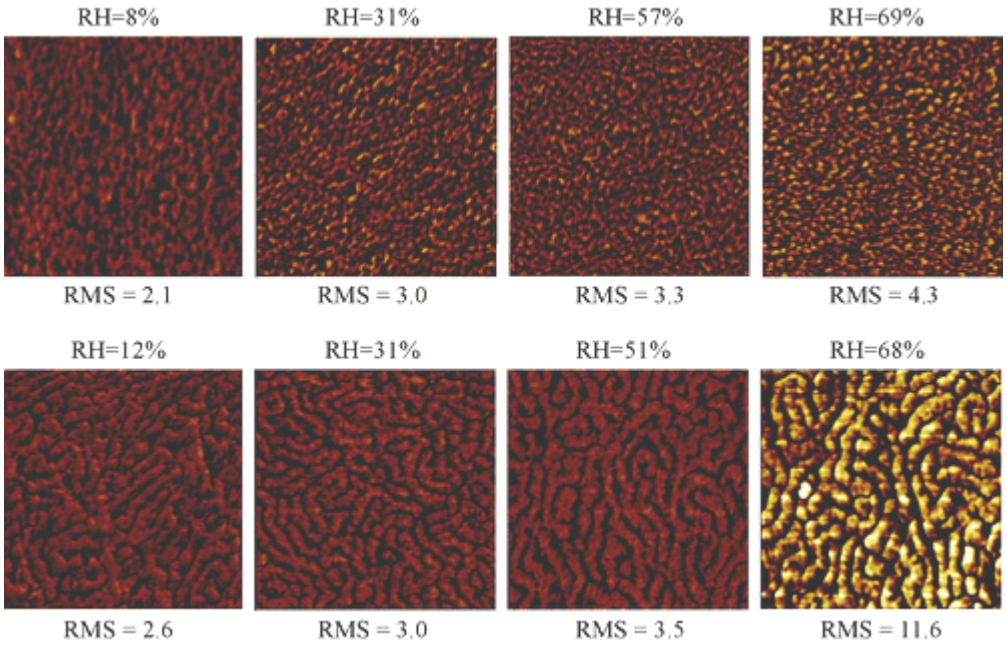

Figure 2.6. Scanning force microscopy images of random (top) and multiblock (bottom) PEMs as a function of RH. Image size is 1 μm, and phase range is 40° for all images. RMS values are the root-mean-square surface roughness. The random copolymer is BPSH35, a copolymer of 4,4′-biphenol, 4,4′-dichlorodiphenylsulfone, and 3,3′-disulfonated-4,4′-dichlorodiphenylsulfone. The multiblock copolymer contains blocks of a hydrophilic poly(arylene ether sulfone) and hydrophobic polyimide. Adapted with permission from Einsla, M. L.; Kim, Y. S.; Hawley, M.; Lee, H.-S.; McGrath, J. E.; Liu, B.; Guiver, M. D.; Pivovar, B. S., *Chemistry of Materials* **2008,** 20, (17), 5636-5642..[38] Copyright 2008 American Chemical Society.

Another example of a block copolymer contained a hydrophilic sulfonated poly(arylene ether sulfone) block and a hydrophobic polyimide block. The final membrane had an IEC of 1.55 meq/g and a low proton conductivity of 1.9 mS/cm at 50% RH, 80°C, half the conductivity of Nafion 212.[38] The block copolymer film swelled considerably more than Nafion 212 in water (51 wt% vs. 19 wt%). Furthermore, when

the copolymer film was incorporated into a MEA it performed worse than a Nafion 212 MEA in a hydrogen/air fuel cell (operated from 40%-70% RH at 100^{o}C).[38]

Generally, sulfonated hydrocarbons require a higher IEC to achieve the same conductivities as PFSAs, partly due to the weaker nature of its acid groups (pKa ~ -1 as compared to -6 for PFSA).[33, 39] The requisite high IEC leads to large water swelling in the wet state and sometimes brittle mechanical properties in the dry state[39], making the manufacturing and durability of these materials suspect. Another drawback of hydrocarbon copolymers is the limitations of polymer chemistry. Covalent attachment of block segments can be difficult and it can be problematic to find a suitable solvent (for the purpose of solution casting) when the blocks have dramatic differences in hydrophilicity/hydrophobicity.[18, 40]

With regards to sulfonated hydrocarbon ionomers for DMFC applications, Kim et al. have shown that BPSH (the random copolymer discussed previously) has lower methanol permeability (ranging from 5% to 80% lower depending on the monomer ratio) and greater selectivity (as high as 3 times higher) than Nafion. These characteristics were primarily attributable to the difference in the microstructure of the hydrophilic and hydrophobic domains between BPSH and Nafion.[39, 41] However, these materials were not tested in a DMFC.

Kim and Guiver[3] provide an excellent summary of the relationship between methanol permeability and proton conductivity in sulfonated hydrocarbon polymers and several other PEMs, demonstrating the trade-off between these two physical properties. In general, decreasing methanol permeability results in an undesirable reduction in proton conductivity. One exception to this rule is McGrath's BPSH polymer (BPSH30) which

has similar proton conductivity to the benchmark Nafion 117 membrane and less than half of Nafion's methanol permeability.

2.3.3 Composite membranes: addition of hygroscopic inorganics

Various studies have been performed to determine the effects of hygroscopic inorganic additives on the performance of PFSA materials.[42-48] These additives can enhance water retention, mechanical properties, and selectivity of PFSA membranes. A variety of inorganics have been investigated, including: metal oxides (e.g., SiO_2, TiO_2), clays (e.g., montmorillonite, zeolites) and heteropolyacids (HPAs).[42-50] Such inorganic-organic composite membranes have had some success at retaining water in high-temperature/low-humidity environments for hydrogen/air fuel cells. For example, Adjemian, et al.[51] adapted the method of Mauritz and co-workers[48] to prepare Nafion and SiO_2 composite membranes via a sol-gel process. Thus, commercial Nafion 115 membranes were immersed in tetraethoxysilane (TEOS) solution and then dried at 100°C. The Nafion/SiO_2 composite membranes had over twice the power output as neat Nafion 115 in a hydrogen/air fuel cell operated at 0.4V, 130°C, and 100% RH (3 atm pressure was applied to permit humidification above 100°C). The improved performance was attributed to additional membrane hydration caused by SiO_2's hydroscopic nature. At lower temperature (~80°C with >100% RH feed streams) the Nafion/SiO_2 composite membranes had 30% lower power output than neat Nafion 115, presumably due to dilution of Nafion's conduction pathways by SiO_2.

Professor Herring's group has developed a scheme for incorporating HPA's into PEMs.[45-47, 52] Crystalline HPAs have high conductivities (i.e., >0.1 S/cm at 25°C, in the

hydrated state),[52] and their incorporation into an ionomer was expected to improve the composite membrane's conductivity. One notable HPA-containing membrane was prepared by copolymerizing butyl acrylate and hexanedioldiacrylate in the presence of the HPA, $H_4[SiW_{11}O_{40}(Si(CH=CH_2))_2]$. The composite had a proton conductivity of 0.17 S/cm at 80°C, 100% RH, slightly higher than Nafion's conductivity (~0.15 S/cm).[52]

Inorganic particles have also been used as methanol-blocking components in DMFC membranes.[49, 53-58] For example, Rhee et al. first functionalized montmorillonite (MMT) with a sulfonic acid group to minimize the loss in conductivity associated with dispersing unfunctionalized MMT into an ionomer. Then the modified MMT was dispersed in a Nafion solution and a composite film was cast. A composite membrane (95 wt% Nafion and 5 wt% modified MMT) had a proton conductivity of ~0.07 S/cm (vs. 0.10 S/cm for Nafion) and a methanol permeability 3 times lower than Nafion's. A MEA with this membrane had 30% higher maximum power output in a DMFC than commercial Nafion 115 when operating at 40°C with a 2 M methanol feed.[58]

The addition of inorganic particles to PEMs has led to some encouraging hydrogen/air fuel cell and DMFC results. However, these additives have given rise to new problems: at high inorganic loadings, the membranes become mechanically brittle and have reduced proton conductivity due to dilution of the ionomer.[59] Also, some of the particles, most notably HPAs, are water soluble and thus have suspect stability in a fuel cell environment.[52, 60]

2.3.4 Composite membranes: impregnated ionomer in macroporous support

The dimensional and mechanical stability of PFSA materials has been enhanced by impregnating PFSA solution into porous, uncharged materials. The most notable example is W.L. Gore's commercially available GORE-SELECT® membrane, which is fabricated by imbedding PFSA polymer into an expanded polytetrafluoroethylene support (see Figure 2.7 for an image of the support).[61, 62] An MEA containing a GORE-SELECT membrane lasted ~150% longer in an accelerated fuel cell durability/humidity-cycling test as compared to a MEA with an extruded Nafion 1035 membrane.[63] The improved durability was attributed to GORE-SELECT's polytetrafluoroethylene reinforcement, though the physical properties of the membrane were not reported. One drawback of GORE-SELECT and other pore-filled membranes is that they often require multiple impregnation steps for complete pore-filling.[61, 62, 64, 65] This complicates manufacture[66] and limits the number of polymer combinations (i.e., the impregnated polymer cannot be in a solution which dissolves or excessively swells the porous, reinforcing polymer).

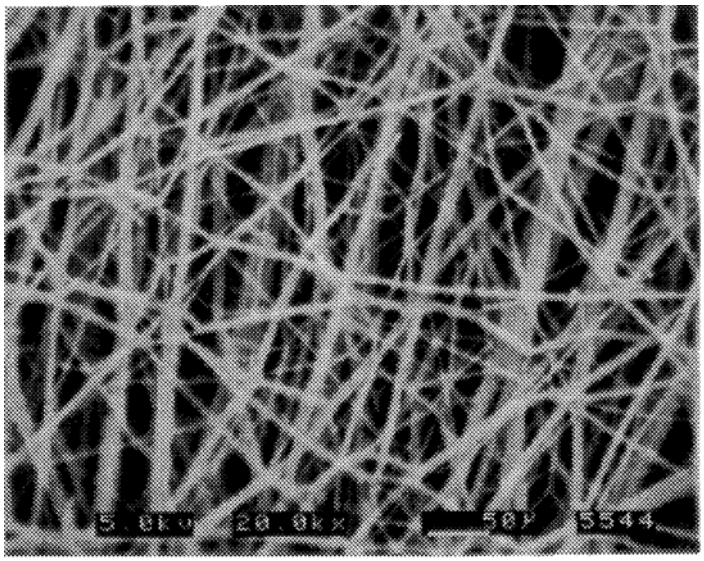

Figure 2.7. Gore's expanded polytetrafluoroethylene support prior to pore-filling by ionomer. Image from Reference (61).

Another dimensionally stabilized membrane is currently being developed by Giner, LLC. PFSA ionomer is imbedded into 2-D or 3-D polymeric, porous supports such as polytetrafluoroethylene (the same polymer as the GORE-SELECT support), polysulfone, polyether-ether ketone, and polyimide (Kapton®).[67, 68] Giner reports that filling the void space of these supports is difficult[68] and making membranes thinner than 25 μm was also problematic,[69] thus providing another example of the difficulties associated with imbedding polymer solutions in porous polymer supports. Still, Giner's membrane is expected to realize durability improvements over the benchmark commercial Nafion membranes because of its impressive mechanical properties and low water swelling. A Giner membrane reinforced by Kapton has a storage modulus 3 orders of magnitude higher than Nafion's and has low in-plane/areal water swelling (<5%). Additionally, a Giner membrane with 700 EW PFSA that was reinforced by Kapton had

higher proton conductivity than commercial Nafion (0.2 S/cm vs. 0.1 S/cm at 80^{o}C, 80% RH).[68]

Another notable pore-filling membrane has been developed by Professor Yamaguchi's group at the University of Tokyo.[70-72] The membrane was prepared by impregnating poly(acrylamide-tert-butylsulfonic acid) into an uncharged, porous support of either high density polyethylene or polyimide with porosities ranging from 40-47%. After impregnation, the poly(acrylamide-tert-butylsulfonic acid) was crosslinked. When this membrane (using the high density polyethylene support) was incorporated into a MEA and tested in a DMFC it had dramatically lower methanol crossover than a MEA with Nafion 117 (4 times lower crossover with a 10 M methanol feed stream). The reduced methanol crossover resulted in ~5 times higher power output for a DMFC operated at 0.2 V and 50^{o}C - 60^{o}C.[71]

2.4 References

(1) MacLean, H. L.; Lave, L. B., *Progress in Energy and Combustion Science* **2003,** 29, (1), 1-69.

(2) Hamrock, S. J., Yandrastis, Michael A., *Polymer Reviews* **2006,** 46, 219-244.

(3) Kim, D. S.; Guiver, M. D., In *Polymer Membranes for Fuel Cells*, Zaidi, S. M. J.; Matsuura, T., Eds. Springer Science + Business Media, LLC: New York, 2009.

(4) Cooper, K. R.; Ramani, V.; Fenton, J. M.; Kunz, H. R., *Experimental Methods and Data Analysis for Polymer Electrolyte Fuel Cells*. 1.8 ed.; Scibner Associates, Inc.: Southern Pines, NC, 2009.

(5) Hickner, M. A.; Ghassemi, H.; Kim, Y. S.; Einsla, B. R.; McGrath, J. E., *Chemical Reviews* **2004,** 104, (10), 4587-4612.

(6) Gronowski, A. A.; Yeager, H. L., *Journal of the Electrochemical Society* **1991,** 138, (9), 2690-2697.

(7) Mauritz, K. A.; Moore, R. B., *Chemical Reviews* **2004,** 104, (10), 4535-4586.

(8) Mohammadi, F.; Rabiee, A., *Journal of Applied Polymer Science* 120, (6), 3469-3476.

(9) Kusoglu, A.; Karlsson, A. M.; Santare, M. H.; Cleghorn, S.; Johnson, W. B., *Journal of Power Sources* **2007,** 170, (2), 345-358.

(10) Heitner-Wirguin, C., *Journal of Membrane Science* **1996,** 120, (1), 1-33.

(11) Banerjee, S.; Curtin, D. E., *Journal of Fluorine Chemistry* **2004,** 125, (8), 1211-1216.

(12) Marrony, M.; Barrera, R.; Quenet, S.; Ginocchio, S.; Montelatici, L.; Aslanides, A., *Journal of Power Sources* **2008,** 182, (2), 469-475.

(13) Atkinson, S., *Membrane Technology* **2005,** 2005, (1), 5-7.

(14) Lin, J.; Wycisk, R.; Pintauro, P. N., In *Polymer Membranes for Fuel Cells*, Zaidi, S. M. J. M., Takeshi, Ed. Spring Science+Business Media, LLC: New York, 2009; pp 341-359.

(15) Beckerbauer, R. US Patent 3714245, 1973.

(16) Grot, W. G. US Patent 3718627, 1973.

(17) Emery, M.; Frey, M.; Guerra, M.; Haugen, G.; Hintzer, K.; Lochhaas, K. H.; Pham, P.; Pierpont, D.; Schaberg, M.; Thaler, A.; Yandrasits, M.; Hamrock, S., *ECS Transactions* **2007,** 11, (1), 3-14.

(18) Choi, J.; Lee, K. M.; Wycisk, R.; Pintauro, P. N.; Mather, P. T., *Journal of Materials Chemistry* **2010,** 20, (30), 6282-6290.

(19) Hamrock, S. J., 2010 Annual Merit Review Proceedings Fuel Cells: Membranes and MEA's for Dry, Hot Operating Conditions. In 2010.

(20) Schaberg, M. S.; Abulu, J. E.; Haugen, G. M.; Emery, M. A.; O'Conner, S. J.; Xiong, P. N.; Hamrock, S., *ECS Transactions* **2010,** 33, (1), 627-633.

(21) Hamrock, S., 2011 Annual Merit Review Proceedings Fuel Cells: Membranes and MEA's for Dry, Hot Operating Conditions. In 2011.

(22) Dang, T. D.; Bai, Z.; Yoonessi, M., In *Polymer Membranes for Fuel Cells*, Zaidi, S. M. J. M., Takeshi, Ed. Spring Science+Business Media, LLC: New York, 2009; pp 115-157.

(23) Bauer, B.; Jones, D. J.; Roziere, J.; Tchicaya, L.; Alberti, G.; Casciola, M.; Massinelli, L.; Peraio, A.; Besse, S.; Ramunni, E., *Journal of New Materials for Electrochemical Systems* **2000,** 3, (2), 93-98.

(24) Zaidi, S. M. J.; Mikhailenko, S. D.; Robertson, G. P.; Guiver, M. D.; Kaliaguine, S., *Journal of Membrane Science* **2000,** 173, (1), 17-34.

(25) Wang, F.; Hickner, M.; Ji, Q.; Harrison, W.; Mecham, J.; Zawodzinski, T. A.; McGrath, J. E., *Macromolecular Symposia* **2001,** 175, 387-395.

(26) Wei, J.; Stone, C.; Steck, A. E. US Patent 5422411, 1995.

(27) Schuster, M.; de Araujo, C. C.; Atanasov, V.; Andersen, H. T.; Kreuer, K. D.; Maier, J., *Macromolecules* **2009,** 42, (8), 3129-3137.

(28) Genies, C.; Mercier, R.; Sillion, B.; Cornet, N.; Gebel, G.; Pineri, M., *Polymer* **2001,** 42, (2), 359-373.

(29) Litt, M.; Granados-Focil, S.; Kang, J.; Si, K.; Wycisk, R., *ECS Transactions* **2010,** 33, (1), 695-710.

(30) de Araujo, C. C.; Kreuer, K. D.; Schuster, M.; Portale, G.; Mendil-Jakani, H.; Gebel, G.; Maier, J., *Physical Chemistry Chemical Physics* **2009,** 11, (17), 3305-3312.

(31) Si, K.; Wycisk, R.; Dong, D.; Cooper, K.; Rodgers, M.; Brooker, P.; Slattery, D.; Litt, M., *Macromolecules* **2013,** 46, (2), 422-433.

(32) Si, K.; Wycisk, R.; Dong, D. X.; Cooper, K.; Rodgers, M.; Brooker, P.; Slattery, D.; Litt, M., *Macromolecules* 46, (2), 422-433.

(33) Wang, F.; Hickner, M.; Kim, Y. S.; Zawodzinski, T. A.; McGrath, J. E., *Journal of Membrane Science* **2002,** 197, (1-2), 231-242.

(34) Ghassemi, H.; McGrath, J. E.; Zawodzinski, T. A., *Polymer* **2006,** 47, (11), 4132-4139.

(35) Lecommandoux, S.; Lazzari, M.; Liu, G., In *Block Copolymers in Nanoscience*, Lazzari, M.; Liu, G.; Lecommandoux, S., Eds. John Wiley & Sons: Darmstadt, 2007.

(36) Li, Y.; Roy, A.; Badami, A. S.; Hill, M.; Yang, J.; Dunn, S.; McGrath, J. E., *Journal of Power Sources* **2007,** 172, (1), 30-38.

(37) Ghassemi, H.; Ndip, G.; McGrath, J. E., *Polymer* **2004,** 45, (17), 5855-5862.

(38) Einsla, M. L.; Kim, Y. S.; Hawley, M.; Lee, H.-S.; McGrath, J. E.; Liu, B.; Guiver, M. D.; Pivovar, B. S., *Chemistry of Materials* **2008,** 20, (17), 5636-5642.

(39) Kreuer, K. D., *Journal of Membrane Science* **2001,** 185, (1), 29-39.

(40) Pintauro, P. N.; Litt, M., Nanofiber Composite Membranes for Electrochemical Applications. Department of Energy Grant Proposal: 2008.

(41) Kim, Y. S.; Hickner, M. A.; Dong, L. M.; Pivovar, B. S.; McGrath, J. E., *Journal of Membrane Science* **2004,** 243, (1-2), 317-326.

(42) Deng, Q.; Moore, R. B.; Mauritz, K. A., *Journal of Applied Polymer Science* **1998,** 68, (5), 747-763.

(43) Damay, F.; Klein, L. C., *Solid State Ionics* **2003,** 162, 261-267.

(44) Bebin, P.; Caravanier, M.; Galiano, H., *Journal of Membrane Science* **2006,** 278, (1-2), 35-42.

(45) Malers, J. L.; Sweikart, M.-A.; Horan, J. L.; Turner, J. A.; Herring, A. M., *Journal of Power Sources* **2007,** 172, (1), 83-88.

(46) Meng, F.; Aieta, N. V.; Dec, S. F.; Horan, J. L.; Williamson, D.; Frey, M. H.; Pham, P.; Turner, J. A.; Yandrasits, M. A.; Hamrock, S. J.; Herring, A. M., *Electrochimica Acta* **2007,** 53, (3), 1372-1378.

(47) Vernon, D. R.; Meng, F.; Dec, S. F.; Williamson, D. L.; Turner, J. A.; Herring, A. M., *Journal of Power Sources* **2005,** 139, (1-2), 141-151.

(48) Deng, Q.; Moore, R. B.; Mauritz, K. A., *Chemistry of Materials* **1995,** 7, (12), 2259-2268.

(49) Herring, A. M., *Polymer Reviews* **2006,** 46, (3), 245-296.

(50) Deng, Q.; Moore, R. B.; Mauritz, K. A., *Journal of Applied Polymer Science* **1998,** 68, (5), 747-763.

(51) Adjemian, K. T.; Lee, S. J.; Srinivasan, S.; Benziger, J.; Bocarsly, A. B., *Journal of the Electrochemical Society* **2002,** 149, (3), A256-A261.

(52) Sachdeva, S.; Turner, J. A.; Horan, J. L.; Herring, A. M., In *Fuel Cells and Hydrogen Storage*, Bocarsly, A.; Mingos, D. M. P., Eds. Springer: 2011; pp 115-168.

(53) Dimitrova, P.; Friedrich, K. A.; Stimming, U.; Vogt, B., *Solid State Ionics* **2002,** 150, (1-2), 115-122.

(54) Silva, V. S.; Ruffmann, B.; Vetter, S.; Mendes, A.; Madeira, L. M.; Nunes, S. P., *Catalysis Today* **2005,** 104, (2-4), 205-212.

(55) Baglio, V.; Arico, A. S.; Blasi, A. D.; Antonucci, V.; Antonucci, P. L.; Licoccia, S.; Traversa, E.; Fiory, F. S., *Electrochimica Acta* **2005,** 50, (5), 1241-1246.

(56) Ruffmann, B.; Silva, H.; Schulte, B.; Nunes, S. P., *Solid State Ionics* **2003,** 162-163, (0), 269-275.

(57) Ren, S.; Sun, G.; Li, C.; Song, S.; Xin, Q.; Yang, X., *Journal of Power Sources* **2006,** 157, (2), 724-726.

(58) Rhee, C. H.; Kim, H. K.; Chang, H.; Lee, J. S., *Chemistry of Materials* **2005,** 17, (7), 1691-1697.

(59) Wycisk, R.; Ballengee, J.; Pintauro, P. N., In *Encyclopedia of Membrane Science and Technology*, John Wiley & Sons: In Press.

(60) Zhu, X.; Liu, Y.; Zhu, L., In *Polymer Membranes for Fuel Cells*, Zaidi, S. M. J.; Matsuura, T., Eds. Spring Science+Business Media, LLC: New York, 2009.

(61) Bahar, B.; Hobson, A. R.; Kolde, J. A. US Patent 5599614 1997.

(62) Bahar, B.; Hobson, A. R.; Kolde, J. A.; Zuckerbrod, D. US Patent 5547551, 1996.

(63) Liu, W.; Ruth, K.; Rusch, G., *Journal of New Materials for Electrochemical Systems* **2001,** 4, (4), 227-232.

(64) Hasani-Sadrabadi, M. M.; Shabani, I.; Soleimani, M.; Moaddel, H., *Journal of Power Sources* 196, (10), 4599-4603.

(65) Mollá, S.; Compañ, V., *Journal of Membrane Science* **2011,** 372, (1-2), 191-200.

(66) Song, M.-K.; Kim, Y.-T.; Fenton, J. M.; Kunz, H. R.; Rhee, H.-W., *Journal of Power Sources* **2003,** 117, (1-2), 14-21.

(67) Brawn, S.; Liu, H.; Mittelsteadt, C. K.; Flach, A.; Johnson, F.; Cabasso, I., Dimensionally Stable Membranes™. In DOE Hydrogen Review, 2010.

(68) Mittelsteadt, C. K.; Braff, W.; VanBlarcom, S.; Liu, H.; Johnson, F.; Cabasso, I., Dimensionally Stable Membranes™. In DOE Annual Merit Review: 2009.

(69) Brawn, S.; Liu, H.; Mittelsteadt, C. K.; Flach, A.; Johnson, F.; Cabasso, I., Dimensionally Stable Membranes™. In DOE Annual Merit Review: 2011.

(70) Yamaguchi, T.; Zhou, H.; Nakazawa, S.; Hara, N., *Advanced Materials* **2007,** 19, (4), 592-596.

(71) Yamauchi, A.; Ito, T.; Yamaguchi, T., *Journal of Power Sources* **2007,** 174, (1), 170-175.

(72) Yamaguchi, T.; Miyata, F.; Nakao, S., *Advanced Materials* **2003,** 15, (14), 1198-1201.

CHAPTER III

MORPHOLOGICAL CONTROL OF ELECTROSPUN NAFION NANOFIBER MATS

Adapted with permission from Ballengee, J. B.; Pintauro, P. N., *Journal of the Electrochemical Society* **2011,** 158, (5), B568-B572.

3.1 Introduction

Electrospinning of polymer solutions has allowed for the production of polymeric fibers with diameters ranging from tens of nanometers to several microns.[1] During electrospinning, an electrostatic field induces a surface charge on a polymer solution or polymer melt as it emerges from a needle-spinneret tip and draws the solution/melt into a Taylor cone configuration. A polymeric fiber-jet (filament) emerges from the Taylor cone and is accelerated toward a grounded collecting surface, during which time solvent evaporates from the polymer (or the polymer melt is cooled). Entangled polymer chains prevent the fiber-jet from breaking up into droplets. As the fiber travels toward the grounded collector, charge repulsion creates a whipping instability which dramatically increases the jet path distance. An electric-field-induced drawing force elongates the jet, resulting in fibers, often of sub-micron diameter. The drawing action ceases when the fiber solidifies or the fiber jet impacts the grounded collector.

Electrospinning of Nafion perfluorosulfonic acid (PFSA) polymer has received recent interest.[2-6] Unfortunately, Nafion polymer electrospinning is notoriously difficult; it does not dissolve completely in alcohol/water solutions and in common organic

solvents like dimethylacetamide or dimethylformamide but rather forms a micellar dispersion.[7] Prior attempts at electrospinning Nafion fibers from commercial or prepared solutions failed because of insufficient polymer chain entanglements, in which case Nafion only electrosprayed as droplets.[3] Researchers found that Nafion could only be electrospun by adding a high molecular weight carrier polymer such as poly(ethylene oxide) (PEO), poly(acrylic acid) (PAA), or poly(vinyl alcohol) (PVA). Thus, several researchers proceeded to fabricate Nafion nanofibers by using a very high concentration of carrier polymer. For example, (i) Laforgue et al.[2] electrospun Nafion nanofiber mats with either 16.7 wt% PEO (200 kDa MW) or PVA (110 kDa MW) for possible use in sensors, actuators, and fuel cell electrodes, (ii) Chen et al.[3] electrospun Nafion with 25 wt% PAA (450kDa MW) for fuel cell applications, (iii) Zhou et al.[6] electrospun $Ru(bpy)_3^{2+}$-doped Nafion mats, where the fibers contained 29% PAA (450 kDa MW), in order to enhance an electrochemiluminescence sensor signal, and (iv) Nah et al.[5] used PEO as the carrier to electrospin a Nafion fiber mat, where the mat was used to increase the response speed of actuator devices.

Utilizing a low relative concentration of carrier polymer during Nafion electrospinning is highly desirable, particularly for fuel cell applications. The presence of carrier polymer compromises some of Nafion's properties (i.e., mechanical strength and proton conductivity). For example, PEO was found to reduce the conductivity of PFSAs far in excess of its volume fraction content in an electrospun fiber mat.[8] Consequently, Pintauro and co-workers, in papers authored recently by Lee et al. and Choi et al.,[4, 8] utilized a low concentration of carrier polymer (≤1 wt% PEO with molecular weights of either 300 kDa or 1,000 kDa) to fabricate nanofiber mats of Nafion and low equivalent

weight PFSA polymer from 3M Company (the mats were subsequently converted into nanofiber composite proton exchange membranes). The focus of these papers was on membrane fabrication and characterization, thus, a thorough study of Nafion electrospinning was not performed.

To date, no study has been devoted to the systematic study of Nafion electrospinning. This deficiency has contributed to the wide range of carrier polymer concentrations and electrospinning conditions found in the open literature. Here, I describe the first systematic investigation of Nafion nanofiber electrospinning with low amounts of carrier polymer (1-2 wt% of the total polymer content, where PEO (300-600 kDa MW) was chosen as the carrier). A guide for controlling the morphology of electrospun Nafion mats is presented. The effect of nanofiber morphology on a variety of electrospinning conditions (air humidity, solvent, carrier polymer molecular weight, applied voltage, and polymer solution flow rate) are described and discussed. While the study was not exhaustive, it was comprehensive. The results demonstrate that, by employing the proper electrospinning conditions, well-formed nanofiber mats of Nafion polymer can be fabricated using only 1 wt% PEO carrier, where the average fiber diameter is controlled between 300 and 900 nm.

3.2 Experimental

3.2.1 Solution preparation

Solutions of Nafion powder (prepared by drying a LIQUION 1115 solution from Ion Power, Inc.) and poly(ethylene oxide) (PEO, from Sigma-Aldrich. Molecular weights of 300 kDa, 400 kDa, and 600 kDa were used) in a 2:1 alcohol:water solvent

were prepared separately (at 23°C) and then combined to make an electrospinning solution with the proper ratio of Nafion to PEO. The electrospinning solution was mixed for 2-4 hours at 23°C. Longer mixing was unnecessary and should be avoided; extended mixing sometimes resulted in the formation of an electrospun bead-on-fiber morphology, for reasons not well understood at this time (but perhaps due to acid-induced hydrolytic PEO degradation).[9] Bead-on-fiber structures are undesirable for applications that require a uniform and isotropic fiber network.

A brief investigation of an alternative carrier polymer, poly(2-acrylamido-2-methyl-1-propanesulfonic acid), was also performed and is discussed in Appendix A.

3.2.2 Electrospinning

The Nafion/PEO electrospinning solution was drawn into a 3 mL syringe and electrospun using a 22 gauge needle-spinneret from Hamilton Company. The electrospinning apparatus is shown schematically in Figure 3.1, where the high voltage power supply was purchased from Glassman High Voltage (#MJ10P1500). Fibers were collected on a custom-built rotating aluminum drum that oscillated horizontally to ensure a nanofiber mat with randomly oriented fibers, where the mat thickness and volume fraction of fibers were uniform. Several parameters were varied in the present study, as summarized in Table 3.1. All electrospinning experiments were conducted at room temperature (~23°C). Humidity was set by the building HVAC system and was monitored with a sensor from Fisher Scientific (#11-661-19). The spinneret-to-collector distance (SCD) was set at either 5 or 6 cm for all experiments. SCD did not have a significant effect on nanofiber morphology over this narrow range.

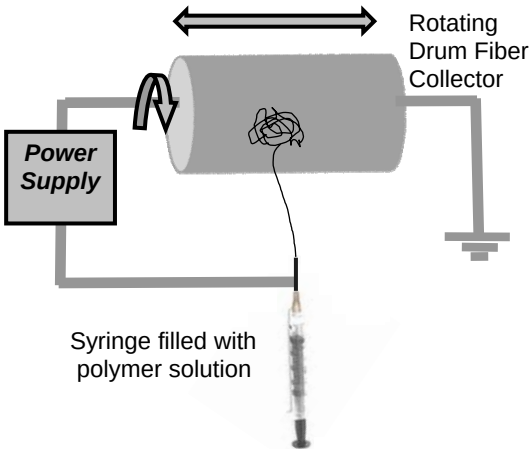

Figure 3.1. Schematic diagram of the rotating drum electrospinning apparatus. The grounded drum collector rotates and oscillates laterally.

Table 3.1. Electrospinning conditions and solution properties.

Parameter	Investigated Range
Electrospinning Conditions:	
Electrospinning Voltage	3.0 – 7.0 kV
Polymer Solution Flow Rate	0.2 – 0.6 mL/hr
Spinneret-to-Collector Distance	5 – 6 cm
Relative Humidity of the Air	20 – 40% (± 4%)
Solution Properties:	
Total Polymer Concentration	15 – 25 wt%
Alcohol Component of Solvent System*	methanol, ethanol, 2-propanol, 1-propanol
PEO Molecular Weight	300 - 600 kDa
PEO Concentration (wt%)	1 – 2 wt%

*Each alcohol was mixed with water in a 2:1 wt. ratio to prepare a solvent system for electrospinning

3.2.3 SEM microscopy

The morphology of electrospun mats was quantified via scanning electron microscopy (Hitachi 2-4200). Samples were sputtered with a gold layer (~5 nm in thickness) before imaging. After imaging, fiber diameters were measured with ImageJ software. A minimum of 30 fibers were measured to calculate an average fiber diameter in a given electrospun mat. If a bead-on-fiber morphology was observed, the bead diameter was excluded from the analysis. Error bars were calculated with 95% confidence intervals.

3.3 Results and discussion

3.3.1 Relative humidity effects

Figure 3.2 shows SEM micrographs of electrospun Nafion/PEO mats (using two different spinning solutions) that were created at low and high relative humidity (20% and 40% RH, this humidity range is typical for many laboratory/working environments). Average fiber diameters for the electrospun mats are shown in Figure 3.3. An increase in air humidity causes the formation of bead-on-fiber structures and increases the fiber diameter. Electrospinning at high humidity causes unwanted sorption of water into the Nafion/PEO fibers and premature polymer precipitation (water is a non-solvent for Nafion). Fast polymer precipitation reduces the time for fiber elongation during electrospinning, thus the increase in average fiber diameter with increasing humidity. Additionally, we hypothesize that Nafion precipitation at high humidity destabilizes the fiber jet and initiates bead-formation. The destabilization mechanism may involve Nafion precipitation within the Taylor cone at the spinneret tip. Prior work has shown

that Taylor cone destabilization causes bead formation.[10] Alternatively, non-uniform precipitation may occur along the polymeric fiber jet after it emerges from the Taylor cone, with the creation of polymer-rich and polymer-poor regions that eventually transform into bead-on-fiber structures.

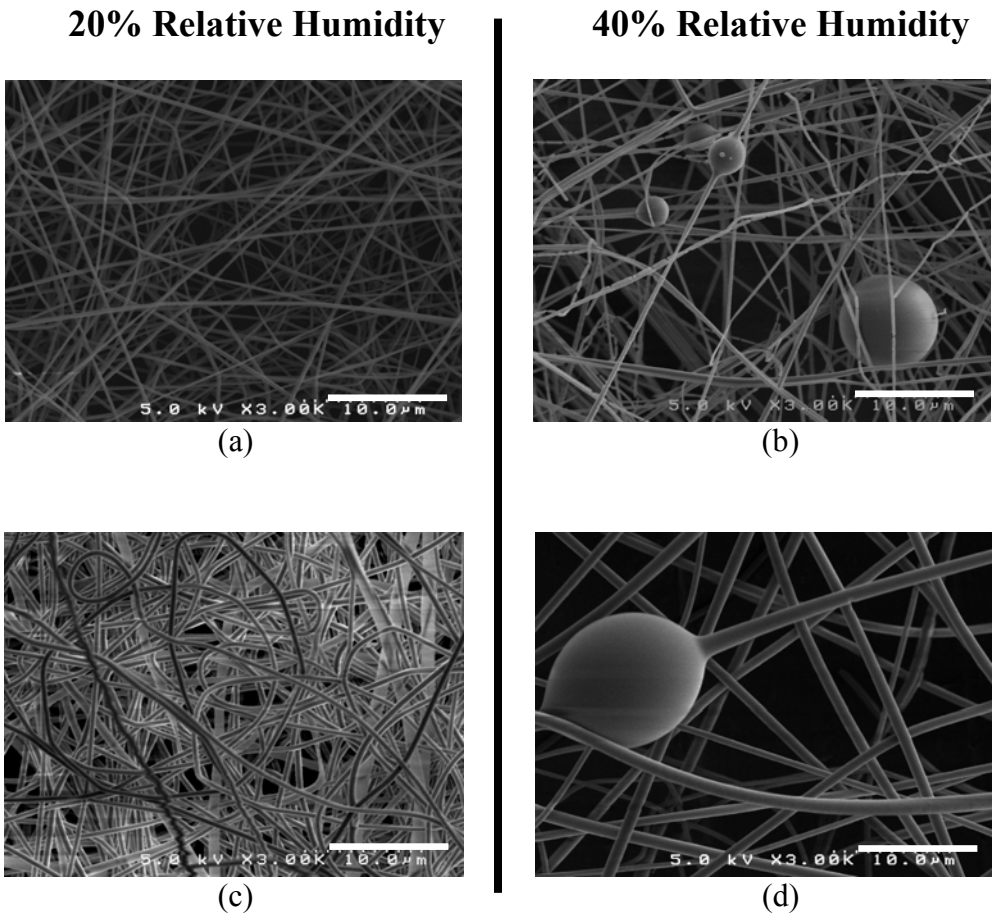

Figure 3.2. SEM micrographs of electrospun Nafion/PEO mats at 20% relative humidity (a, b) and 40% relative humidity (c, d). Scale bar is 10 microns. Electrospinning conditions for (a-d): 4.5 kV, 5 cm spinneret-to-collector distance, and 0.2 mL/hr solution flow rate. Electrospinning solution for (a, b) 15 wt% total polymer solution with a 99:1 Nafion:PEO weight ratio (300 kDa MW PEO) and 2-propanol/water solvent. Electrospinning solution for (c, d): 20 wt% total polymer solution with a 98:2 Nafion:PEO weight ratio (300 kDa MW PEO), and 2-propanol/water solvent.

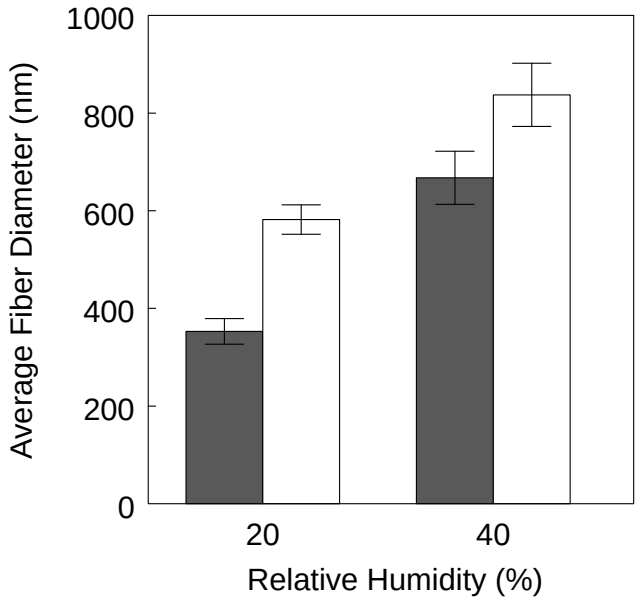

Figure 3.3. Effect of relative humidity on fiber diameter for two different electrospinning solutions. (■) 15 wt% Nafion:PEO (99:1 wt. ratio) and (□) 20 wt% Nafion:PEO (98:2 wt. ratio). Electrospinning conditions: 4.5 kV, 5cm spinneret-to-collector distance, 0.2 mL/hr flow rate, 300 kDa MW PEO carrier, 2-propanol/water solvent.

Bead-free fiber mats of Nafion/PEO were successfully electrospun at high air humidity by decreasing the applied voltage. Thus, at 40% relative humidity a well-formed Nafion nanofiber mat with no beads was created using a voltage of 4.0 kV and 1 wt% PEO (vs. the bead-on-fiber morphology in Figure 3.2 at 4.5 kV and 2 wt% PEO). An SEM micrograph of such a mat is shown in Figure 3.4, where the average fiber diameter is 498 nm. Lowering the PEO content between the fiber mats shown in Figures 3.3 and 3.4 would generally be expected to increase bead formation due to reduced polymer chain entanglements. This was not observed and thus the absence of beads can be attributed to the reduction in electrospinning voltage.

Understanding the interrelationship between voltage and humidity during Nafion electrospinning will require additional experiments. However, high voltages have previously been shown to result in bead formation with polymers other than Nafion.[10] With a high electric field strength the polymer solution is drawn from the spinneret too rapidly, causing the Taylor cone to recede into the needle. The confined Taylor cone is less stable and results in bead formation. The results with Nafion indicate that the maximum, stable electrospinning electric field strength is reduced at elevated air humidity, presumably due to the additional destabilizing effect of polymer precipitation by adsorbed water, as discussed above.

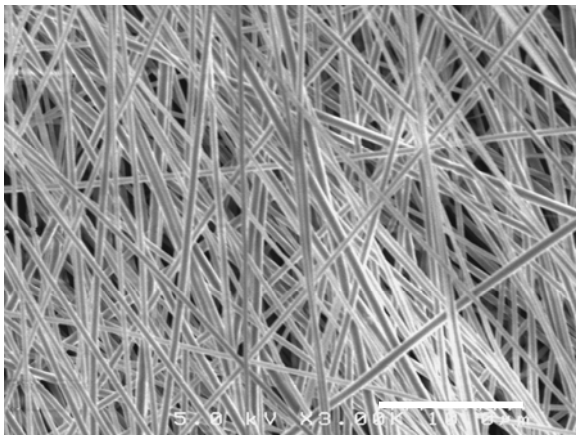

Figure 3.4. Bead-free Nafion/PEO nanofiber mat that was electrospun at 40% RH. Scale bar is 10 μm. Electrospinning conditions: 4 kV, 6 cm SCD, 0.2 mL/hr. Solution properties: 20 wt% polymer, 99:1 wt. ratio of Nafion:PEO (300 kDa MW), 2-propanol/water solvent.

3.3.2 Voltage and flow rate effects

The effect of electrospinning voltage on the average diameter of Nafion/PEO fibers is shown in Figure 3.5. Fiber diameter increases from 3 to 4 kV, however the fiber

diameter slightly decreases as the applied voltage is increased from 4 to 7 kV. Also, unwanted bead-on-fiber structures were more prevalent in mats that were electrospun at an applied voltage greater than 4 kV, as seen in Figure 3.6 (bead formation is not reflected in the average fiber diameters shown in Figure 3.5). A modest decrease in nanofiber diameter with increasing voltage is normal for many electrospinning systems.[11-13] A high applied voltage increases the rate at which a polymer filament is drawn out of the Taylor cone, which results in greater fiber elongation and a reduced fiber diameter.

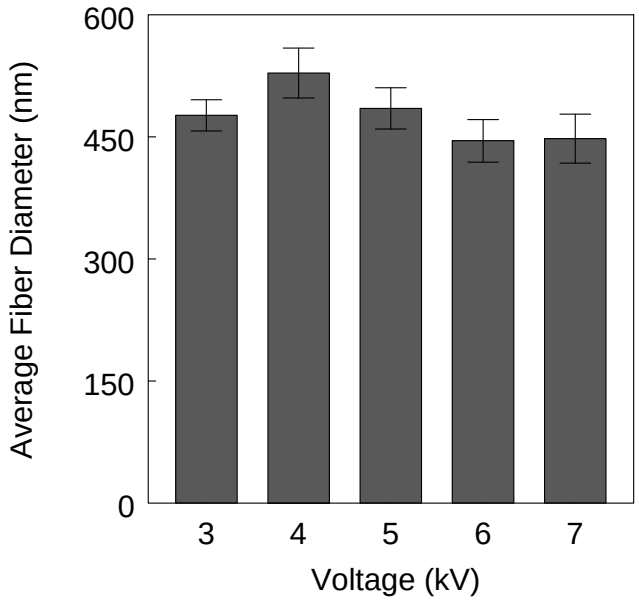

Figure 3.5. Effect of applied voltage on the average fiber diameter of Nafion/PEO electrospun nanofiber mats. Electrospinning conditions: 0.2 mL/hr, 6 cm SCD, 40% RH. Solution properties: 20 wt%, 99:1 wt. ratio of Nafion:PEO (400 kDa MW), 1-propanol/water solvent

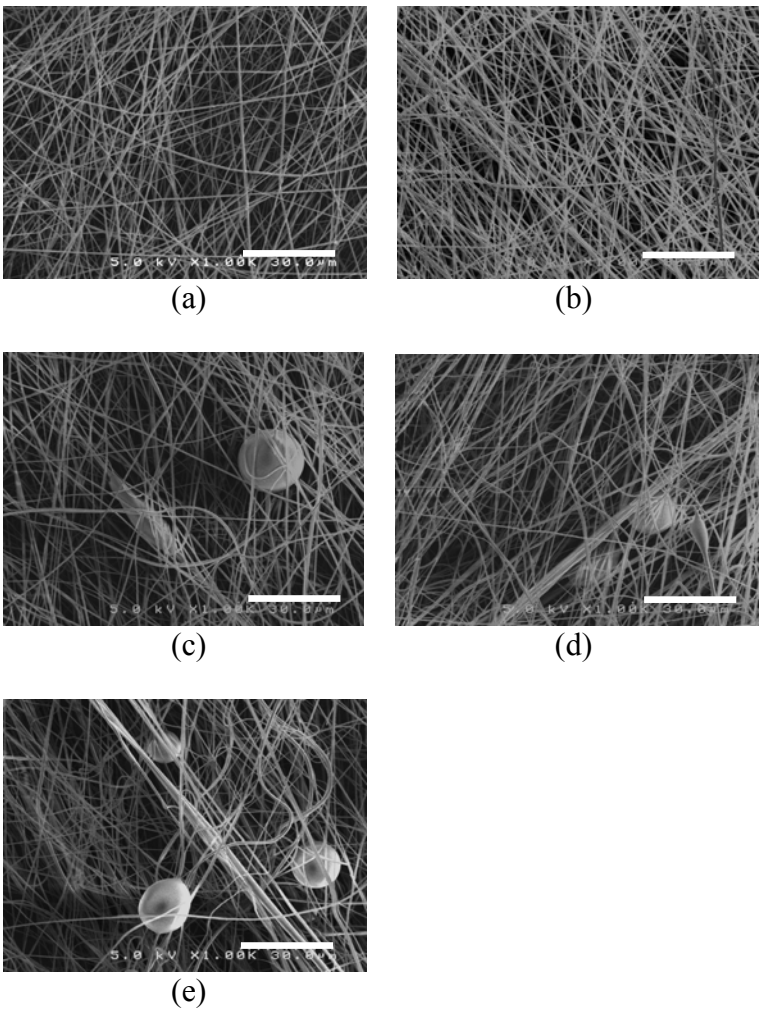

Figure 3.6. SEM micrographs of electrospun Nafion/PEO mats electrospun at (a) 3kV, (b) 4 kV, (c) 5 kV, (d), 6 kV, and (e) 7 kV. Scale bar is 30 μm.

Figure 3.7 shows that higher polymer solution flow rates produce larger average fiber diameters (data was collected at 30% relative humidity). This effect is common for electrospun polymers[14-16] and is attributable to the higher volume of material ejected from the spinneret. Conservation of mass requires a higher jet velocity for a high flow rate, if the fiber diameter is to remain constant. Wang et al.[17] showed that the jet velocity is constant and independent of flow rate when the applied voltage is fixed, as is the case for

the experimental conditions in Figure 3.7, in which case the fiber diameter can not be constant.

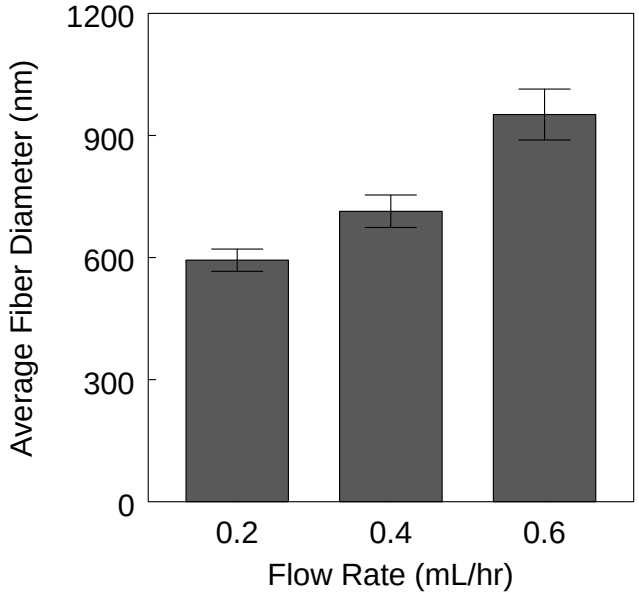

Figure 3.7. Effect of solution flow rate on the average fiber diameter of Nafion/PEO electrospun nanofiber mats. Electrospinning conditions: 4 kV, 5 cm SCD, 30% air RH. Solution properties: 25 wt% polymer, 99:1 wt. ratio of Nafion:PEO (400 kDa MW), 1-propanol/water solvent.

3.3.3 Solvent effects

The effect of solvent type on fiber diameter is shown in Figure 3.8 for methanol/water, ethanol/water, and 1-propanol/water solvents, where the alcohol/water ratio is held constant at 2:1 by weight. The average fiber diameter decreases with increasing boiling point of the solvent's alcohol component. Thus, the average fiber diameter is 1,070 nm for the solvent with methanol (b.p. 65^{o}C), whereas the average fiber diameter is 529 nm when the solvent contains 1-propanol (b.p. 97^{o}C). By using a higher boiling point solvent for electrospinning, the time for full solvent evaporation is

prolonged, allowing the polymer jet to be further drawn (elongated) into a fiber of smaller diameter before it contacts the collector surface. From a practical viewpoint, the electrospinning needle-spinneret often clogged when Nafion/PEO was electrospun with ethanol/water and methanol/water solvents, presumably due to rapid solvent evaporation.

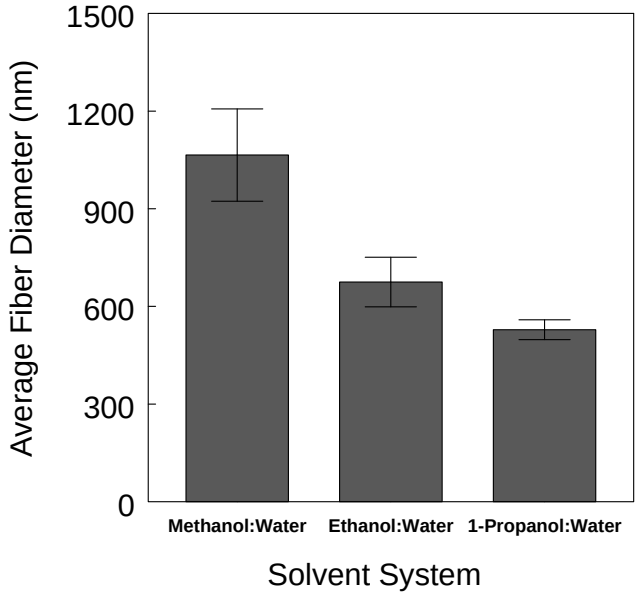

Figure 3.8. Effect of electrospinning solvent on Nafion/PEO nanofiber diameter. Electrospinning conditions: 4 kV, 6 cm SCD, 0.2 mL/hr solution flow rate, and 40% RH air humidity. Solution properties: 20 wt% polymer, 99:1 wt. ratio of Nafion:PEO (400 kDa MW). Boiling points of the alcohol components are as follows: methanol (65^{o}C), ethanol (78^{o}C), and 1-propanol (97^{o}C).

3.3.4 Effect of carrier polymer molecular weight

SEM micrographs for Nafion/PEO electrospun mats using three different PEO molecular weights are shown in Figure 3.9. The corresponding average fiber diameters are shown in Figure 3.10. The average fiber diameter is a strong function of PEO MW, increasing from 498 nm for 300 kDa PEO to 1138 nm for 600 kDa PEO (where the PEO

concentration was 1 wt% and the solvent was 2-propanol:water). The viscosity of a polymer solution is generally known to increase with polymer molecular weight[18] and an increase in polymer solution viscosity has been shown to increase electrospun fiber diameters.[19, 20] High viscosity solutions have greater resistance to the electric-field-induced drawing force as the solution emerges from the spinneret. Additionally, higher viscosity solutions undergo less bending instabilities before contacting the collector surface, thus reducing the distance and time under which the drawing (elongation) force acts.[20] For the two highest PEO MWs (400 and 600 kDa), ribbons are created in addition to nanofibers (see Figures 3.9b and 3.9c). Figure 3.9d shows a Nafion/PEO ribbon from an alternative perspective. The folds in the ribbon give evidence of the higher aspect ratio of a ribbon's cross-section as compared to a cylindrical fiber. Ribbon structures are known to form during electrospinning when the spinning solution solvent evaporates from the polymer filament's surface, leaving a solid film encapsulating a liquid core. Atmospheric pressure collapses this tube, resulting in a flat ribbon.[21] Generally, this phenomenon is more common when electrospinning large diameter fibers under conditions such as high polymer concentration in solution or high polymer MW.[4, 12, 22]

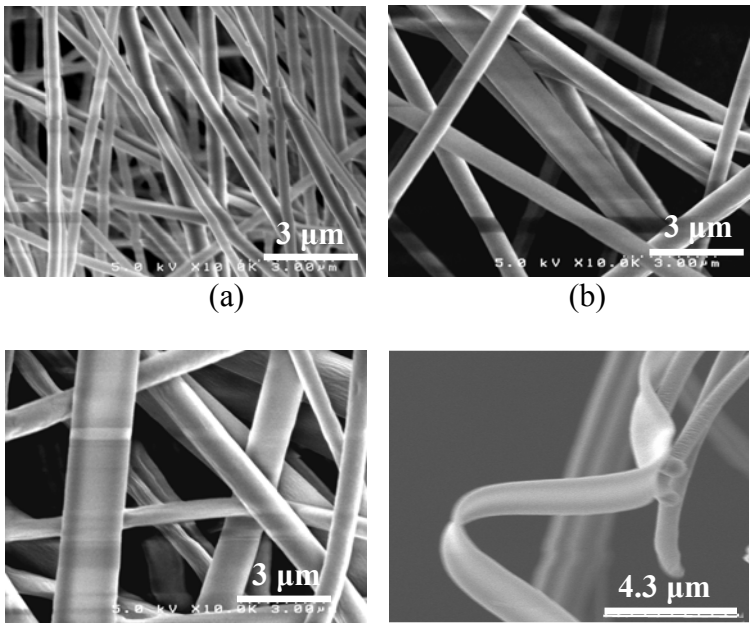

Figure 3.9. SEM micrographs for Nafion/PEO electrospun mats with (a) 300 kDa MW PEO, (b) 400 kDa MW PEO, (c-d) 600 kDa MW PEO. Electrospinning conditions: 4kV, 6 cm SCD, 0.2 mL/hr, and 40% RH. Electrospinning solution: 20 wt% polymer, 99:1 wt. ratio of Nafion:PEO, 2-propanol/water solvent.

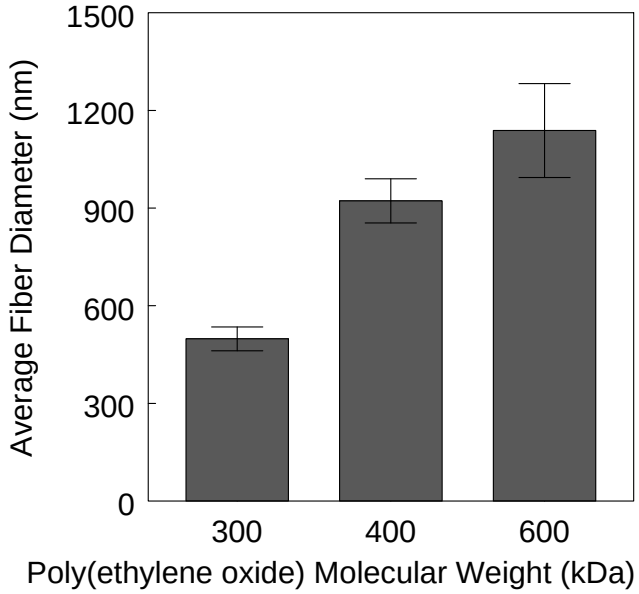

Figure 3.10. Effect of poly(ethylene oxide) molecular weight on the average fiber diameter of the Nafion/PEO electrospun mats shown in Figure 3.9.

3.3.5 Overview of Nafion mat morphology

Based on the above results, procedures for electrospinning Nafion nanofiber mats with 1 wt% PEO (as a required carrier) of different average fiber diameter can now be specified. Table 3.2 lists solution properties and electrospinning conditions to obtain Nafion/PEO mats with an average fiber diameter of 300 nm, 500 nm, 700 nm, and 900 nm.

Table 3.2. Solution properties and electrospinning conditions to produce Nafion nanofiber mats with different average fiber diameters. For solution properties, a 2:1 wt. ratio alcohol:water solvent was always used and the PEO carrier polymer loading was always 1 wt% (on a total polymer weight basis). Under electrospinning conditions, SCD denotes the spinneret-to-collector distance.

Average Nanofiber Diameter	**Solution Properties**	**Electrospinning Conditions**
300 nm	Total polymer concentration: 15 wt% Solvent: 2-propanol/water PEO MW: 300 kDa	Applied voltage: 4.5 kV Flow rate: 0.2 mL/hr SCD: 5 cm Relative humidity: 20%
500 nm	Total polymer concentration: 20 wt% Solvent: 2-propanol/water PEO MW: 300 kDa	Applied voltage: 4 kV Flow rate: 0.2 mL/hr SCD: 6 cm Relative humidity: 40%
700 nm	Total polymer concentration: 25 wt% Solvent: 1-propanol/water PEO MW: 400 kDa	Applied voltage: 4 kV Flow rate: 0.4 mL/hr SCD: 5 cm Relative humidity: 30%
900 nm	Total polymer concentration: 25 wt% Solvent: 1-propanol/water PEO MW: 400 kDA	Applied voltage: 4 kV Flow rate: 0.6 mL/hr SCD: 5 cm Relative humidity: 30%

3.4 Conclusions

Nafion has been electrospun into a nanofiber mat using 1-2 wt% poly(ethylene oxide) (PEO) as a carrier polymer. The effect of electrospinning conditions on the resulting nanofiber mat morphology was investigated. The experimental conditions and solution composition required to generate mats with an average fiber diameter of 300 nm to 900 nm have been identified. In general, slower polymer solidification rates favor the creation of fibers of smaller diameter. Nafion/PEO fibers which are electrospun into low humidity air have a smaller average diameter, with a lower occurrence of undesirable bead-on-fiber structures. The average fiber diameter of a mat decreases with decreasing molecular weight of PEO carrier and with increasing boiling point of the spinning solution solvent. The applied voltage and the polymer solution flow rate during electrospinning also influence the nanofiber morphology; high flow rates lead to fibers of larger diameter and an applied voltage greater than 4 kV resulted in the formation of bead-on-fiber structures, particularly when electrospinning into higher humidity (40% RH) air.

The Nafion electrospinning conditions identified here will be used throughout the coming chapters. However, the remainder of this dissertation will focus of fabricating and characterizing proton exchange membranes from electrospun nanofiber mats, not on more fundamental electrospinning studies. Still, several avenues of research related solely to Nafion electrospinning remain to be explored. For example, the carrier polymer concentration could be reduced even below 1 wt%; finding additional carrier polymers which may not effect Nafion's proton conductivity would be worthwhile; and a more

exhaustive study may reveal a wider range of Nafion fiber diameters, i.e., <300 nm and >900 nm.

3.5 References

(1) Huang, Z.-M.; Zhang, Y. Z.; Kotaki, M.; Ramakrishna, S., *Composites Science and Technology* **2003,** 63, (15), 2223-2253.

(2) Laforgue, A.; Robitaille, L.; Mokrini, A.; Ajji, A., *Macromolecular Materials and Engineering* **2007,** 292, (12), 1229-1236.

(3) Chen, H.; Snyder, J. D.; Elabd, Y. A., *Macromolecules* **2008,** 41, (1), 128-135.

(4) Lee, K. M.; Choi, J.; Wycisk, R.; Pintauro, P. N.; Mather, P., *ECS Transactions* **2009**, 25, 1451-1458.

(5) Nah, C.; Lee, Y. S.; Cho, B. H.; Yu, H. C.; Akle, B.; Leo, D. J., *Composites Science and Technology* **2008,** 68, (14), 2960-2964.

(6) Zhou, C. S.; Liu, Z.; Dai, J. Y.; Xiao, D., *Analyst* **2010,** 135, (5), 1004-1009.

(7) Loppinet, B.; Gebel, G.; Williams, C. E., *The Journal of Physical Chemistry B* **1997,** 101, (10), 1884-1892.

(8) Choi, J.; Lee, K. M.; Wycisk, R.; Pintauro, P. N.; Mather, P. T., *Journal of Materials Chemistry* **2010,** 20, (30), 6282-6290.

(9) Yang, B.; Guo, C.; Chen, S.; Ma, J.; Wang, J.; Liang, X.; Zheng, L.; Liu, H., *The Journal of Physical Chemistry B* **2006,** 110, (46), 23068-23074.

(10) Deitzel, J. M.; Kleinmeyer, J.; Harris, D.; Beck Tan, N. C., *Polymer* **2001,** 42, (1), 261-272.

(11) Buchko, C. J.; Chen, L. C.; Shen, Y.; Martin, D. C., *Polymer* **1999,** 40, (26), 7397-7407.

(12) Kidoaki, S.; Kwon, I. K.; Matsuda, T., *Biomaterials* **2005,** 26, (1), 37-46.

(13) Lee, J. S.; Choi, K. H.; Ghim, H. D.; Kim, S. S.; Chun, D. H.; Kim, H. Y.; Lyoo, W. S., *Journal of Applied Polymer Science* **2004,** 93, (4), 1638-1646.

(14) Zong, X.; Kim, K.; Fang, D.; Ran, S.; Hsiao, B. S.; Chu, B., *Polymer* **2002,** 43, (16), 4403-4412.

(15) Munir, M. M.; Iskandar, F.; Yun, K. M.; Okuyama, K.; Abdullah, M., *Nanotechnology* **2008,** 19, (14), 6.

(16) Megelski, S.; Stephens, J. S.; Chase, D. B.; Rabolt, J. F., *Macromolecules* **2002,** 35, (22), 8456-8466.

(17) Wang, C.; Hsu, C. H.; Lin, J. H., *Macromolecules* **2006,** 39, (22), 7662-7672.

(18) Krigbaum, W. R.; Flory, P. J., *Journal of Polymer Science* **1953,** 11, (1), 37-51.

(19) Fong, H.; Chun, I.; Reneker, D. H., *Polymer* **1999,** 40, (16), 4585-4592.

(20) Mit-uppatham, C.; Nithitanakul, M.; Supaphol, P., *Macromolecular Chemistry and Physics* **2004,** 205, (17), 2327-2338.

(21) Koombhongse, S.; Liu, W.; Reneker, D. H., **2001,** 39, (21), 2598-2606.

(22) Koski, A.; Yim, K.; Shivkumar, S., *Materials Letters* **2004,** 58, (3-4), 493-497.

CHAPTER IV

COMPOSITE FUEL CELL MEMBRANES FROM DUAL-NANOFIBER ELECTROSPUN MATS

4.1 Introduction

Nafion has been widely studied as the membrane material in hydrogen/air fuel cells due to its high proton conductivity and inherent thermal/mechanical/chemical stability.[1] For long-term use with numerous on/off cycles, such as the case for automotive applications, researchers have found that Nafion undergoes undesirable dimensional swelling and shrinking which eventually leads to membrane degradation.[2, 3] During hydrogen/air fuel cell operation at an elevated temperature (e.g., 80^{o}C), the proton-exchange membrane swells with water due to the presence of humid feed gases and the production of water at the cathode. After shutdown, the system cools, the supply of humid gases ceases, and the membrane dehydrates and shrinks. Tensile and compressive forces on the membrane are generated during membrane swelling/shrinking events due to physical constraints on the membrane (as part of the membrane-electrode-assembly, MEA) in a fuel cell fixture.[4] These forces cause unwanted membrane/electrode delamination, membrane creep, and pinhole formation.[5, 6] Few membrane materials have been fabricated to address this problem, although there have been numerous studies where Nafion swelling has been investigated.[5, 7-10]

Water swelling of a charged polymer can be controlled by the presence of physical crosslinks. Such crosslinks are generated by blending the ionomer with a hydrophobic/uncharged polymer. Solution cast blended films of Nafion and an uncharged polymer are problematic due to the incompatibility of Nafion with typical membrane casting solvents (i.e., Nafion forms a micellar dispersion and not a true polymer solution in typical membrane casting solvents such as dimethylformamide and dimethylacetamide) and with the uncharged polymer itself. With poorly dispersed blends there is little or no control of membrane swelling and no improvement in membrane mechanical properties.[11] Nonetheless, there have been a number of Nafion blending studies in the fuel cell literature involving the addition of polyvinylidene fluoride (PVDF).[12-15] One study found that PVDF and Nafion had poor miscibility below 60 wt% Nafion loading.[16] Water swelling was controlled (reduced from 37% for Nafion to ~27% for a blend membrane with 80 wt% Nafion), but the proton conductivity was dramatically reduced (from 0.052 S/cm for neat Nafion to 0.012 S/cm for the Nafion/PVDF blend).

An alternative strategy to blended Nafion fuel cell membranes is an impregnated composite membrane construct. For fuel cell applications, the most well known impregnated membrane material is the GORE-SELECT® product line from W. L. Gore & Associates where Nafion is impregnated into an expanded Teflon® sheet. In one iteration of the GORE-SELECT membrane, the conductivity was half that of Nafion 112 (due to the presence of the inert PTFE support material), but dimensional stability was improved (linear in-plane shrinkage upon dehydration was reduced from 11% for Nafion to 3%).[17] The impregnation processing step is the primary drawback of this type of composite membrane material. Typically, multiple ionomer solution impregnations are required

with intermittent solvent evaporation (membrane drying) steps. Complete filling of the inert matrix void volume is often challenging and there could be undesirable membrane swelling issues if the solvent of the ionomer impregnation solution sorbs into the inert matrix polymer.

In the present chapter, an alternative technique for fabricating composite ion-exchange membranes is presented. Two distinct membrane structures are described herein: (1) Nafion nanofibers embedded in inert/uncharged polyphenylsulfone polymer (2) a Nafion film reinforced by a polyphenylsulfone nanofiber network. Whereas the latter structure is similar to that of GORE-SELECT films, the former is a new morphology for Nafion/hydrocarbon polymer blends. The two membrane types are fabricated from the same dual fiber mat that was formed by simultaneously electrospinning Nafion and polyphenylsulfone (PPSU) from two separate spinnerets. Simple post-electrospinning processing steps were developed to create the two final membrane morphologies (see Figure 4.1). For structure #1, the Nafion component of the fiber mat is allowed to soften and flow to fill the PPSU interfiber void space without damaging the PPSU fiber structure (by use of a mat compression step followed by thermal annealing). For structure #2, the PPSU material in the mat is allowed to soften and flow into the void space between Nafion nanofibers without damaging the Nafion fiber structure (by mat compression, exposure to chloroform solvent vapor, and then thermal annealing). The method is inherently simpler and more robust than an impregnation scheme and the final polymer morphology is not limited by dispersion/compatibility problems that often plague blended membrane systems. As will

be shown below, the resulting nanofiber composite membranes have attractive properties for fuel cell applications.

The current work is an advancement over previously electrospun nanofiber-based fuel cell membranes in which ionomer fibers were electrospun and impregnated with a hydrophobic polymer component.[18-22] Our new approach provides i) ease of manufacture (no impregnation), ii) versatility of morphology (two distinct structures are fabricated from the same dual fiber mat where the diameter and volume fraction of the nanofibers can be controlled), and iii) a robust framework for future membrane design and fabrication (e.g., the method can be easily extended to other polymer composite combinations and the number of polymers incorporated into the composite membrane via electrospinning can be easily increased to three or more).

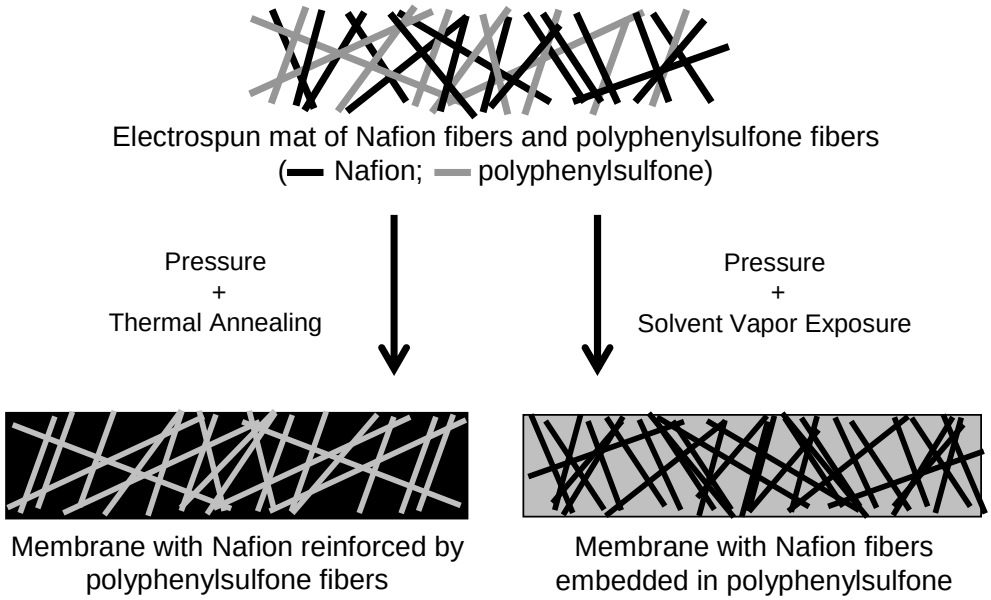

Figure 4.1. Schematic representation of two nanofiber-composite membrane structures fabricated from a single dual fiber electrospun mat.

4.2 Experimental

4.2.1 Electrospinning

Separate Nafion and polyethylene oxide (PEO) solutions were prepared by dissolving Nafion powder (prepared by evaporating the solvent from LIQUION 1115, Ion Power, Inc.) and PEO powder (Sigma-Aldrich, 400 kDa MW) into a 2:1 weight ratio n-propanol:water mixture. These two solutions were then combined to form a Nafion/PEO electrospinning solution where PEO constituted 1 wt% of the total polymer content.

Polyphenylsulfone (Radel R 5500NT, 63 kDa MW, from Solvay Advanced Polymers, LLC) solutions were prepared by dissolving polymer powder in an 80:20 wt. ratio of n-methyl-2-pyrrolidone:acetone. The polyphenylsulfone (PPSU) solution and Nafion/PEO solution were each drawn into separate syringes and electrospun using 22 g needles (Hamilton Company). PPSU fibers and Nafion/PEO fibers were simultaneously collected on a rotating aluminum drum that also oscillated laterally to ensure a random distribution and orientation of fibers with a uniform fiber density (as depicted in Figure 4.2 and Figure 4.3). The flow rates and concentrations of Nafion/PEO and PPSU were varied to produce fiber mats of varying compositions (i.e., different Nafion volume fractions). Nafion/PEO was electrospun at flow rates ranging from 0.10 mL/hr to 0.60 mL/hr and concentrations from 20 wt% to 25 wt%. PPSU was electrospun at flow rates from 0.04 mL/hr to 0.40 mL/hr, at a constant concentration of 25 wt%. For Nafion/PEO electrospinning, the spinneret-to-collector distance (SCD) was fixed at 5.5 cm and the voltage was set between 3.75 and 4 kV. PPSU was electrospun at 7.5 kV with a SCD of 8.5 cm. All electrospinning experiments were performed at room temperature, where the relative humidity (RH) was 22-40%.

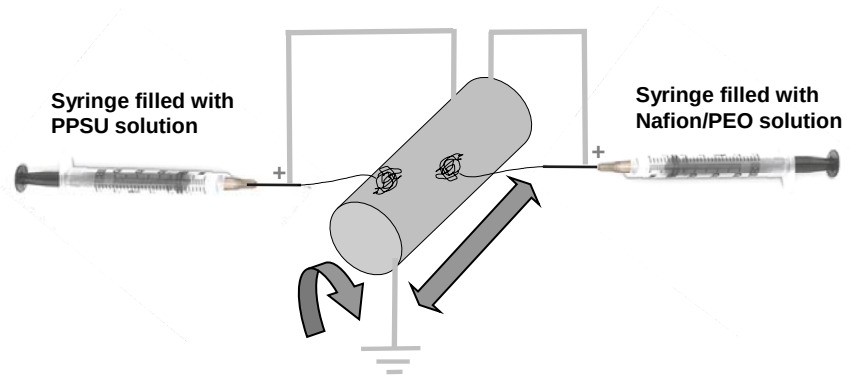

Figure 4.2. Schematic of dual-fiber electrospinning process.

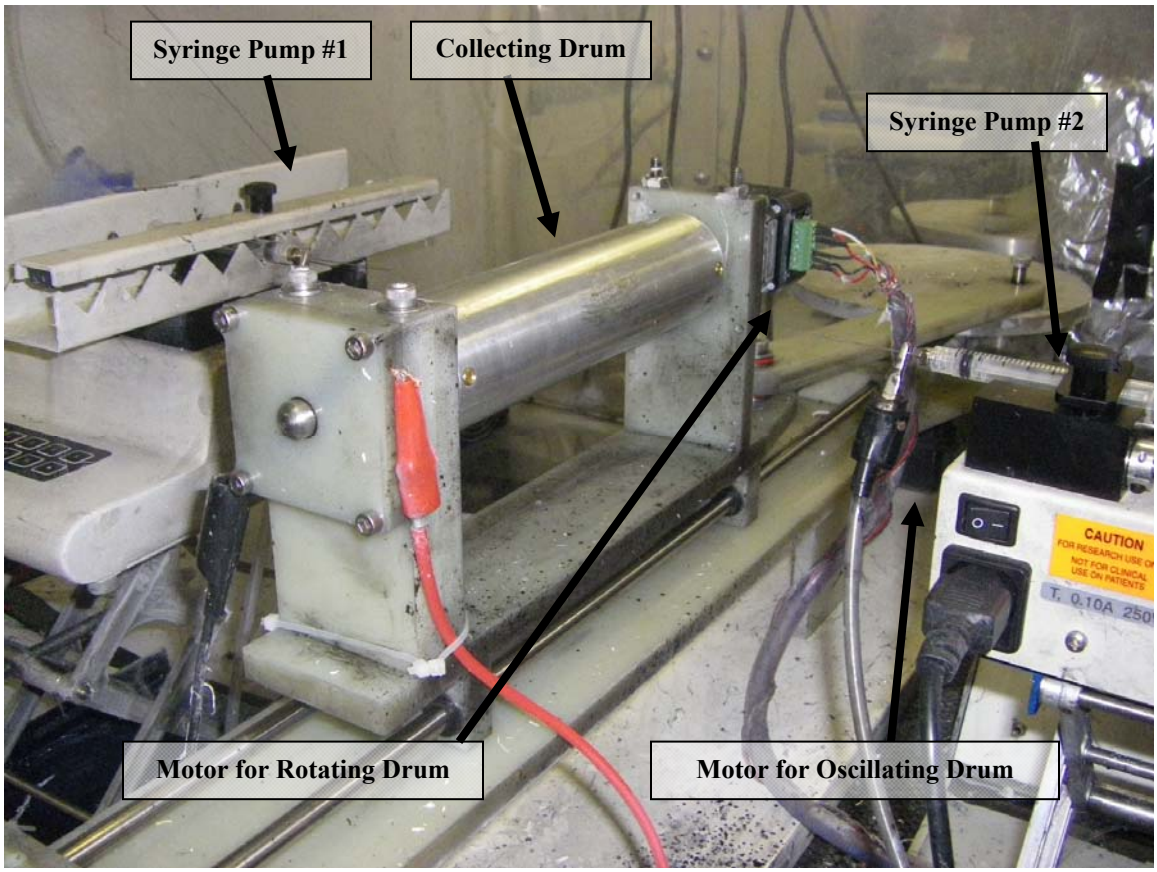

Figure 4.3. Photograph of dual-fiber electrospinning apparatus.

4.2.2 Nanofiber mat processing

Electrospun mats were processed in two different ways to give two distinct membrane morphologies.

Method 1 (for membranes where a Nafion film is reinforced by a PPSU nanofiber network). The electrospun mat was compressed at 15,000 psi and 127^{o}C for ~10 seconds. The sample was rotated 90^{o} three times and successively compressed to ensure even compression. The mat was then annealed in vacuum at 150^{o}C for 2 hours. The resulting membrane was boiled in 1 M sulfuric acid and deionized water for one hour each to remove residual PEO and to protonate all ion-exchange sites. Membranes were fabricated with Nafion volume fractions ranging from 0.33 to 1.0 (for a membrane with a Nafion volume fraction of 1.0, a mat with no PPSU fibers was processed as described above).

Method 2 (for membranes where Nafion nanofibers are embedded in PPSU). Electrospun mats were compressed at 3,500 psi and 23^{o}C. The sample was rotated 90^{o} 3 times and successively compressed to ensure even compression. The mat was suspended above liquid chloroform at 23^{o}C (i.e., exposed to chloroform vapor) in a sealed jar for 8-16 minutes (depending on the Nafion volume fraction, e.g., 16 minutes for mats with 70 vol% Nafion; 8 minutes for mats with 30 vol% Nafion). The membranes were immediately dried at 70^{o}C for 1 hour and then at 140^{o}C for 10 minutes, followed by thermal annealing of the Nafion (150^{o}C for 2 hours under vacuum). The membranes were then boiled in 1 M sulfuric acid for one hour and boiled in deionized water for one hour. Membranes with Nafion nanofibers embedded in PPSU were fabricated with Nafion volume fractions ranging from 0.09 to 0.68. Membranes composed solely of

PPSU (0.00 Nafion volume fraction) were fabricated from electrospun PPSU nanofiber mats by this same method.

4.2.3 Scanning electron microscopy

Electrospun mats and membranes were imaged with a Hitachi S-4200 scanning electron microscope. Samples were sputter-coated with a gold layer (~5 nm) to provide electrical conductivity. Freeze-fractured membrane cross-sections were prepared by immersing samples in liquid nitrogen. Fiber diameters were calculated using the ImageJ software package.

4.2.4 Proton conductivity

In-plane proton conductivity was measured by AC impedance. Water-equilibrated membrane samples were loaded into a BekkTech 4-electrode cell and immersed in water. Conductivity was calculated using Equation 4.1.

$$\sigma = \frac{L}{Rw\delta} \tag{4.1}$$

where σ [S/cm] is proton conductivity, R [Ω] is the measured resistance between the electrodes, L [cm] is the distance between the electrodes, w [cm] is the width of the sample (usually 1 cm), and δ [cm] is the thickness of the sample (typically between 0.0030 and 0.0060 cm).

4.2.5 Ion-exchange capacity

Ion-exchange capacity (IEC) was determined by a standard acid exchange and base titration experiment. A membrane sample of known dry weight in the H+ counterion form was soaked in 1 M NaCl for a minimum of 48 hours to exchange protons with Na+. The soak solution was then titrated to pH 7 with 0.01 N NaOH. IEC was calculated by Equation 4.2.

$$IEC = \frac{VN}{m_{dry}} x 1000 \tag{4.2}$$

where IEC [meq/g] is ion-exchange capacity (on a dry polymer weight basis), V [L] is the volume of the NaOH titrating solution, N [mol/L] is the normality of the NaOH titrating solution, and m_{dry} [g] is the dry mass of the membrane. The Nafion volume fraction in a composite membrane was determined from the measured IEC, as per Equation 4.3.

$$Nafion\ Volume\ Fraction = \frac{IEC_{Composite}}{IEC_{Nafion}} x \frac{\rho_{Composite}}{\rho_{Nafion}} \tag{4.3}$$

where $IEC_{composite}$ and $\rho_{composite}$ are the measured ion-exchange capacity and dry density of a nanofiber composite membrane and IEC_{Nafion} and ρ_{Nafion} are the same quantities for a neat solution cast and annealed Nafion film.

4.2.6 Water uptake and swelling

Gravimetric, volumetric, and areal (in-plane) swelling (water uptake) was measured by boiling samples in 1 M sulfuric acid for one hour and then boiling in 100°C water for one hour. Samples were removed from the water bath, quickly wiped dry, and then membrane mass, area, and volume were measured. Swelling was determined by Equation 4.4.

$$Water\ Swelling\ (\%) = \frac{x_{wet} - x_{dry}}{xdry} x100 \tag{4.4}$$

where x is either the membrane's mass, geometric area, or volume, corresponding to mass swelling, in-plane/areal swelling, or volumetric swelling, respectively.

4.2.7 Mechanical properties

Mechanical properties were measured with a TA Instrument Q800 Dynamic Mechanical Analyzer (DMA). Stress-strain curves were obtained for dry membranes at 30°C and ~20% RH (all membranes were pre-dried at ambient conditions for a minimum of three days and in vacuum at 40°C for one hour before the measurements). The DMA was operated in tension using the controlled force mode, where the force was increased at 0.1000 N/min until the sample yielded.

4.2.8 Fuel cell polarization

Fuel cell polarization curves were obtained for a 5 cm^2 membrane-electrode assembly (MEA) at a cell temperature of 80°C, a feed gas humidity of 100%, and

ambient pressure. For all experiments, the Pt electrode catalyst loading was 0.4 mg/cm^2, with 30 wt% Nafion binder. Catalyst inks were prepared from Pt/C catalyst (Alfa Aesar #42204) and Nafion solution (Sigma-Aldrich #527084). MEAs were fabricated using a standard decal method, where electrodes were painted onto Kapton films and then transferred to a membrane by hot-pressing for 10 minutes at 140^{o}C and 100 psi. Prior to a fuel cell test, the MEA was pre-conditioned overnight at room temperature by repeatedly cycling the cell for 5 minutes at a low current density (150 mA/cm^2) and then 5 minutes at a low voltage (0.2 V).[23] In a fuel cell experiment, feed gases were supplied at 100 sccm (hydrogen) and 500 sccm (air) for the anode and cathode, respectively. Polarization curves were obtained by measuring the current at specified voltages after 60 seconds of equilibration.

4.2.9 Fuel cell durability/open circuit voltage experiment

Fuel cell durability was determined by an accelerated open circuit voltage (OCV) test, where 100% and 0% hydrogen and air feed gases were successively and repeatedly passed through the fuel cell test fixture (2 min. each), while continuously monitoring the OCV. A 25 cm^2 fuel cell was operated at 80^{o}C for the test. The catalyst layers were prepared via a decal method, as stated above. The hydrogen limiting current was periodically measured during an OCV experiment by linear sweep voltammetry (0.0 to 0.5 V, using a Gamry Series G300 Potentiostat) after changing the feed gases (humidified hydrogen to the anode and nitrogen to the cathode at 200 sccm).[3]

4.3 Results and discussion

4.3.1 Membrane morphology

Nafion and polyphenylsulfone (henceforth abbreviated as PPSU) solutions were simultaneously electrospun from separate syringes to produce a nanofiber mat. Electrospinning perfluorosulfonic acid (PFSA) polymer solutions (e.g., DuPont's Nafion in alcohol:water solvents) is difficult because PFSAs do not dissolve in normal organic solvents but rather form micellar dispersions. Without the requisite chain entanglements, such solutions can only be electrospun by addition of a neutral high molecular weight carrier polymer like poly(ethylene oxide) (PEO), poly(acrylic acid) (PAA), or poly(vinyl alcohol).[20, 21, 25] A high concentration of the carrier (as much as 25 wt%) was required in early studies to electrospin Nafion fibers.[24-26] More recently, electrospinning conditions have been identified for electrospinning Nafion and other PFSA materials with a much lower concentration of the carrier material (e.g., $\leq$ 1 wt% PEO).[21, 22, 27] In the present study, Nafion and PEO (400 kDa MW) were mixed and electrospun in a 99:1 wt. ratio (400 kDa MW) using a 2:1 n-propanol:water solvent. PEO was later removed from a fully processed membrane during the standard Nafion membrane pre-treatment sequence of boiling in sulfuric acid and then boiling in water.

Figure 4.4a shows the fiber morphology of an electrospun mat containing Nafion/PEO and PPSU fibers where there is a uniform distribution of Nafion and PPSU nanofibers, with an average fiber diameter of 340 nm (see Figure 4.5 for a histogram of the fiber diameter distribution). In Figure 4.4a, the two types of fibers are indistinguishable. However, 60% of the fibers are composed of Nafion/PEO fibers, as determined by ion-exchange capacity and membrane density measurements. In its present

form, the dual fiber mat is highly porous and cannot be used as a fuel cell membrane, so further processing of the mat is required to create a dense and defect-free film. This processing can follow two different paths: (i) the Nafion/PEO fibers can fill the voids between PPSU fibers (resulting in a Nafion membrane reinforced by PPSU nanofibers) or (ii) the PPSU polymer can fill the void space between Nafion nanofibers, resulting in a membrane where proton conducting PFSA nanofibers are embedded in an inert/uncharged PPSU matrix.

The processing steps for converting a dual fiber electrospun mat into a Nafion membrane with reinforcing PPSU nanofibers are as follows: hot press at ~15,000 psig and 127^{o}C and then anneal at 150^{o}C for 2 hours (this time and temperature are the normal annealing conditions for Nafion). In a previous study, Choi et al.[20] observed that Nafion nanofibers in a low fiber volume fraction mat would fuse/weld at an elevated temperature, thus creating a three-dimensional PFSA nanofiber network. We have found in our work that Nafion nanofibers will soften, flow, and fully fill the void space between PPSU nanofibers when a high fiber volume fraction mat is subjected to a high temperature annealing step. The softening and flow of Nafion/PEO nanofibers is attributed to partial plasticization of Nafion by trace amounts of adsorbed water and to morphological rearrangement of ionic and amorphous domains since compression and annealing occurs above Nafion's α-transition temperature (~100^{o}C).[28, 29] After annealing, the membrane is boiled in 1 M sulfuric acid and water (1 hour each) to remove residual PEO from the membrane (the presence of PEO is known to suppress proton conductivity in a Nafion nanofiber membrane)[20] and to insure that all sulfonic acid ion-exchange sites are in the proton counter-ion form. A freeze-fracture SEM cross-section of a completely processed

Nafion membrane reinforced by PPSU nanofibers is shown in Figure 4.4b. The PPSU fibers are clearly visible and uniformly distributed throughout the membrane thickness and Nafion appears to completely fill the interfiber void volume.

A membrane with Nafion nanofibers embedded in PPSU (a morphology inverse to that in Figure 4.4b), was fabricated by: compacting the mat at ~3,500 psig, exposing the mat to chloroform vapor at room temperature to induce softening and flow of PPSU into the void space between Nafion nanofibers, drying the mat to remove chloroform, and then annealing the Nafion at 150^{o}C for 2 hours in vacuum. After the annealing step the membrane was pretreated in the normal fashion, by boiling in sulfuric acid and water. A SEM freeze-fractured cross-section of a membrane with Nafion nanofibers embedded in PPSU is shown in Figure 4.4c. The Nafion fiber morphology cannot be seen in this image, so to confirm the membrane morphology a fully processed film was soaked in liquid chloroform for two hours to dissolve/remove all of the PPSU. An SEM of the resulting membrane surface is shown in Figure 4.4d, where an interconnected (welded) network of Nafion nanofibers is clearly visible. Thus, it can be concluded that encapsulation of the Nafion nanofibers by PPSU prevents Nafion flow during the high temperature annealing step, but it does allow for intersecting Nafion fibers to weld.

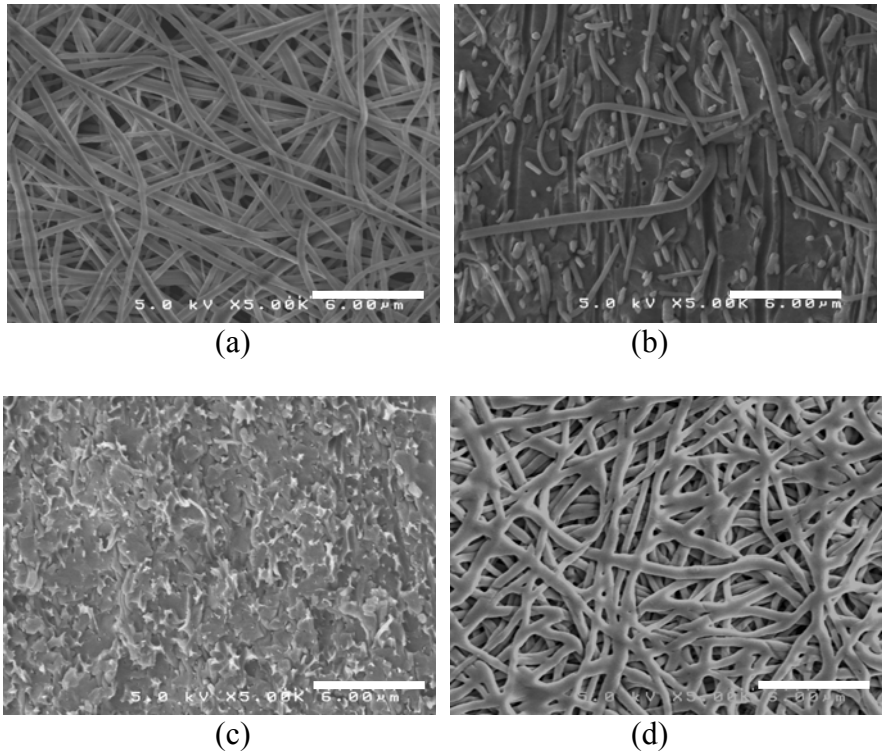

(a) (b)

(c) (d)

Figure 4.4. SEM micrographs of a) an electrospun dual nanofiber mat surface (fibers are visually indistinguishable but are composed of either PPSU or Nafion), b) freeze-fractured cross-section of a Nafion film reinforced by a PPSU nanofiber network, c) freeze-fractured cross-section of a membrane with Nafion nanofiber embedded in PPSU, and d) surface of the Nafion nanofiber structure membrane after removal of all PPSU (by soaking in liquid chloroform). Scale bars are 6 μm.

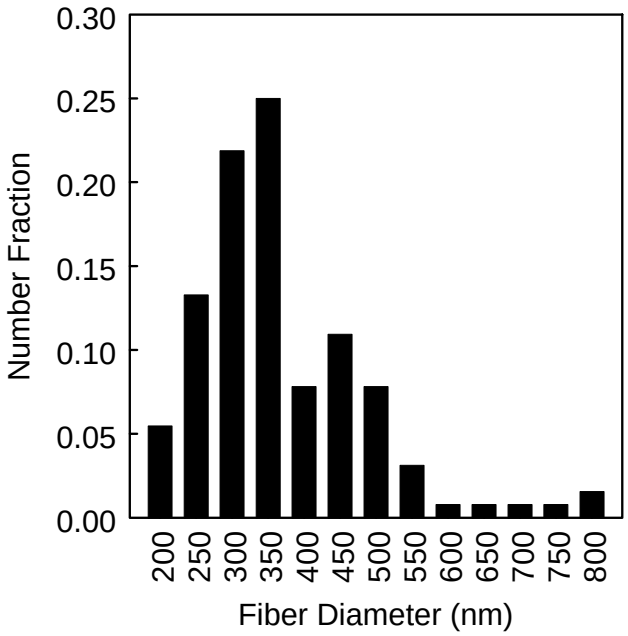

Figure 4.5. Representative histogram of fiber diameter distribution for an electrospun dual-fiber mat.

Cross-sectional SEMs of electrospun composite membranes are compared to a solution-cast composite membrane in Figure 4.6. Each membrane in Figure 4.6 is ~70 wt% Nafion and 30 wt% PPSU. During dual-fiber electrospinning Nafion and PPSU mix in the dry state with a much lower domain size (~500 nm diameter fibers) than in a solution-cast film (where there are PPSU discs with a ~5 μm diameters). The solution-cast membrane was cast at 70^{o}C from a 15 wt% clear/transparent polymer solution in dimethylacetamide solvent

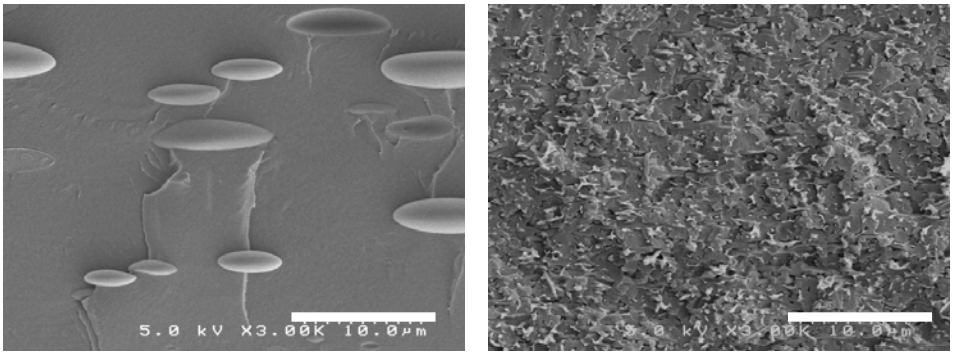

(a) (b)

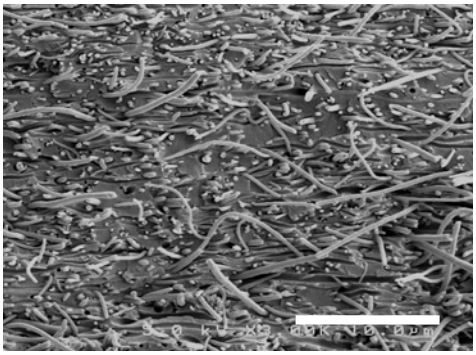

(c)

Figure 4.6. (a) Cross-section of a solution-cast Nafion/PPSU composite membrane compared to (b) an electrospun film with Nafion fibers encapsulated in PPSU and (c) an electrospun membrane with a Nafion film being reinforced by PPSU fibers. Each membrane is ~70 wt% Nafion. The solution-cast membrane was cast at 70°C from a 15 wt% clear/transparent polymer solution in dimethylacetamide solvent. Cross-sections were obtained by freeze-fracturing. Scale bars are 10 μm.

4.3.2 Reproducibility of electrospinning experiments and nanofiber membranes

Electrospun nanofiber composite membranes were found to have variations in polymer composition from membrane to membrane. For a given set of electrospinning flow rates, there is typically a ±5% difference in the resulting membranes' average Nafion volume fraction, as shown in Table 4.1. This variability is primarily attributed to differences in the amount of electrospun fibers deposited on the collecting drum (on-the-drum) as compared to the amount of fibers deposited on other portions of the electrospinning apparatus (off-the-drum, e.g., the motor that rotates the collecting drum).

For some experiments, a greater proportion of fibers are collected on-the-drum versus off-the-drum; thus the membranes' average Nafion volume fraction changes between experiments. The reason for the variation in on-the-drum versus off-the-drum fiber deposition is not well understood at this time and requires further investigation.

Table 4.1. Variation in Nafion volume fraction for a given set of electrospinning flow rates. The volume fraction is determined after processing an electrospun dual-fiber mat into a dense membrane. Nafion was electrospun form 20 wt% solutions and PPSU was electrospun from 25 wt% solutions.

	Nafion flow rate (mL/hr)	**PPSU flow rate (mL/hr)**	**Final membrane's average Nafion volume fraction**
Experiment 1	.20	.04	0.53
Experiment 2	.20	.04	0.58
Experiment 3	.20	.04	0.65
Experiment 4	.20	.04	0.56
Experiment 5	.20	.04	0.62

In addition to variations in the average/global Nafion volume fraction between separate membranes that was discussed above, there are less pronounced compositional and thickness variations within a single electrospun membrane. Figure 4.7 shows a representation of how membrane composition varies across a given membrane (as determined by later proton conductivity and ion-exchange capacity experiments). Figure 4.8 shows a representation how the thickness varies across a dry electrospun membrane. This variability is largely attributed to the lab-scale electrospinning unit using only two syringes, i.e., nanofibers immerge from a point source to cover a relatively large area, thus less material reaches the edges of the electrospinning deposition area/collecting drum. Additionally, the oscillation of the collecting drum is driven by a rotatory motor

and fly wheel (see Figure 4.3) and thus the drum's linear velocity is not constant as it oscillates back and forth.

When membrane composition and thickness are reported in this dissertation, the average/global composition and thickness is given.

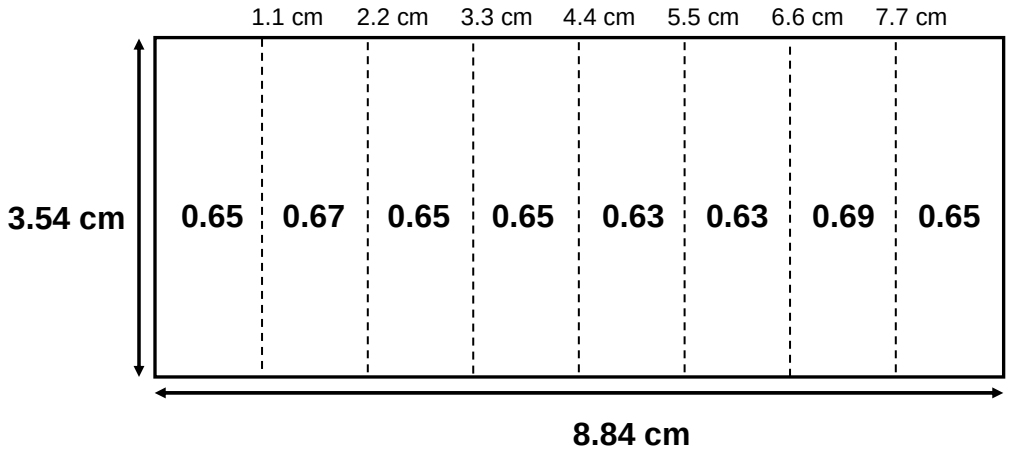

Figure 4.7. Example composition distribution for a nanofiber composite membrane. Compositions are given as Nafion volume fractions. The membrane's length is 3.54 cm, the width the 8.84 cm (in the wet state).

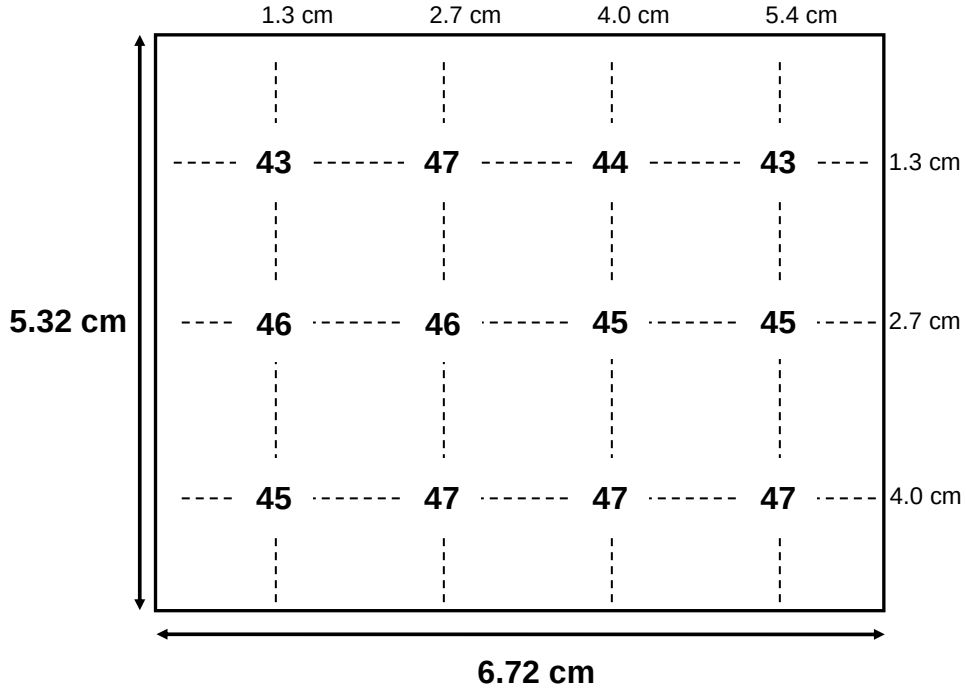

Figure 4.8. Example dry thickness distribution for a dry nanofiber composite membrane. The thickness measurements are given in microns and were measured with a Mitutoyo micrometer (No. 227-211). The membrane's length is 5.32 cm, the width is 6.72 cm.

4.3.3 Membrane properties

The in-plane proton conductivity of membrane samples for the two Nafion/PPSU composite structures in room temperature water is shown in Figure 4.9 as a function of Nafion volume fraction. There is no significant difference in conductivity between the two membrane morphologies, with proton conductivity being solely a function of the volume fraction of Nafion in the membrane (i.e., conductivity varies linearly with Nafion volume fraction, as shown by the straight line in Figure 4.9). Extrapolation of the linear data to a fiber volume fraction of 1.0 gives a proton conductivity identical to that of bulk Nafion (0.095 S/cm). The results in Figure 4.9 differ significantly from data in reference 30 where the authors report conductivities of a non-annealed electrospun Nafion fiber at 30^{o}C and 90% relative humidity that were unusually high (>1 S/cm) for small fibers

(<300 nm diameter) and anomalously low (0.025 S/cm) for larger fibers (5 μm diameter).[30] In Figure 4.9, the membrane conductivity for the two different Nafion/PPSU morphologies obey the same Nafion volume fraction mixing rule (with zero conductivity for PPSU), as has been reported for other nanofiber composite fuel cell membranes.[18-22] Also, there is no percolation threshold for conductivity at low Nafion volume fractions; composite films with as little as 9 vol% Nafion fit the linear straight line conductivity correlation. This is well below the 16-30 vol% ionomer percolation minimum for composite membranes fabricated by traditional blending methods.[31, 32] Furthermore, the proton conductivities of the nanofiber composite films are much higher than those reported for Nafion/PVDF solution cast blends. For example, a solution-cast Nafion/PVDF film with 80 wt% Nafion was found to have a conductivity of 0.012 S/cm in water at 25^{o}C (23% the measured conductivity for a neat Nafion film), whereas a nanofiber composite of similar Nafion content has a conductivity of 0.070 S/cm, or 70% that of neat Nafion. (Note that nanofiber composite membranes that are ~80 wt% Nafion are ~70 vol% Nafion due to differences in Nafion's and PPSU's density).

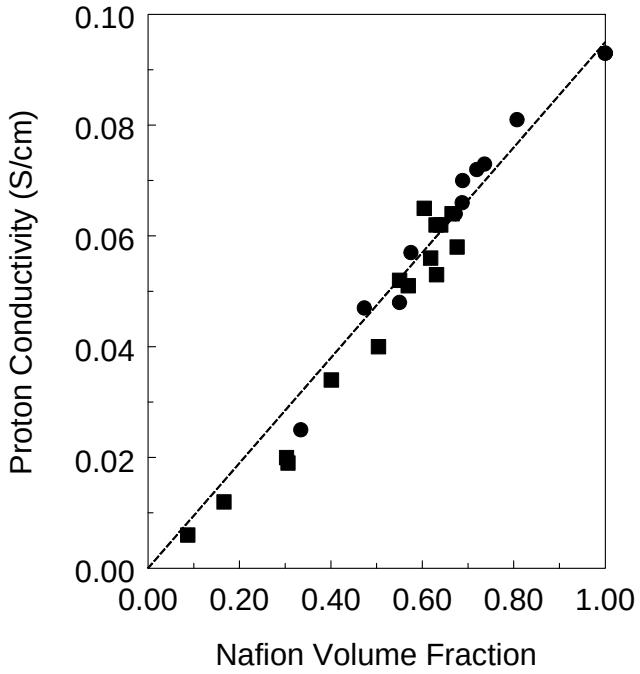

Figure 4.9. In-plane proton conductivity of nanofiber composite membranes as a function of Nafion volume fraction. Conductivity was measured in liquid water at room temperature. (■) Nafion nanofibers embedded in PPSU, (●) Nafion reinforced by PPSU nanofibers. Dashed line represents a simple volume fraction mixing rule (with zero ionic conductivity for PPSU) and Nafion 212 conductivity for a Nafion volume fraction of 1.0.

Volumetric and gravimetric water swelling of the two Nafion/PPSU composite membrane structures is shown in Figure 4.10 as a function of Nafion volume fraction. As was the case for proton conductivity, there is no obvious difference in swelling for the two different membrane structures (Nafion nanofibers embedded in PPSU and Nafion reinforced by a PPSU nanofiber network). However, the swelling is lower than would be predicted by a simple Nafion volume fraction mixing rule below 70 vol% Nafion (but not so low as to adversely affect proton conductivity) because the presence of PPSU causes the Nafion component to swell less in the composite films (this has been observed in other Nafion blended membranes).[31] For example, a membrane with 50 vol% Nafion has a λ (moles of water per mole of sulfonic acid sites in Nafion) of 19 as compared to 21.5

for commercial Nafion 212. The low water content of the composite membranes in Figure 4.10 is an important finding in terms of future applications of the membrane fabrication method with very high ion-exchange capacity (IEC) ionomer polymers that swell excessively in water.

In-plane (areal) water swelling of the two nanofiber composite membranes is shown in Figure 4.11 for films of different Nafion volume fraction. Unlike conductivity and volumetric/mass swelling, the in-plane swelling for the two membrane morphologies differ substantially, with Nafion films reinforced by PPSU nanofibers swelling less for a wide range of Nafion volume fractions. The swelling difference is attributed to differences in PPSU connectivity for the two membrane structures. A membrane with Nafion fibers embedded in PPSU has strong interconnectivity in three dimensions, with more isotropic water swelling. When PPSU is in the fiber form, there is minimal PPSU connectivity in the membrane thickness direction (the PPSU nanofibers were never welded to create a 3-D interconnecting network), with stronger connectivity for the in-plane direction (due to the presence of closed-form cells created by the PPSU fiber network). Thus, there is more membrane swelling in the thickness direction for membranes with reinforcing PPSU nanofibers, as compared to the inverse structure. For example, a membrane with 60 vol% Nafion had a thickness swelling of 29% for the Nafion film reinforced by PPSU nanofibers, but only 18% for the membrane with Nafion fibers embedded in PPSU. It should be noted that the in-plane swelling of both composite membrane morphologies was lower than that of neat Nafion (37% in-plane swelling for Nafion 212) and lower than that of a hypothetical PPSU/Nafion composite film based on a simple Nafion volume fraction mixing rule. The swelling properties of

the Nafion/PPSU nanofiber membranes compare favorably with other composite membranes found in the literature. A Nafion film reinforced by PPSU nanofibers had ~0.080 S/cm conductivity (in room temperature water) and an in-plane swelling of 8%, compared to 15% for a film of similar conductivity, as report by Lee and co-workers for a Nafion nanofiber mat impregnated with Norland Optical Adhesive 63.[22] Similarly, a GORE-SELECT membrane with a conductivity similar to that of Nafion 212 has a reported in-plane water swelling of ~31% in 100°C water.[33] Under similar experimental conditions, the Nafion film reinforced by PPSU fibers exhibited 73% lower in-plane swelling with a small (20%) loss in proton conductivity relative to the GORE-SELECT film (the loss in proton conductivity can be offset by simply making the membrane 20% thinner; changing membrane thickness will not alter in-plane swelling).

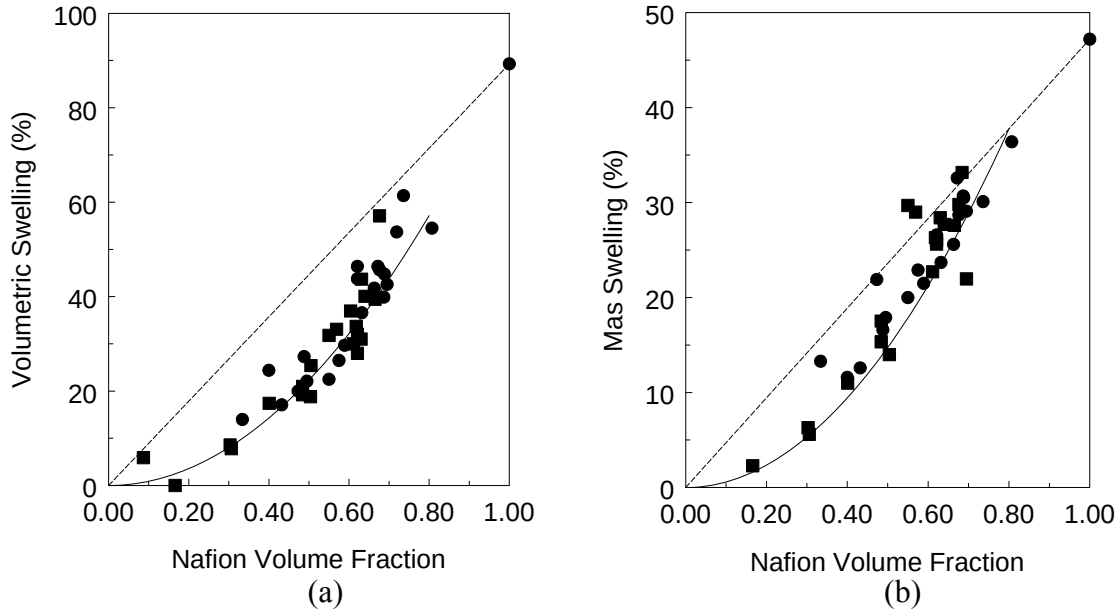

Figure 4.10. Water swelling of nanofiber composite membranes as a function of Nafion volume fraction at 100°C. (a) Volumetric swelling, (b) mass swelling. (■) Nafion nanofibers embedded in PPSU, (●) Nafion reinforced by PPSU nanofibers.

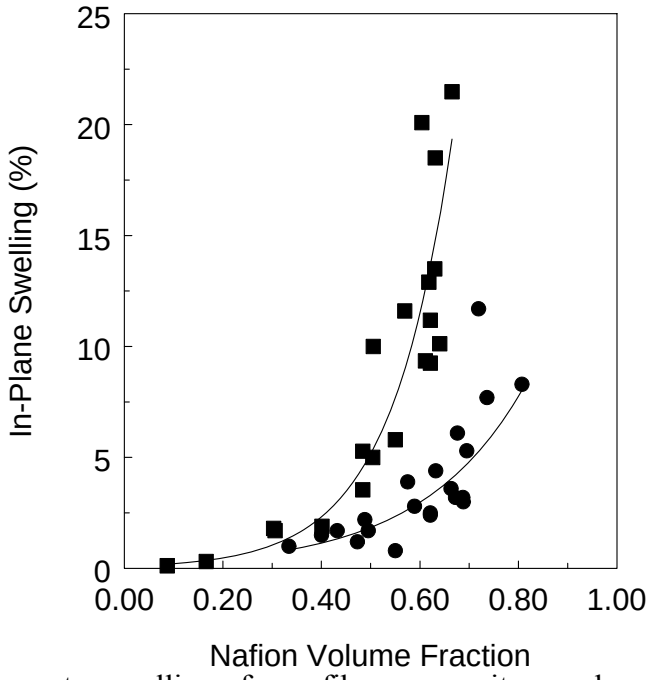

Figure 4.11. In-plane water swelling of nanofiber composite membranes as a function of Nafion volume fraction. Swelling was measured in 100°C water. (■) Nafion nanofibers embedded in PPSU, (●) Nafion reinforced by PPSU fibers.

PPSU has excellent mechanical properties and its presence improved the overall mechanical properties of the nanofiber composite membranes, as compared to commercial Nafion films. Typical stress-strain curves for the two nanofiber composite membrane structures and for Nafion 212 are shown in Figure 4.12. Mechanical properties (Young's modulus and the proportional limit stress, abbreviated as PLS) are summarized in Table 4.2. PLS is a measure of yield strength which is useful for characterizing materials such as Nafion that do not undergo a clear transition from elastic to plastic deformation; PLS is determined by extrapolating lines tangent to the low- and high-strain regions of a stress-strain curve,[34] as shown in Figure 4.12. As can be seen, the nanofiber composite membranes have a higher modulus and proportional limit stress than Nafion 212 and the mechanical properties improve as the volume fraction of PPSU in the

composite membrane increases. For all Nafion volume fractions tested, the membranes with Nafion nanofibers embedded in PPSU exhibited superior mechanical properties as compared to the inverse morphology. This is attributed to the greater connectivity of PPSU when it is the matrix material, surrounding Nafion nanofibers in a membrane, as opposed to having PPSU in the fiber form as a reinforcing non-woven network.

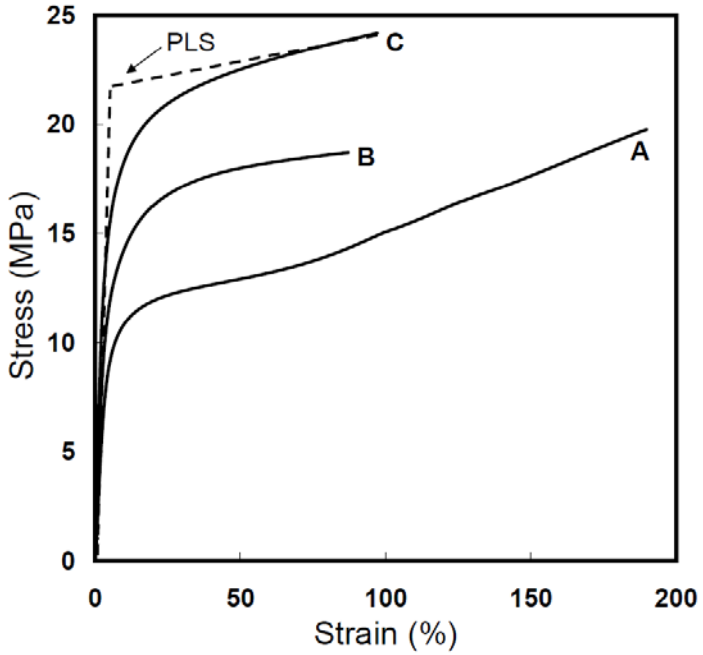

Figure 4.12. Stress-strain curves for Nafion 212 and nanofiber composite membranes. Stress-strain curves were measured at 30°C and ~20% RH. (a) Nafion 212, (b) Nafion reinforced by PPSU nanofibers (61 vol% Nafion), (c) Nafion nanofibers embedded in PPSU (61 vol% Nafion).

Table 4.2. Young's modulus and proportional limit stress (PLS) for nanofiber composite membranes of different Nafion volume fractions.

	Nafion Nanofibers Embedded in PPSU		Nafion Reinforced by PPSU Nanofibers	
Nanofiber Composite	**Young's Modulus (MPa)**	**PLS (MPA)**	**Young's Modulus (MPa)**	**PLS (MPA)**
61 vol% Nafion	566	21.1	444	15.9
48 vol% Nafion	733	24.6	601	22.3
39 vol% Nafion	852	29.2	624	23.4
Neat Membrane	**Young's Modulus (MPa)**		**PLS (MPa)**	
Nafion 212	294		11.9	
Polyphenylsulfone film	1057		64.3	

Uncharged/hydrophobic polymers other than PPSU were also investigated as reinforcing materials for dual-fiber composite membranes. Specifically, either poly(vinylidene fluoride) (PVDF) or poly-[(1-(4,4′-diphenylether)-5-oxybenzimidazole)-benzimidazole (PBI-OO) fibers were used to reinforce Nafion films, though such membranes did not perform as well as PPSU-reinforced Nafion. Further descriptions of membrane fabrication and material properties are given in Appendix B for Nafion/PVDF and Nafion/PBI-OO nanofiber composites.

4.3.4 Fuel cell performance

The low in-plane swelling of a Nafion film reinforced by PPSU nanofibers should translate into improved membrane-electrode-assembly (MEA) durability in a hydrogen/air fuel cell. To test this hypothesis, fuel cell data were collected for such a film containing 65 vol% Nafion. At this Nafion volume fraction, the membrane had a conductivity of 0.066 S/cm in water (at 25^{o}C) and an in-plane swelling of 6% in 100^{o}C water. The composite film was fabricated into a MEA by attachment of Pt/C catalytic

powder electrodes using a standard decal technique (see section 4.2.8). Voltage vs. current density fuel cell performance curves are shown in Figure 4.13a for a 30 μm PPSU/Nafion membrane and a commercial Nafion 212 film (51 μm dry thickness) at 80°C for two different feed gas humidification levels. The area-specific resistance of the Nafion 212 and nanofiber composite membranes is approximately the same (the composite membrane has 65% of the conductivity and 60% of the thickness) and the fuel cell power output (voltage multiplied by current density) is essentially identical for the two MEAs. The high open circuit voltage and low gas crossover (<2 mA/cm^2) for the composite membrane MEA indicates a membrane free of pin-holes and defects.

Membrane durability for the Nafion-film reinforced by PPSU fibers was evaluated by an open circuit voltage (OCV) humidity cycling experiment at 80°C with repeated cycling of 2 minutes 100% relative humidity (RH) hydrogen gas and air and then 2 minutes 0% RH hydrogen and air. This OCV experiment was used to evaluate the membrane for both mechanical durability (the membrane undergoes stresses from swelling and shrinking when the gases cycle between wet and dry) and chemical durability (the diffusion of hydrogen and oxygen into the membrane can result in the formation of harmful peroxides which can degrade Nafion for both the neat membrane and nanofiber composite).[35] In the present study, only OCV and hydrogen gas crossover were monitored during humidity cycling; there was no attempt to quantify any membrane chemical degradation with time by measuring, for example, fluoride release rates. The change in OCV (during the wet cycle) vs. time is shown in Figure 4.13b. Failure criteria for this test is defined as a drop in OCV (for a fully humidified MEA) below 0.8 V. As can be seen, the nanofiber composite membrane failed after 842 hours vs. 546 hours for

Nafion 212 (a 54% improvement in membrane durability). Additionally, the hydrogen limiting current (measured in-situ at 100% RH) dramatically increased at membrane failure (increasing from <2 mA/cm2 at the beginning of the test to over 13 mA/cm^2 at failure, see Table 4.3).

Additional fuel cell studies on nanofiber membranes are reported in Appendix C. Most notably, further durability studies were conducted by General Motors. Similarly to the accelerated durability test described above, humidified and dry gases were alternately supplied to the fuel cell in two minute intervals while at 80^{o}C. General Motors' accelerated durability experiment indicated an 87% improvement for a Nafion film reinforced by PPSU fibers when compared to Nafion 211.

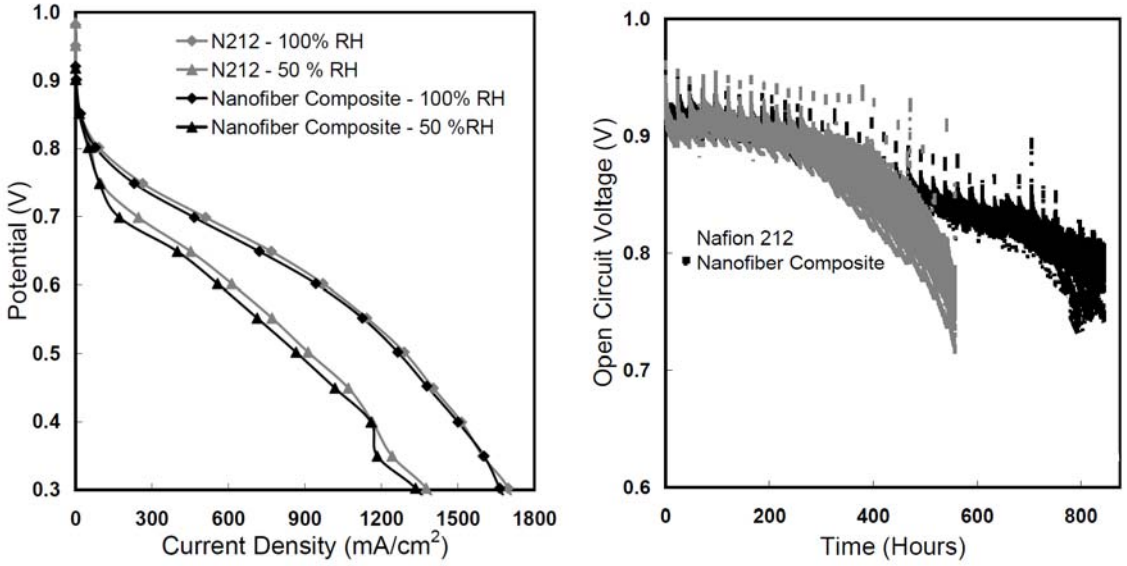

(a) (b)

Figure 4.13. (a) Fuel cell polarization and (b) accelerated durability tests. The nanofiber composite membrane (with Nafion reinforced by PPSU nanofibers) was ~65 vol% Nafion and 31 μm thick for all fuel cell testing.

Table 4.3. Limiting current of Nafion 212 and nanofiber composite membranes during durability cycling.

Time (hours)	Limiting Current - Nafion 212 (mA/cm^2)	Limiting Current - Nanofiber Composite (mA/cm^2)
0	1.5	1.9
515	>13	5.2
845	n/a	>13

4.4 Conclusions

A new approach to the design and fabrication of composite ion-exchange membranes has been presented. Nanofiber mats of two dissimilar polymers (Nafion perfluorosulfonic acid polymer and polyphenylsulfone) were simultaneously and separately electrospun into the same mat and then the resulting dual fiber web was processed into two different defect-free dense film morphologies: (1) a Nafion film reinforced by polyphenylsulfone nanofibers and (2) an interconnecting nanofiber mat of Nafion embedded in polyphenylsulfone. The procedures for converting a dual-fiber mat into either of the two membrane morphologies are simple and straightforward. Both membrane structures exhibited similar volumetric/gravimetric water swelling and proton conductivity, where the in-plane conductivity scaled linearly with Nafion volume fraction and the swelling was less than expected based on the relative amounts of Nafion and polyphenylsulfone. Compared to other fuel cell membranes, the nanofiber composite membranes exhibited very low in-plane water swelling and better mechanical properties, which translated into improved membrane/MEA longevity in a hydrogen/air open circuit voltage humidity cycling durability test with no loss in power production as compared to a Nafion 212 membrane. The in-plane liquid water swelling of membranes with Nafion reinforced by a polyphenylsulfone nanofiber network was always less than that of the

inverse structure. On the other hand, the mechanical properties of membranes with Nafion nanofibers embedded in polyphenylsulfone were superior to membranes with the opposite structure.

The impregnation-free dual-fiber electrospinning approach to composite membrane design can be expanded to produce composite films with any two polymers that are: (i) electrospin-able and ii) have sufficient differences in solubility and/or thermal properties so as to allow for one component to soften, flow, and fill the interfiber void volume of the other. Additionally, one can fabricate a composite membrane for non-fuel-cell applications, e.g., as separators in electrochemical reactors, for sensors, and in industrial electrodialysis separations. Also, it is entirely possible to fabricate nanofiber composite membranes with three or more different fiber compositions, e.g., one charged polymer for normal fuel cell operating temperatures, and a second nanofiber for low (sub-zero) fuel cell operation, and a third polymer fiber for membrane reinforcement.

Chapters V-VII will build on the dual-fiber membrane platform described in Chapter IV to further investigate the effect of processing conditions (Chapter V), replace Nafion with a more conductive, high IEC polymer (Chapter VI), and to prepare multi-layered membranes with applications in direct methanol fuel cells (Chapter VII).

4.5 References

(1) Grot, W. G.; Rajendran, G. US Patent 5919583, 1999.

(2) Huang, X. Y.; Solasi, R.; Zou, Y.; Feshler, M.; Reifsnider, K.; Condit, D.; Burlatsky, S.; Madden, T., *Journal of Polymer Science Part B-Polymer Physics* **2006,** 44, (16), 2346-2357.

(3) Tang, H.; Peikang, S.; Jiang, S. P.; Wang, F.; Pan, M., *Journal of Power Sources* **2007,** 170, (1), 85-92.

(4) Wu, J.; Yuan, X. Z.; Martin, J. J.; Wang, H.; Zhang, J.; Shen, J.; Wu, S.; Merida, W., *Journal of Power Sources* **2008,** 184, (1), 104-119.

(5) Kusoglu, A.; Karlsson, A. M.; Santare, M. H.; Cleghorn, S.; Johnson, W. B., *Journal of Power Sources* **2006,** 161, (2), 987-996.

(6) Patil, Y. P.; Jarrett, W. L.; Mauritz, K. A., *Journal of Membrane Science* In Press, Corrected Proof.

(7) Bauer, F.; Denneler, S.; Willert-Porada, M., *Journal of Polymer Science Part B: Polymer Physics* **2005,** 43, (7), 786-795.

(8) Kundu, S.; Simon, L. C.; Fowler, M.; Grot, S., *Polymer* **2005,** 46, (25), 11707-11715.

(9) Kusoglu, A.; Karlsson, A. M.; Santare, M. H.; Cleghorn, S.; Johnson, W. B., *Journal of Power Sources* **2007,** 170, (2), 345-358.

(10) Sethuraman, V. A.; Weidner, J. W.; Haug, A. T.; Protsailo, L. V., *Journal of the Electrochemical Society* **2008,** 155, (2), B119-B124.

(11) Kerres, J. A., *Fuel Cells* **2005,** 5, (2), 230-247.

(12) Kyu, T.; Yang, J. C., *Macromolecules* **1990,** 23, (1), 176-182.

(13) Landis, F. A.; Moore, R. B., *Macromolecules* **2000,** 33, (16), 6031-6041.

(14) Taylor, E. P.; Landis, F. A.; Page, K. A.; Moore, R. B., *Polymer* **2006,** 47, (21), 7425-7435.

(15) Yang, J. C.; Kyu, T., *Macromolecules* **1990,** 23, (1), 182-186.

(16) Song, M.-K.; Kim, Y.-T.; Fenton, J. M.; Kunz, H. R.; Rhee, H.-W., *Journal of Power Sources* **2003,** 117, (1-2), 14-21.

(17) Kolde, J. A.; Bahar, B.; Wilson, M. S.; Zawodzinski, T. A.; Gottesfeld, S., *Electrochemical Society Proceedings* **1995,** 95-23, 193-201.

(18) Choi, J.; Lee, K. M.; Wycisk, R.; Pintauro, P. N.; Mather, P. T., *Macromolecules* **2008,** 41, (13), 4569-4572.

(19) Choi, J.; Lee, K. M.; Wycisk, R.; Pintauro, P. N.; Mather, P. T., *Journal of the Electrochemical Society* **2010,** 157, (6), B914-B919.

(20) Choi, J.; Lee, K. M.; Wycisk, R.; Pintauro, P. N.; Mather, P. T., *Journal of Materials Chemistry* **2010,** 20, (30), 6282-6290.

(21) Choi, J.; Wycisk, R.; Zhang, W. J.; Pintauro, P. N.; Lee, K. M.; Mather, P. T., *ChemSusChem* **2010,** 3, (11), 1245-1248.

(22) Lee, K. M.; Choi, J.; Wycisk, R.; Pintauro, P. N.; Mather, P., *ECS Transactions* **2009,** 25, (1), 1451-1458.

(23) Muldoon, J.; Lin, J.; Wycisk, R.; Takeuchi, N.; Hamaguchi, H.; Saito, T.; Hase, K.; Stewart, F. F.; Pintauro, P. N., *Fuel Cells* **2009,** 9, (5), 518-521.

(24) Chen, H.; Snyder, J. D.; Elabd, Y. A., *Macromolecules* **2008,** 41, (1), 128-135.

(25) Laforgue, A.; Robitaille, L.; Mokrini, A.; Ajji, A., *Macromolecular Materials and Engineering* **2007,** 292, (12), 1229-1236.

(26) Zhou, C. S.; Liu, Z.; Dai, J. Y.; Xiao, D., *Analyst* **2010,** 135, (5), 1004-1009.

(27) Ballengee, J. B.; Pintauro, P. N., *Journal of the Electrochemical Society* **2011,** 158, (5), B568-B572.

(28) Osborn, S. J.; Hassan, M. K.; Divoux, G. M.; Rhoades, D. W.; Mauritz, K. A.; Moore, R. B., *Macromolecules* **2007,** 40, (10), 3886-3890.

(29) Page, K. A.; Landis, F. A.; Phillips, A. K.; Moore, R. B., *Macromolecules* **2006,** 39, (11), 3939-3946.

(30) Dong, B.; Gwee, L.; Salas-de la Cruz, D.; Winey, K. I.; Elabd, Y. A., *Nano Letters* **2010,** 10, (9), 3785-3790.

(31) Lin, J.; Lee, J. K.; Kellner, M.; Wycisk, R.; Pintauro, P. N., *Journal of the Electrochemical Society* **2006,** 153, (7), A1325-A1331.

(32) McLachlan, D. S.; Blaszkiewicz, M.; Newnham, R., *Journal of the American Ceramic Society* **1990,** 73, (8), 2187-2203.

(33) Cleghorn, S.; Kolde, J.; Liu, W., Catalyst Coated Composite Membranes. In *Handbook of Fuel Cells - Fundamentals, Technology and Applications*, Vielstich, W.; Lamm, A.; Gasteiger, H. A., Eds. John Wiley & Sons, Ltd: Chichester, 2003; Vol. 3, pp 566-575.

(34) Tang, Y. L.; Karlsson, A. M.; Santare, M. H.; Gilbert, M.; Cleghorn, S.; Johnson, W. B., *Materials Science and Engineering a-Structural Materials Properties Microstructure and Processing* **2006,** 425, (1-2), 297-304.

(35) de Bruijn, F. A.; Dam, V. A. T.; Janssen, G. J. M., *Fuel Cells* **2008,** 8, (1), 3-22.

CHAPTER V

EFFECT OF DUAL-FIBER MAT PROCESSING CONDITIONS ON FINAL MEMBRANE PROPERTIES

5.1 Introduction

Electrospun nanofiber composite proton exchange membranes (PEMs) are a promising alternative to traditional polymer blends, phase-separated block copolymers, and pore-filled (impregnated) films. Thus far, two PEM morphologies have been fabricated and investigated: (1) an uncharged polymer surrounding a 3D interconnected mat of ionomer nanofibers or (2) an ionomer surrounding an electrospun mat of uncharged polymer nanofibers. Electrospun PEMs offer a high degree of compositional and morphological control in that the volume fraction and diameter of the charged or uncharged polymer fibers can be independently fixed. Additionally, electrospun membranes can be made via solid-state "forced-assembly" of nanofibers on a collector surface, as opposed to self-assembly in solution, thus circumventing problems of phase-separation and poor dispersion leading to large (micron) size domains of the minor blend component. Nanofiber composite membranes have exhibited impressive proton conductivity, water swelling, and mechanical properties, e.g., a proton conductivity near 0.10 S/cm at 120^{o}C and 50% relative humidity.[1] In a different study (Chapter IV), nanofiber PEMs were significantly more durable than Nafion® 212 during an accelerated humidity/temperature fuel cell cycling test.[2]

The preparation method for nanofiber composite membranes has evolved over time, as described in a series of papers by Pintauro and co-workers. In early

experiments,[1,3-5] membranes were prepared by: (i) electrospinning a nanofiber mat of sulfonated poly(arylene ether sulfone) or perfluorosulfonic acid (PFSA) ionomer with/without sulfonated molecular silica (to add additional fixed charge sites to the membrane), (ii) compacting the mat to increase the volume fraction of ionomer fibers, (iii) welding ionomer fibers at intersection points to create a 3D interconnected network, (iv) impregnating into the interfiber void space Norland Optical Adhesive 63 (NOA 63), a solventless polyurethane prepolymer which was subsequently UV crosslinked into a dense and tough matrix, and (v) soaking the final membrane in 1 M H_2SO_4 and water.

To simplify the membrane fabrication procedure and to eliminate the NOA impregnation step, a new dual nanofiber processing scheme for preparing fuel cell PEMs was introduced in Chapter IV and in Reference 2. Membranes were made by separately and simultaneously electrospinning two polymers (charged Nafion polymer and uncharged polyphenylsulfone, hereafter abbreviated as PPSU) from separate syringes. The resulting dual fiber mat was then processed in two different ways to produce two distinct membrane structures: (i) Nafion nanofibers encapsulated by PPSU and (ii) Nafion polymer surrounding PPSU fibers (where the PPSU mat acts as a nonwoven reinforcing mesh). For the first structure, the processing steps are: mechanical mat compaction, chloroform vapor exposure, thermal annealing of Nafion, and acid/water washings. For the second type of membrane, the processing steps are mat compaction with heating, thermal annealing of Nafion, and acid/water washings. The total time for such processing steps as reported previously was ca. 4-5 hours.[2] The dual fiber technique offers several advantages over the original electrospinning membrane fabrication method, namely the elimination of a separate impregnation step (where complete void space

filling is often problematic), the choice of making two distinct structures from the same initial dual fiber mat, the possibility of expanding the number of polymers that are spun simultaneously to three or more in order to add other properties to the membranes, and the ability to control the spatial distribution of charged and uncharged polymers in the membrane thickness direction (i.e., by changing the relative flow rates of charged and uncharged polymers during electrospinning, mats with a layered or gradient compositional morphology can be created).

While the dual-fiber electrospinning technique is a robust platform for the fabrication of a wide variety of membrane structures, fiber mat processing (the conversion of a highly porous dual fiber mat into a dense and defect-free membrane) is poorly understood. In the present Chapter I report on an examination of the various processing steps required for transforming a dual fiber electrospun mat into a functional PEM, where the initial mat is composed of Nafion perfluorosulfonic acid and polyphenylsulfone nanofibers. The rationale for such a study was two-fold: (i) I sought to decrease the overall time required to process a dual fiber mat into a PEM, and (ii) I sought to better understand the effects of post-electrospinning processing conditions on the final membrane properties. I focused my attention on thermal annealing of Nafion, void-space filling by either Nafion or PPSU fibers, and the acid/water washing step. The effectiveness of each step was assessed by measuring relevant fuel cell membrane properties, e.g., proton conductivity, water swelling, mechanical strength, and hydrogen crossover.

5.2 Experimental

5.2.1 Membrane fabrication

Dual-fiber mats of 1100 EW Nafion (LIQUION 1115 from Ion Power, Inc.) and PPSU (Radel® polymer from Solvay Advanced Polymers, with a molecular weight of 63 kDa) were electrospun from separate syringes, as described in Chapter IV. Nafion was always co-spun with poly(ethylene oxide) carrier (400 kDa, from Sigma-Aldrich) at a 99:1 wt. ratio, using n-propanol/water solvent. Mats contained between 55 and 70 vol% ionomer, where the average diameter of the Nafion and PPSU fibers was essentially the same and typically 400-500 nm. The mats were processed into two distinct membrane structures: (i) Nafion films reinforced by PPSU fibers and (ii) Nafion fibers encapsulated by PPSU.

5.2.2 Membrane fabrication: Nafion reinforced by PPSU fibers

Fiber mats were compressed for 10 seconds at 127^{o}C and 15,000 psi using a Carver heated press (Model 3851-0). Each mat was compacted 4 times, after rotating 90^{o} between presses to ensure even compression. The samples were then annealed in vacuum, where the annealing time was varied systematically from 5 to 120 minutes and the annealing temperature ranged from 130^{o}C to 250^{o}C. During hot pressing and annealing, Nafion flowed into the void space between PPSU nanofibers to create a fully dense membrane structure. Ionomer flow is attributed to plasticization of Nafion above its α-transition temperature (~100^{o}C).[6,7] After densification/annealing, membranes were boiled in 1 M H_2SO_4 and then in H_2O for times ranging from 1 to 60 minutes for each soaking step; acid/water immersion is required to remove PEO carrier and insure that

Nafion fixed charge sites are in the H^+ counterion form. The "base-case" annealing and boiling procedure from previous studies (Chapter IV) was an annealing time of 120 minutes at 150°C followed by a 60 minute soak in boiling 1 M H_2SO_4 followed by soaking for 60 minutes in boiling H_2O.

5.2.3 Membrane fabrication: Nafion fibers encapsulated in PPSU

Mats were compressed at room temperature and 3,500 psi for several seconds to increase the fiber void fraction (samples were compacted four times, with intermittent sample rotation of 90° to ensure even compression). Compacted mats were then exposed to chloroform vapor in a sealed vessel for a specified time between 1.5 and 16 minutes at either 25°C or 50°C to allow the PPSU fibers to soften and flow, thus filling the void space between Nafion nanofibers. After sample drying at 70°C for 1 hour to remove chloroform, the films were annealed and boiled in 1 M H_2SO_4 and H_2O. The "base-case" processing conditions for this membrane morphology (from Chapter IV) were a chloroform vapor treatment of 16 minutes at 25°C, drying at 70°C for 1 hour and at 140°C for 10 minutes, annealing for 120 minutes at 150°C, immersion for 60 minutes in boiling 1 M H_2SO_4, and a 60 minute soak in boiling H_2O.

5.2.4 Proton conductivity

In-plane proton conductivity was measured using the same technique described in Chapter IV, section 4.2.4.

5.2.5 Equilibrium water swelling

Water swelling was determined as discussed in Chapter IV, section 4.2.6.

5.2.6 Proportional limit stress

Stress-strain curves for membranes at 30°C and 20% relative humidity were generated using a TA instruments Q800 Dynamic Mechanical Analyzer (DMA) that was operated in tension mode. The force was ramped at 0.10 N/min until the sample yielded. The proportional limit stress, a measure of yield strength for materials that do not exhibit a clear transition from elastic to plastic deformation, is the intersection point of two extrapolated straight line asymptotes to the actual stress-strain curve for large stresses and as the stress approaches zero.[8]

5.2.7 Scanning electron microscopy and x-ray diffraction

Samples were sputtered with ~5 nm of gold and then imaged using a Hitachi S-4200 scanning electron microscope. Wide angle x-ray diffraction spectra were obtained with a Rigaku diffractometer with nickel filtered CuKα (λ=1.5418 Å) radiation in long-line focus mode. Samples were scanned from 2.5° to 12.5° at a rate of 0.2°/min. Percent cyrstallinity was determined using methods described elsewhere.[9]

5.2.8 Hydrogen crossover flux

Hydrogen crossover was determined by a limiting current experiment in a fuel cell test fixture.[10] Membranes were fabricated into 5 cm^2 membrane-electrode-assemblies (MEAs) using the decal method with Pt/C catalyst powder (Alfa Aesar 42204)

and Nafion binder.[2] Limiting current was measured by linear sweep voltametry (ramping the cell voltage from 0.0 to 0.5 volts) while supplying fully humidified hydrogen to the anode and humidified nitrogen gas to the cathode, each at a flow rate of 200 sccm.

5.3 Results and discussion

5.3.1 Nafion films reinforced by polyphenylsulfone nanofibers

5.3.1.1 Nafion annealing time and temperature

The effect of annealing time on mass swelling and proton conductivity for an annealing temperature of 150^{o}C is shown in Figure 5.1. For these experiments, the PEMs contained ~58 vol% Nafion and all membranes were fully dense, as suggested by membrane density measurements (the density was found to be a simple mixing rule additive function of the volume fraction adjusted densities of Nafion and PPSU). Thus, changes in mass swelling and proton conductivity were associated with the properties of poorly annealed Nafion polymer and not due to the presence of void space imperfections in the membrane. As can be seen, mass swelling dramatically falls from 35% (no annealing) to 31% (five minute anneal) to 19% for annealing times of 15 minutes or longer. Volumetric swelling (not shown) followed a similar trend. In-plane swelling for all samples was ~2% and independent of annealing time. The constancy of in-plane swelling is attributed to the anisotropic nature of the membrane structure. Namely, the PPSU reinforcing fiber mat, which has high in-plane and low through-plane connectivity, favors swelling in the membrane thickness direction and strongly inhibits areal swelling (low areal swelling is particularly desirable for fuel cell membrane applications).[2] Figure 5.1 also shows that conductivity is not strongly dependent on annealing time. All

films adsorbed a sufficient amount of water for proton dissociation and migration through the Nafion phase. Nevertheless, there was a modest (10%) increase in proton conductivity for films that were annealed at 150°C for less than 15 minutes; the specific reason for the conductivity increase is not known.

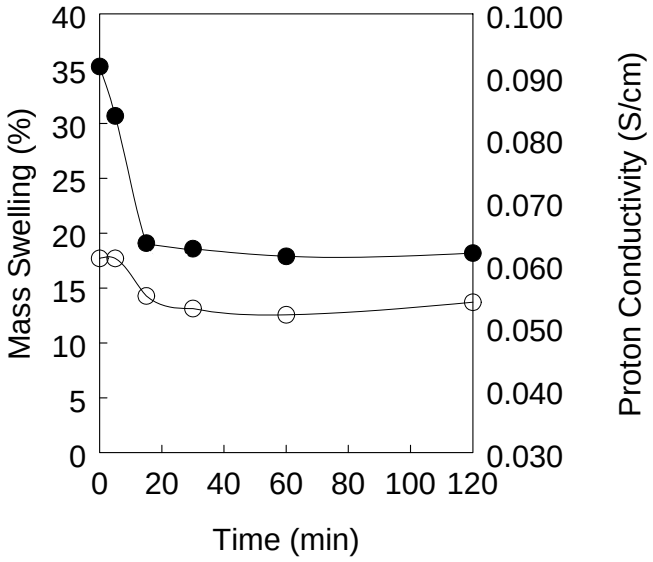

Figure 5.1. Mass swelling and proton conductivity as a function of annealing time at 150°C. (●) mass swelling in 100°C water, (○) proton conductivity at 25°C in liquid water.

The effect of annealing time at 150°C on membrane mechanical properties, as quantified by the proportional limit stress (PLS), is shown in Figure 5.2. A small increase in PLS with annealing time was observed during the first 15 minutes of heating, but all samples (with and without annealing) exhibited excellent mechanical properties, i.e., the PLS of all nanofiber composite films was significantly greater than that for Nafion 212 (a common fuel cell benchmark material with a PLS of 11.1 MPa). The improved mechanical properties of the composite membranes is due to the presence of the reinforcing PPSU mat (the PLS of neat PPSU is 64.3 MPa).[2] Better PEM mechanical

properties can enhance the durability and manufacturability of fuel cell MEAs, thus the high PLS is desirable.[11]

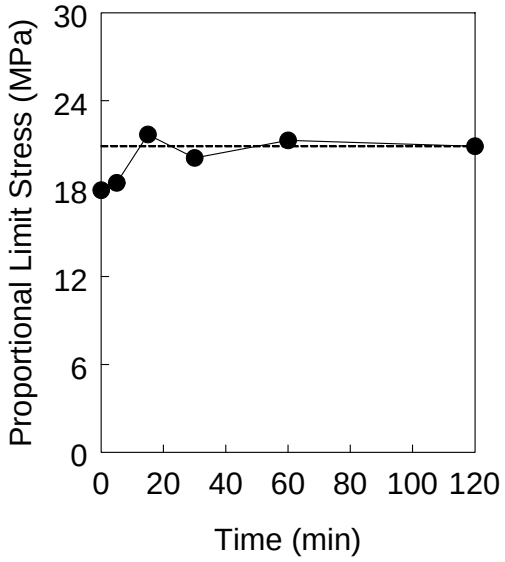

Figure 5.2. Proportional limit stress as a function of annealing time at 150°C. Data points are the average of three tests. The membranes were tested at 30°C and 20% relative humidity. The dashed line represents the proportional limit stress of the "base-case" annealing procedure of 2 hours at 150°C.

The effect of annealing temperature on membrane swelling and conductivity is shown in Figure 5.3a and 5.3b for an annealing time of five minutes. All nanofiber composite membranes in this Figure had a Nafion volume fraction of 65%. When the annealing temperature was increased from 130°C to 210°C, there was a dramatic reduction in mass swelling by liquid water. Annealing at 210°C for five minutes gave the same swelling as a membrane annealed for 120 minutes at 150°C. Proton conductivity, conversely, was essentially constant for all annealing temperatures.

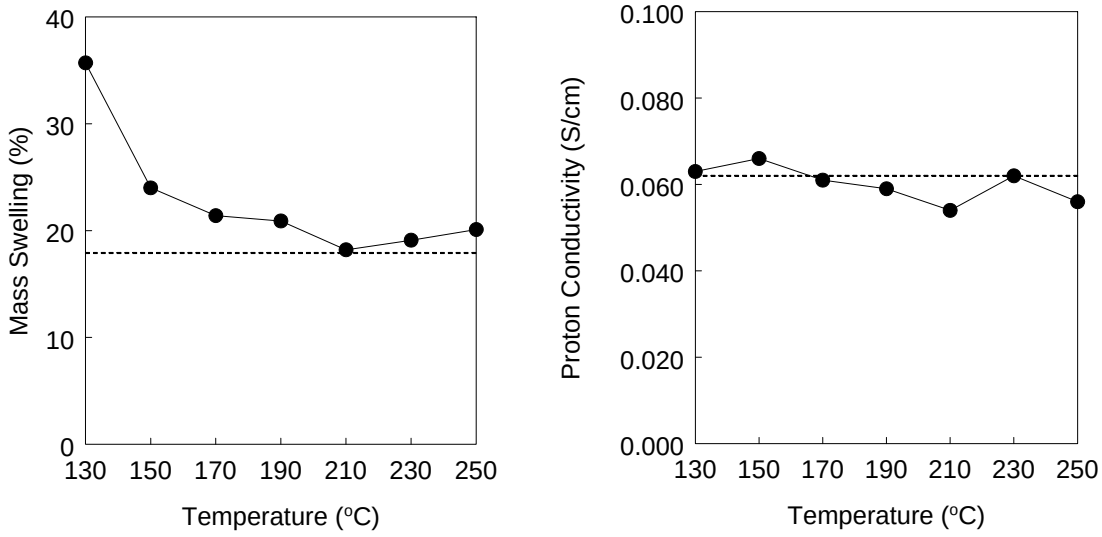

Figure 5.3. (a) Equilibrium mass swelling of liquid water and (b) proton conductivity as a function of annealing temperature. All samples were annealed for five minutes. Dashed lines represent a membrane annealed two hours at 150°C. Mass swelling was measured in 100°C water and proton conductivity measured in liquid water at 25°C.

In-plane membrane swelling is shown as a function of annealing temperature in Figure 5.4 for a 5 minute annealing time. Planar swelling is constant for temperatures between 130°C and 210°C, but increases at 230°C and 250°C. The higher areal swelling at the two highest temperatures is attributed to PPSU fiber-welding above PPSU's glass transition temperature, 220°C.[12] To confirm this hypothesis, a mat consisting of only PPSU fibers was heated to 210°C, 230°C, and 250°C for five minutes. SEMs of the resulting mats (Figure 5.5) indicate no welding at 210°C and interfiber welding at the two higher temperatures. When PPSU welding occurs in a composite membrane, there is 3D connectivity of the PPSU reinforcing fibers which causes water swelling to be more isotropic. The increased planar swelling of films annealed at the two highest temperatures is undesirable because such swelling reduces membrane durability in a fuel cell during on/off (wet/dry) operation.[13,14]

As shown in Figure 5.6, the PLS of composite membrane samples was independent of Nafion annealing temperature for an annealing time of 5 minutes, with a value between that of neat PPSU (64.3 MPa) and neat Nafion (11.1 MPa)**.** The constancy in PLS, even at high annealing temperatures when PPSU fibers weld together, indicates that the welds are not enhancing mechanical strength. The results in Figures 5.4-6, when taken together, strongly suggest that interfiber welds of the reinforcing PPSU mat are not desirable for optimum functioning of a PEM in a fuel cell.

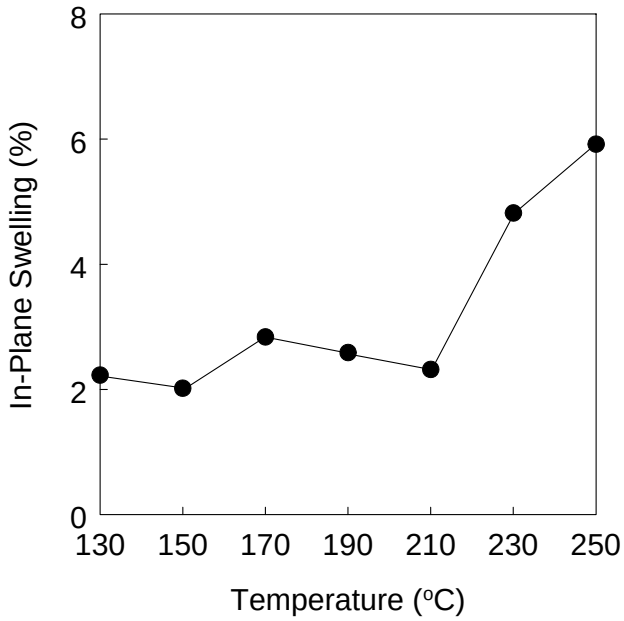

Figure 5.4. In-plane swelling as a function of annealing temperature. All samples were annealed for five minutes. Swelling was measured in 100°C liquid water.

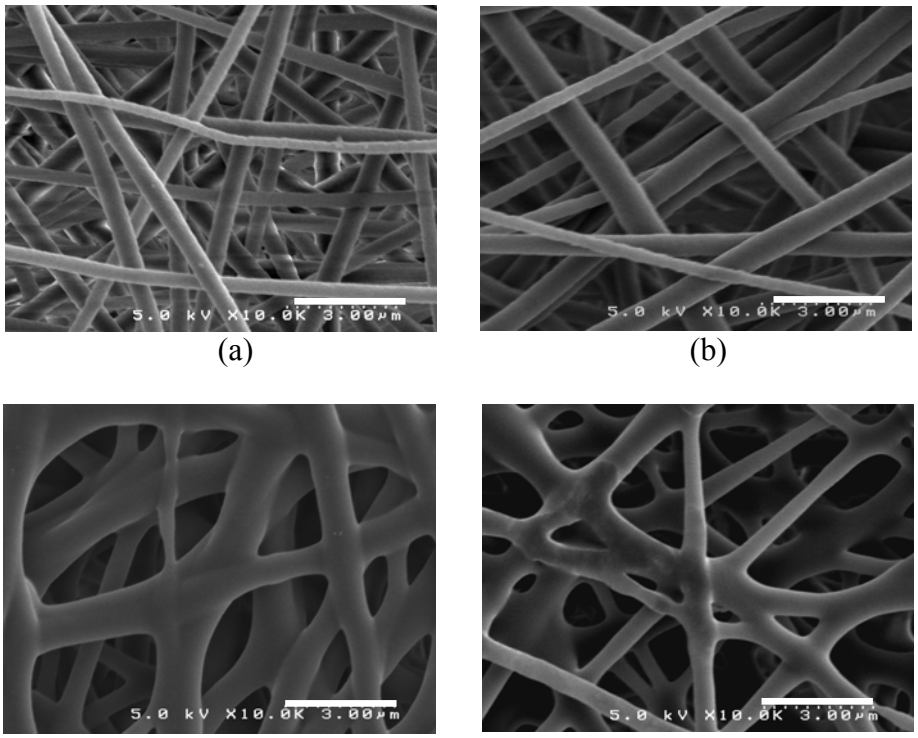

(a) (b)

(c) (d)

Figure 5.5. Effect of annealing temperature on PPSU fiber mat welding. (a) As-spun mat (no annealing), (b) annealed at 210°C, (c) annealed at 230°C (d) annealed at 250°C. The annealing time was constant at five minutes. Scale bar is 3 µm.

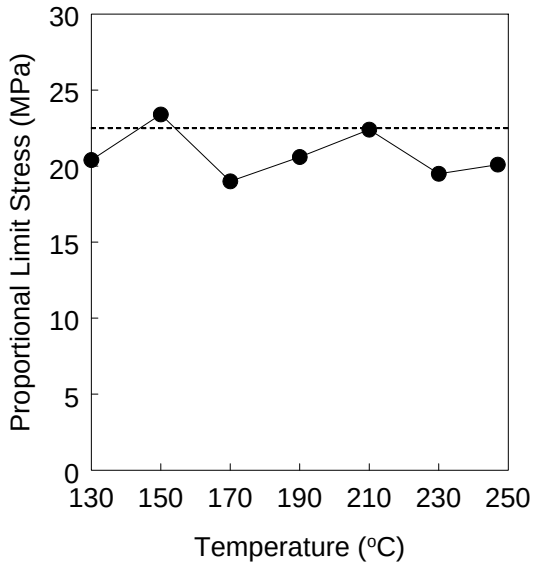

Figure 5.6. Proportional limit stress as a function of annealing temperature. Data points are the average of three tests. All samples were annealed for five minutes. The dashed line represents the PLS for a membrane annealed two hours at 150°C and which had the same structure and Nafion volume loading.

Figure 5.7 shows XRD spectra for several electrospun Nafion fiber samples (electrospun mats containing no PPSU) and for a sample of commercial Nafion 212. There is an increase in the size of the crystalline peak at 18° (associated with Nafion's polytetrafluoroethylene backbone)[15] upon annealing, where properly annealed Nafion nanofibers have a similar degree of crystallinity as Nafion 212 (~20% crystallinity)

.

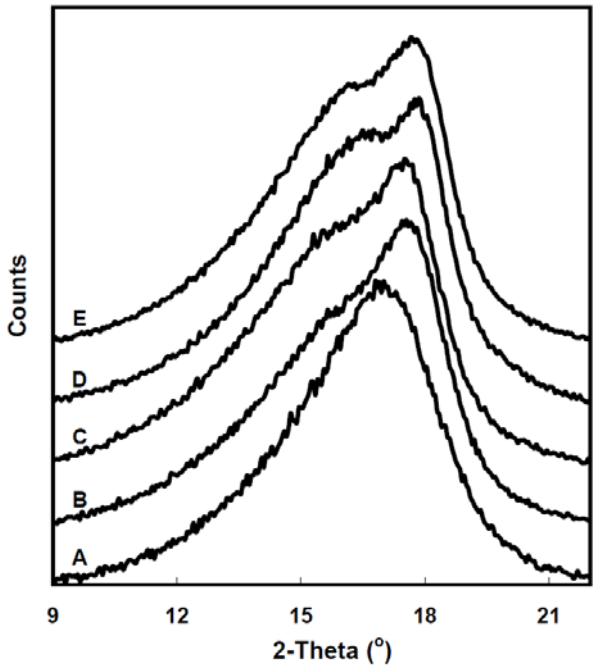

Figure 5.7. XRD spectra of Nafion fiber mats and Nafion 212. (a) As-spun Nafion fiber mat (not annealed), (b) Nafion fiber mat annealed for 15 minutes at 150°C, (c) Nafion fiber mat annealed for 120 minutes at 150°C, (d) Nafion fiber mat annealed for five minutes at 210°C, (e) a commercial sample of Nafion 212.

5.3.1.2 Acid/water washing

The standard pretreatment procedure for solution-cast Nafion membranes is film soaking for one hour in boiling dilute H_2SO_4 and for one hour in boiling water.[16, 17] This treatment ensures that Nafion's sulfonic acid sites are protonated and hydrated. In the case of electrospun composite Nafion membranes, these two pretreatment steps perform

an additional function: during the soakings, PEO carrier polymer is removed from the Nafion fibers. It has been shown by Choi et al.[5] that: (i) the presence of PEO lowers the proton conductivity of water-equilibrated homogeneous Nafion films and (ii) boiling Nafion/PEO fiber mats in acid and water (one hour each) effectively removes PEO with complete recovery of proton conductivity. In the present study, the minimum acid/water pretreatment soaking times were determined for nanofiber composite films containing ~70 vol% Nafion. Proton conductivity was used as a measure of complete PEO removal, where a properly pretreated membrane exhibited a proton conductivity of 59 mS/cm at 80^{o}C and 80% relative humidity. Table 5.1 shows the effect of boiling in water only (no acid washing) on the proton conductivity of the nanofiber composite membrane, where an untreated composite membrane had a very low proton conductivity, 33 mS/cm. After boiling a nanofiber membrane in water for 10 minutes, there is partial recovery of the proton conductivity to 44 mS/cm, with no further increase in conductivity for longer (60 minutes) water boiling times. One might have predicted that water-soluble PEO could be removed from nanofiber composite membranes after water boiling, but this does not appear to be the case. PEO was effectively removed from the membrane with full recovery of proton conductivity by boiling membrane samples for five minutes in 1 M sulfuric acid and then 5 minutes in boiling water (see Table 5.1). In a final experiment, nanofiber membrane samples were soaked at room temperature (25^{o}C) in 1 M H_2SO_4 and water for 24 hours each. Full restoration of conductivity could not be achieved; the resulting membrane conductivity was only 47 mS/cm. Thus one can conclude that hot acid, which is known to degrade PEO,[18] is necessary to extract this carrier material from composite membranes. Soaking membranes in hot sulfuric acid solutions at a

concentration > 1.0 M might further decrease the treatment time; such experiments were not performed in the present study.

Table 5.1. Effect of boiling membranes in 1 M sulfuric acid and water. Conductivity was measured at 80°C, 80% RH.

Boiling Time in 1 M Sulfuric Acid (min)	Time Boiled in Water (min)	Conductivity (mS/cm)
0	0	33
0	10	44
0	60	44
1	5	53
2	5	56
5	5	59
60	5	59

5.3.1.3 Hydrogen limiting current

Hydrogen limiting current experiments were performed to confirm that the new and more rapid processing steps resulted in a fully dense and pinhole-free membrane. A nanofiber mat with 65 vol% Nafion was rapidly processed into a membrane (i.e., hot-pressing at 127°C, 5 minutes annealing at 210°C, 5 minutes soaking in boiling 1 M sulfuric acid, and 5 minutes soaking in boiling water) and then transformed into a fuel cell membrane-electrode-assembly (MEA) by hot pressing a Pt/C anode and cathode to the opposing membrane surfaces. The limiting current for hydrogen crossover under fully humidified (100% relative humidity) feed gas conditions was found to be comparable to that for a Nafion 212 MEA, even though the composite film was considerably thinner than the Nafion membrane (see Table 5.2). Thus, it can be concluded that: (i) the new processing steps create defect-free membranes and (ii) the hydrogen gas permeability of a nanofiber composite membrane is very low.

Table 5.2. Hydrogen limiting current for composite membranes and commercial Nafion at 80°C and 100% relative humidity. Nanofiber membranes were ~65 vol% Nafion and rapid-processed.

Membrane	Limiting Current (mA/cm^2)	Dry Membrane Thickness (μm)
PPSU-fiber/Nafion-matrix	1.27	30
Nafion 212	1.15	51

5.3.2 Nafion fibers encapsulated in polyphenylsulfone

5.3.2.1 Densification by solvent vapor exposure

The nanofiber composite membranes analyzed in section 5.3.1 had a reinforcing fiber mat of polyphenylsulfone (PPSU) embedded in a Nafion matrix. Membranes with the inverse morphology (created from the same dual fiber Nafion/PPSU mat) were also examined in terms of post-electrospinning processing conditions. For these films, our attention was focused on softening and flowing PPSU around Nafion nanofibers.

The effect of chloroform vapor exposure at 25°C and 50°C on final membrane properties is presented in Table 5.3. As expected, there is faster PPSU void space filling at 50°C vs. 25°C (3 minutes vs. 16 minutes), due to the higher partial pressure of chloroform (the vapor pressure of chloroform is 193 mmHg at 25°C and 514 mmHg at 50°C) which presumably increased the membrane-phase concentration of solvent. The proportional limit stress and the equilibrium water swelling properties after chloroform vapor exposure at 50°C for 3 minutes are similar to those obtained at 25°C and 16 minutes. In the present study, no attempt was made to use a chloroform vapor temperature > 50°C, but one would expect a decrease in membrane exposure time for the higher temperature.

Table 5.3. Effect of chloroform vapor exposure time on nanofiber composite membrane properties. Conductivity was measured in water at 25°C, swelling was in 100°C water, and proportional limit stress was determined from the average of three stress-strain curves taken at 30°C, 20% RH.

Temperature	Chloroform Vapor Exposure Time (min)	Conductivity (mS/cm)	Mass Swelling (%)	Volumetric Swelling (%)	Proportional Limit Stress (MPa)
25°C	5	39	23	35	20.2
	16	51	20	27	25.0
50°C	1.5	45	59	48	19.6
	3	53	23	28	23.3
	5	52	25	27	21.7

5.3.2.2 Hydrogen limiting current

Hydrogen limiting current experiments were performed to confirm that the new/rapid chloroform vapor treatment resulted in dense, defect-free membranes. Membrane samples were processed as follows: cold compaction, 3 minute chloroform vapor exposure at 50°C, 5 minutes Nafion annealing at 210°C, and 5 minute soakings in boiling 1.0 M H_2SO_4 and water (the preferred annealing and acid/water soaking steps for this membrane morphology were assumed to be the same as those used in section 5.3.1, where Nafion was reinforced by a PPSU fiber mat). The resulting membrane was fabricated into a MEA and loaded in a fuel cell test fixture. As observed previously for a Nafion-film reinforced by PPSU fibers, the low steady-state hydrogen current density (flux) in Table 5.4 is clear evidence that the nanofiber membranes are defect-free, with a hydrogen permeability that is lower than that in a commercial Nafion sample.

Table 5.4. Hydrogen limiting current for composite membranes and commercial Nafion at 80°C and 100% relative humidity. The nanofiber membrane contained 65 vol% Nafion with a dry thickness of 50 μm.

Membrane	Limiting Current (mA/cm^2)	Dry Membrane Thickness (μm)
Nafion-fiber/PPSU-matrix	0.89	31
Nafion 212	1.15	51

5.4 Conclusions

An in-depth study was conducted on processing conditions for transforming an electrospun Nafion/polyphenylsulfone dual fiber mat into a functional composite membrane. Two distinct membrane structures were created from the same dual fiber mat: (1) Nafion fibers encapsulated in PPSU and (2) Nafion films reinforced by PPSU fibers. The mat processing steps of Nafion annealing, void space filling of PPSU by chloroform vapor exposure, and acid/water washing were studied. The effects of these processing conditions on membrane properties were determined.

A summary of the new processing conditions for nanofiber composite membranes is presented in Table 5.5. There was a substantial decrease in the overall processing time for the dual fiber mats relative to those reported in Chapter IV. In order to demonstrate the applicability of the rapid processing results and to confirm the substantial decrease in overall membrane processing time (a >15 fold reduction in dual nanofiber mat processing time from ca. 4-5 hours to 16-19 minutes), nanofiber mats were processed in real-time using the new/rapid methods. The properties of these membranes (for mats containing 56 vol% Nafion) are also summarized in Table 5.5. The new/faster processing procedures yielded membranes with properties similar to those made under baseline conditions (data not shown).

Table 5.5. Summary of membrane processing conditions and membrane properties. Conductivity was measured at 80°C, 80% RH; mass swelling in 100°C water; and proportional limit stress was determined at 30°C for dry membranes.

	Processing Conditions	Conductivity (mS/cm)	Mass Swelling (%)	Proportional Limit Stress (MPa)
Rapid Processing of Nafion-films reinforced by PPSU	1. Hot-press fiber mat ~40 seconds at 127°C 2. Anneal 5 min., 210°C 3. Boil 5 min. in 1 M H_2SO_4 and 5 min. in H_2O	48	18	23.5
Rapid Processing of Nafion fibers encapsulated in PPSU	1. Compact mat ~10 seconds at 25°C 2. Expose to 50°C chloroform vapor, 3min. 3 Anneal 5 min., 210°C 4. Boil 5 min. in 1 M H_2SO_4 and 5 min. in H_2O	48	23	21.9

5.5 References

(1) Choi, J.; Wycisk, R.; Zhang, W. J.; Pintauro, P. N.; Lee, K. M.; Mather, P. T., *ChemSusChem* **2010,** 3, (11), 1245-1248.

(2) Ballengee, J. B.; Pintauro, P. N., *Macromolecules* **2011,** 44, (18), 7307-7314.

(3) Choi, J.; Lee, K. M.; Wycisk, R.; Pintauro, P. N.; Mather, P. T., *Macromolecules* **2008,** 41, (13), 4569-4572.

(4) Choi, J.; Lee, K. M.; Wycisk, R.; Pintauro, P. N.; Mather, P. T., *Journal of the Electrochemical Society* **2010,** 157, (6), B914-B919.

(5) Choi, J.; Lee, K. M.; Wycisk, R.; Pintauro, P. N.; Mather, P. T., *Journal of Materials Chemistry* **2010,** 20, (30), 6282-6290.

(6) Osborn, S. J.; Hassan, M. K.; Divoux, G. M.; Rhoades, D. W.; Mauritz, K. A.; Moore, R. B., *Macromolecules* **2007,** 40, (10), 3886-3890.

(7) Page, K. A.; Landis, F. A.; Phillips, A. K.; Moore, R. B., *Macromolecules* **2006,** 39, (11), 3939-3946.

(8) Tang, Y. L.; Karlsson, A. M.; Santare, M. H.; Gilbert, M.; Cleghorn, S.; Johnson, W. B., *Materials Science and Engineering a-Structural Materials Properties Microstructure and Processing* **2006,** 425, (1-2), 297-304.

(9) Zhang, W.; Kish, D. L.; Pintauro, P., *ECS Transactions* **2010,** 33, (1), 635-645.

(10) Tang, H.; Peikang, S.; Jiang, S. P.; Wang, F.; Pan, M., *Journal of Power Sources* **2007,** 170, (1), 85-92.

(11) Yun, S.-H.; Woo, J.-J.; Seo, S.-J.; Wu, L.; Wu, D.; Xu, T.; Moon, S.-H., *Journal of Membrane Science* **2011,** 367, (1-2), 296-305.

(12) Solvay Advanced Polymers, *Radel Resins Design Guide*, 2004.

(13) Kusoglu, A.; Karlsson, A. M.; Santare, M. H.; Cleghorn, S.; Johnson, W. B., *Journal of Power Sources* **2006,** 161, (2), 987-996.

(14) Kusoglu, A.; Karlsson, A. M.; Santare, M. H.; Cleghorn, S.; Johnson, W. B., *Journal of Power Sources* **2007,** 170, (2), 345-358.

(15) Scigala, R.; Wlochowicz, A., *Acta Polymerica* **1989,** 40, (1), 15-19.

(16) Sone, Y.; Ekdunge, P.; Simonsson, D., *Journal of the Electrochemical Society* **1996**,143, (4) 1254-1259.

(17) Zawodzinski, T. A.; Springer, T. E.; Davey, J.; Jestel, R.; Lopez, C.; Valerio, J.; Gottesfeld, S., *Journal of the Electrochemical Society* **1993,** 140, (7), 1981-1985.

(18) Yang, B.; Guo, C.; Chen, S.; Ma, J.; Wang, J.; Liang, X.; Zheng, L.; Liu, H., *The Journal of Physical Chemistry B* **2006,** 110, (46), 23068-23074.

CHAPTER VI

PROPERTIES AND FUEL CELL PERFORMANCE OF A NANOFIBER COMPOSITE MEMBRANE WITH 660 EQUIVALENT WEIGHT PERFLUOROSULFONIC ACID

6.1 Introduction

High-temperature/low-humidity hydrogen/air fuel cell operation has a number of advantages. Elevated temperature operation (>100^{o}C) improves electrode kinetics and enhances anode resistance to carbon monoxide poisoning (thus allowing for the use of less pure, less expensive hydrogen), and allows for the use of smaller radiators in automotive applications.[1,2] Low humidity operation simplifies fuel cell system design by reducing the need for feed gas pressurization for operating temperatures above 100^{o}C. The benchmark fuel cell membrane, DuPont's Nafion®, performs well in fuel cells that operate up to 80^{o}C at high humidification. At hotter and drier conditions, however, Nafion's proton conductivity decreases due to insufficient water content to dissociate sulfonic acid fixed-charge groups and form water-filled channels through which protons migrate.[3]

One approach to increasing the high-temperature/low-humidity fuel cell operating range of perfluorosulfonic acid (PFSA) materials and other fuel cell ionomers is to increase the polymer ion-exchange capacity (IEC) above that of Nafion (which has an IEC of 0.91 meq/g). 3M Company, for example, has synthesized a series of high IEC

PFSA polymers with equivalent weights (EWs) in the 580-825 range. The 580 EW material (with an IEC of 1.72 meq/g) is highly conductive, with a proton conductivity at 120^{o}C and 50% RH of 0.146 S/cm vs. 0.039 S/cm for Nafion.[4] Similarly, highly sulfonated poly(p-phenylene sulfone) films with an IEC of 4.5 meq/g were found to be very good proton conductors, with a conductivity seven-times higher than that of Nafion at 135^{o}C and 35% RH.[5] Unfortunately, most/all high IEC proton conducting polymers suffer from one or more problems associated with: (i) membrane brittleness when dry, (ii) water solubility (especially in hot water), and (iii) dimensional stability (i.e., excessive swelling/shrinking in the wet/dry states).[6-8] Methods to alleviate these problems include ionomer crosslinking, blending, and the use of block copolymers, see for example references.[9-15]

Recently, nanofiber electrospinning methods have been employed to fabricate fuel cell proton conducting composite (two component) membranes with a high IEC, high proton conductivity, and improved/lower water swelling.[16-20] Such an approach decouples the properties of the proton conducting ionomer from the uncharged polymer which provides mechanical strength and improves the membrane's dimensional stability. Ionomers such as 1.21 meq/g and 1.36 meq/g PFSA (from 3M Company) and 2.1-2.5 meq/g sulfonated polysulfone were electrospun into porous nanofiber mats with fiber diameters <200 nm. The mats were compressed to increase the ionomer fiber volume fraction and then impregnated with Norland Optical Adhesive 63 (NOA 63), a polyurethane liquid pre-polymer which was subsequently UV-crosslinked in-situ to create a mechanically robust reinforcing matrix that surrounded every ionomer fiber. Highly sulfonated polyhedral oligomeric silsesquioxane (sPOSS, with an IEC of 4.8

meq/g) was added to PFSA nanofibers to further increase the proton conductivity. Thus, a membrane consisting of 1.21 meq/g PFSA + sPOSS nanofibers embedded in a NOA 63 matrix had a proton conductivity of 0.107 S/cm at 120^{o}C and 50% RH with half the in-plane dimensional water swelling of a neat PFSA/sPOSS film.[19]

Chapters IV and V of this dissertation introduce a new and simpler approach for the fabrication of nanofiber composite membranes, where the ionomer and the uncharged polymer components are electrospun simultaneously from separate spinnerets to form a dual-fiber mat which is subsequently processed into a dense membrane.[21] The membranes described in Chapters IV and V are well-suited for use in fuel cells operated at ~80^{o}C. In this chapter, I seek to develop membranes suitable in fuel cells where the temperature exceeds 80^{o}C. Specifically, I report on the use of the dual-fiber electrospinning technique to fabricate composite membranes of 3M Company's 660 equivalent weight ionomer (IEC = 1.52 meq/g), hereafter referred to as 3M660, and polyphenylsulfone (PPSU) (see Figure 6.1 for the polymer structures). The two polymers were simultaneously electrospun into a dual-fiber electrospun mat with follow-on processing that allowed for the softening and flow of the 3M660 ionomer into the PPSU interfiber void space. The resulting membrane was a 3M660 film reinforced by a mat of PPSU nanofibers, henceforth designated 3M660/PPSU. Proton conductivity, water swelling, and fuel cell performance for the composite membranes is presented and discussed with that of Nafion 211.

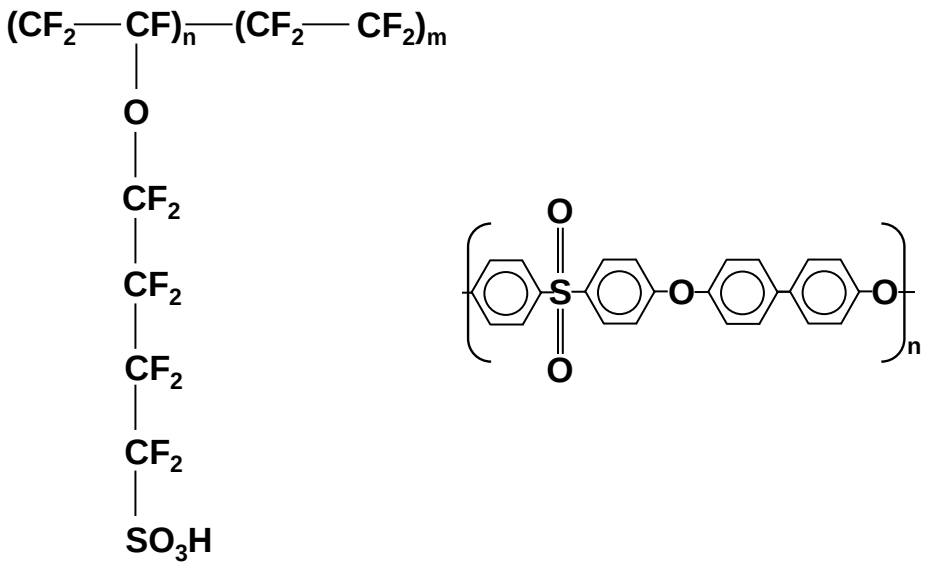

(a) (b)

Figure 6.1. The repeating monomer unit of (a) 660 equivalent weight perfluorosulfonic acid, where m =2.8, n=1 (b) and polyphenylsulfone.

6.2 Experimental

6.2.1 Electrospinning

PFSA polymers do not form true solutions, but rather micellar dispersions in organic solvents.[22] Thus, PFSA lacks the requisite chain entanglements for electrospinning and a carrier polymer must be added to improve electrospin-ability, as described elsewhere.[18,19, 22,23] In the present study, 1,000 kDa MW polyethylene oxide (PEO) was used as the carrier polymer.

3M660 and PEO solutions were prepared separately by dissolving 3M660 powder (from an evaporated liquid solution that was provided by 3M Company) and PEO powder

(Sigma-Aldrich) into a mixed solvent of 2:1 wt. ratio n-propanol:water. The solutions were then combined where PEO constituted 0.3% of the total polymer weight.

Polyphenylsulfone (Radel® R 5500NT from Solvay Advanced Polymers LLC) solutions were prepared by dissolving polymer in an 80:20 wt. ratio n-methyl-2-pyrrolidone:acetone solvent. The PPSU and 3M660/PEO solutions were drawn into separate syringes and electrospun onto a common rotating drum collector surface using 22 gauge needles (Hamilton Company). Electrospinning conditions are summarized in Table 6.1. The total electrospun volume of each polymer component fixed the composition of the final membrane

Table 6.1. Electrospinning conditions for a 3M660/PPSU dual-fiber mat.

Parameter	3M660	PPSU
Polymer Comp.	99.7:0.3 wt. ratio, 3M660:PEO (30 wt% total polymer in solution)	25 wt%
Solvent	n-propanol:water in a 2:1 wt. ratio	NMP:acetone in a 8:2 wt. ratio
Voltage	7.0 kV	7.5 kV
SCD	5.5 cm	8.5 cm
Flow Rate	0.40 mL/hr	0.10 mL/hr

Two electrospun mats with 3M's 825 EW PFSA polymer and PPSU were also prepared. The conditions for electrospinning these mats are provided in Appendix D, along with dense membrane properties.

6.2.2 Membrane fabrication

An electrospun dual-fiber mat (where ~72 vol% of the fibers are PFSA) was compressed three times for ~10 seconds, each at ~15,000 psi and 127°C. The sample was rotated 90° after each compression to ensure uniform compaction. The mat was then annealed in vacuum at 150°C for 2 hours. During hot pressing and annealing, the 3M660 softened and flowed to fill the interfiber void space between PPSU fibers, as was reported in Chapter IV and V for Nafion-PEO/PPSU dual fiber mats. The membranes were then soaked at room temperature in 1 M H_2SO_4 for 16 hours and liquid water for 6 hours to ensure full protonation of sulfonic acid sites.

A membrane boiled in 1 M H_2SO_4 and H_2O lost ~40% of its dry weight due to 3M660's high IEC. However, a membrane soaked in 25°C water had much milder mass loss, only ~6%, and no mass was removed upon a second 25°C water washing.

Typically, electrospun membranes have been boiled in 1 M H_2SO_4 and H_2O to ensure complete PEO removal,[18,23] and thus the room temperature soaking of the 3M660-PEO/PPSU membranes may not completely remove PEO. However, since the PEO content is small, only 0.3 wt% relative to the total 3M660 and PEO polymer content, no significant effect on membrane properties is expected.

6.2.3 Scanning electron microscopy

Scanning electron microscope (SEM) images were obtained as discussed in Chapter IV, section 4.2.3.

6.2.4 Proton conductivity

In-plane membrane conductivity below 120°C was measured by an AC impedance technique using a BekkTech BT-110 clamp. Measurements were performed in an ESPEC Corp. temperature/humidity controlled environmental chamber (Model: SH-241). Conductivity was also measured in room temperature liquid water. In-plane proton conductivity at 120°C was measured by Scribner Associates, Inc. using a BekkTech BT-110 clamp. The temperature was fixed at 120°C and the relative humidity was varied between 18% and 95%, where the humidity was changed in 10% increments and the membrane was equilibrated at each relative humidity for 15 minutes prior to taking a measurement. In all cases, conductivity was calculated by Equation 6.1, using membrane dimensions recorded at dry ambient (room temperature) conditions.

$$\sigma = \frac{L}{Rw\delta} \tag{6.1}$$

where σ [S/cm] is proton conductivity, R [Ω] is the resistance between the electrodes in the BekkTech cell, L [cm] is the distance between the electrodes, w [cm] is the width of the sample in the dry state (usually 1 cm), and δ [cm] is the sample's dry thickness.

6.2.5 Water uptake

Water uptake as a function of relative humidity was determined with a sorption analyzer (TA Instruments Q5000 SA). A membrane sample was dried at 80°C under dry nitrogen gas until the weight stabilized (~3 hours) and then equilibrated at 20%, 40%,

60% and 80% relative humidity for 1 hour. After each humidity equilibration step, the membrane weight was recorded.

Liquid water uptake at room temperature was determined after soaking the membrane in 1 M H_2SO_4 for 16 hours, and then water for 6 hours. The surface of the membrane was wiped dry and the membrane's mass, area, and volume were recorded. The volumetric, gravimetric, and in-plane (areal) swelling were determined by Equation 6.2.

$$Water\ Swelling(\%) = \frac{x_{wet} - x_{dry}}{x_{dry}} x\,100 \tag{6.2}$$

where x is the membrane's volume, mass, or area.

6.2.6 Ion-exchange capacity

Ion-exchange capacity (IEC) was determined as discussed in Chapter IV, section 4.2.5.

6.2.7 Mechanical properties

Stress-strain curves were obtained with a TA instruments Q800 dynamic mechanical analyzer (DMA). Dry samples were tested at 30°C and ~10% RH. The DMA was operated in tension mode, where the force was ramped at 0.10 N/min until the sample yielded. The mechanical properties of water-swollen membranes at 25°C were also tested. Samples were soaked in room temperature water for over 72 hours, then rapidly loaded into the DMA and strained at 20% per minute until failure.

6.2.8 MEA fabrication

3M660/PPSU nanofiber membrane samples were converted into fuel cell membrane-electrode-assemblies (MEAs) at 3M Company by static transfer of electrodes at 140°C and a compression force of 1.5 metric tons for 10 minutes. The electrodes each had a platinum loading of 0.25 mg/cm^2 with 3M's 825 EW PFSA serving as the binder. MEAs were briefly soaked in 1 M H_2SO_4 and water at 25°C prior to fuel cell testing.

Commercial Nafion 211 membranes were converted into MEAs at Vanderbilt University by static transfer of electrodes at 140°C and a compression force of 1.58 metric tons for 10 minutes. The electrodes had a platinum loading of 0.25 mg/cm^2 and used 1000 EW Nafion PFSA as the binder. MEAs were boiled in 1 M H_2SO_4 and water (1 hour for each boiling step) prior to testing.

6.2.9 Fuel cell testing

Fuel cell voltage vs. current density polarization curves were obtained for 5 cm^2 MEAs at atmospheric pressure with a Scribner Associates 850e fuel cell test system. The hydrogen and air flow rates were set at 125 sccm and 500 sccm, respectively. Prior to testing, the MEAs were pre-conditioned overnight at 30°C by cyclic operation at low current (150 mA/cm^2) and then at low voltage (0.2 V). MEAs were then further conditioned at 80°C until the current output (when operating at 0.2 V) and voltage output (when operating at 150 mA/cm^2) stabilized, typically after 3 hours. During polarization experiments, the current was recorded 30 seconds after setting a given voltage.

Electrochemical impedance spectroscopy (EIS) was used to determine each MEA's high frequency (ohmic) resistance (R_{ohm}) and charge-transfer resistance (R_{ct}). EIS

experiments were performed with Scribner's 880 Impedance Analyzer at 100 mA/cm^2 with a 5% oscillation in the DC current. A typical resulting Nyquist plot is shown in Figure 6.2a (actual test data). The equivalent circuit shown in Figure 6.2b was assumed for data analysis. (Note that a constant phase element is analogous to the presence of a capacitor in the equivalent circuit). The reported R_{ohm} is the real resistance x-intercept at high frequency, i.e., where the imaginary resistance is equal to 0. The reported R_{ct} is the x-intercept at low frequency minus R_{ohm}. Resistances determined in this manner were typically within 5% of those calculated by fitting the equivalent circuit in Figure 6.2b to experimental data using Scribner's ZView software.

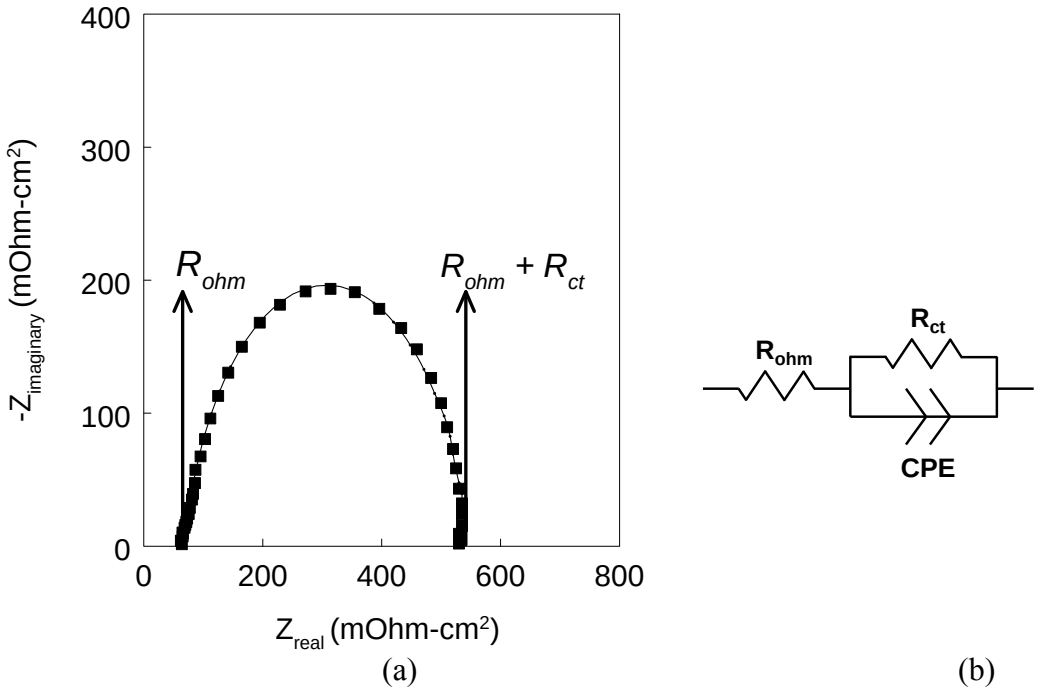

Figure 6.2. (a) Representative Nyquist plot for a MEA at 80^{o}C and 93% RH. The MEA was composed of a nanofiber membrane (3M660 EW film reinforced by PPSU nanofibers) and 3M 825 EW binder with platinum catalyst. (b) Equivalent circuit for a MEA in a hydrogen/air fuel cell. R_{ohm} is the ohmic (high frequency) resistance, R_{ct} is the charge transfer resistance, and CPE is a constant phase element, analogous to a capacitor. The line in Figure 6.2a was calculated using Scribner's Zview software and the equivalent circuit in Figure 6.2b.

6.3 Results and discussion

A SEM image of the surface of a dual-fiber electrospun mat is shown in Figure 6.3a. The 3M660/PEO fibers and the PPSU fibers are visually indistinguishable. In this particular image 72% of the fibers are composed of 3M660/PEO, as anticipated by the polymer electrospinning volumes and determined by later IEC experiments. The average fiber diameter for the mat is 335 nm. The fiber mat was processed into a dense membrane by hot-pressing and annealing, at 150^{o}C for 2 hours. The cross-section of a densified/annealed membrane is shown in Figure 6.3b. The PFSA has softened and flowed into the PPSU inter-fiber void space. PFSA flow during nanofiber mat annealing has been observed by other investigators[18, 24] and is attributed to morphological re-arrangements of the ionic domains above the α-transition temperature.[25, 26] Fully processed membranes were typically 40-60 μm in dry thickness.

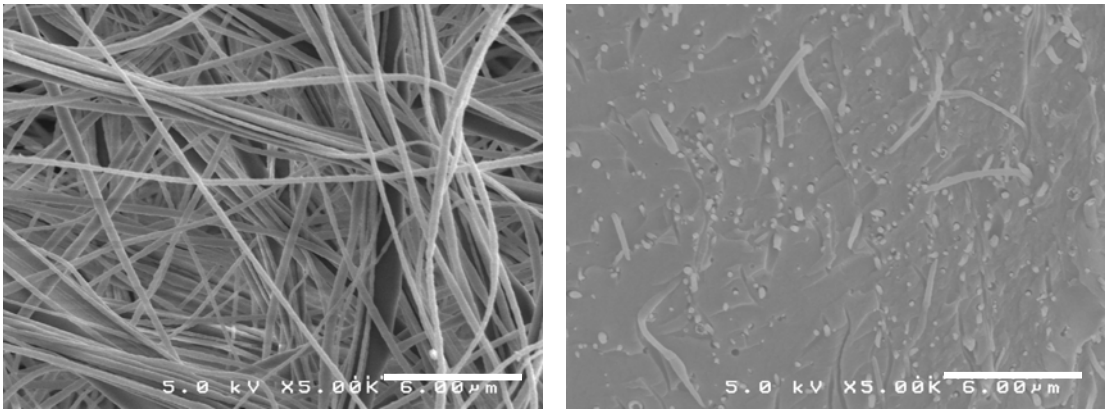

(a) (b)

Figure 6.3. SEM micrographs of (a) an electrospun dual-fiber mat of 3M660/PEO fibers and PPSU fibers and (b) a freeze-fracture cross-section of a dense 3M660/PPSU nanofiber composite membrane where 3M660 has been softened and allowed to flow between PPSU fibers. Scale bars are 6 μm.

3M660/PPSU nanofiber composite dense membranes had a high concentration of fixed-charge sulfonic acid groups; the measured IEC was 1.23 meq/g, corresponding to a 3M660 membrane mass fraction of 0.81 (a volume fraction of 0.72). The additional number of charge carriers, as compared to Nafion, results in a proton conductivity that is significantly higher than commercial Nafion 212, as can be seen in Figure 6.4, where in-plane proton conductivity is plotted as a function of relative humidity at 80°C. Over the entire 20-80% humidity range, the conductivity of the EW 660 nanofiber composite membrane was twice that of Nafion. The composite film's conductivity is lower than a neat solution-cast 3M660 membrane due to effective dilution of PFSA polymer by PPSU. Thus, at 80°C and 50% RH the composite has a conductivity of 0.070 S/cm, as compared to 0.032 S/cm for Nafion and 0.090 S/cm for solution-cast 3M660.

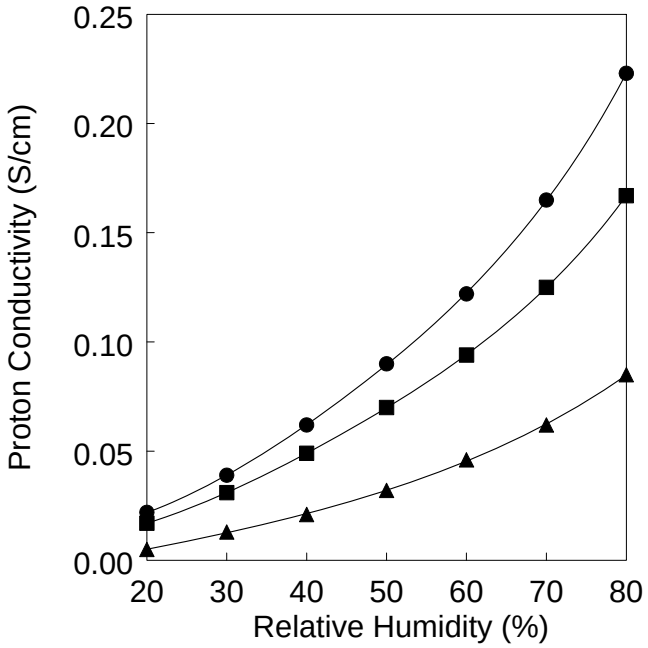

Figure 6.4. In-plane proton conductivity as a function of relative humidity at 80°C (conductivity based on dry membrane sample dimensions). (●) Solution-cast 3M660 membrane, (■) 3M660/PPSU composite membrane, (▲) Nafion 212 membrane (1100 EW).

The proton conductivity of membrane samples at 120°C is shown as a function of relative humidity in Figure 6.5. At 120°C and 50% RH, the composite membrane has a proton conductivity of 93 mS/cm. This conductivity closely approaches the Department of Energy's target of 100 mS/cm at these conditions.[27] A slight increase in membrane PFSA content above 72 vol% would result in a conductivity that surpasses the DOE target; such membranes were not made in the present study (i.e., there was no optimization of membrane composition and properties). The proton conductivity of the 3M660/PPSU nanofiber membrane in Figure 6.5 is considerably higher than that of a commercial Nafion 212 film over the entire humidity range (e.g., Nafion's conductivity is only 37 mS/cm at 120°C and 50% RH). Figure 6.5 also shows the proton conductivity of the nanofiber membrane created by Choi et al.[19] which was composed of 74 vol% charged ionomer fibers that are embedded in an uncharged matrix of Norland Optical Adhesive 63, where the fibers contained 3M 825 EW PFSA, sulfonated POSS (4.8 meq/g IEC), and poly(acrylic acid) carrier at a relative weight ratio composition of 65:35:5. As can be seen, this particular membrane had exceptionally high proton conductivities at moderate/high relative humidities, but lost conductivity at a RH < 30%.

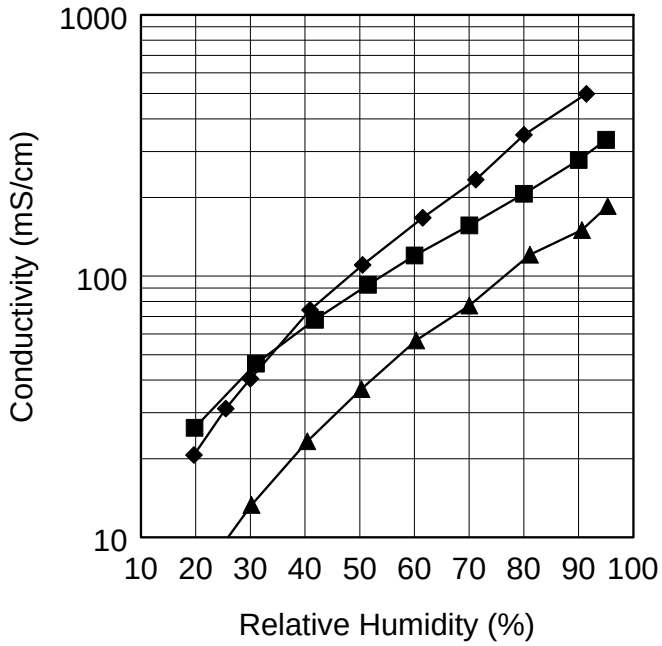

Figure 6.5. Conductivity at 120°C as a function of relative humidity. (■) 3M660/PPSU nanofiber membrane with ~72 vol% 3M660 EW polymer, (▲) Nafion 212, (♦) 3M 825/sPOSS/NOA 63 nanofiber membrane, from reference 19.

High IEC films are more hydrophilic than ionomer films with a lower IEC. The increased concentration of acidic functional groups increases the osmotic driving force for membrane water swelling. As seen in Figure 6.6A, gravimetric water uptake is a strong function of the effective membrane IEC. A solution-cast film of 3M660 (IEC of 1.51 meq/g) sorbs more water than the 3M660/PPSU composite film (IEC of 1.23 meq/g), which, in turn, sorbs more than commercial Nafion 212 (IEC of 0.91 meq/g). Since the PPSU component of the nanofiber composite does not contain acidic functional groups and does not sorb water, there is a reduction in both IEC and water sorption for nanofiber composites as compared to a solution-cast film of 3M660. While there is significantly higher water uptake for the solution-cast 3M660 film, the number of water molecules per

sulfonic acid site is constant, regardless of the effective membrane IEC and the PFSA polymer type (Nafion vs. PFSA), as shown in Figure 6.6B.

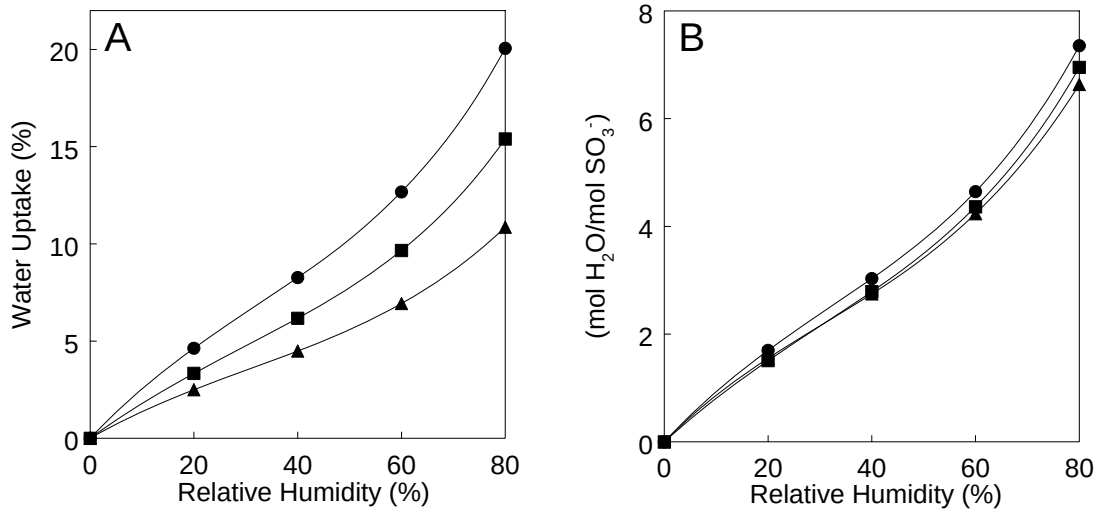

Figure 6.6. Membrane water uptake as a function of relative humidity at 80°C. (A) Gravimetric water uptake and (B) water molecules per sulfonic acid group. (●) Cast 3M660 membrane (IEC of 1.51 meq/g), (■) 3M660/PPSU composite membrane (effective IEC of 1.23 meq/g), (▲) Nafion 212 membrane (1100 EW with an IEC of 0.91 meq/g).

The combination of high water content and minimal changes in areal swelling are desirable membrane properties for fuel cell applications.[7, 8] High water content is required for high proton conductivity whereas low in-plane swelling (i.e., preferential swelling in the membrane thickness direction) is highly desirable for increasing the useful lifetime (i.e., durability) of a membrane/MEA during on/off fuel cell cycling.[28, 29] The 3M660/PPSU composite membrane exhibited excellent dimensional stability, with an areal swelling of only 5%, which is lower than that that of commercial Nafion (see Table 6.2). The low in-plane swelling is attributed to the absence of through-plane connectivity between the reinforcing PPSU fibers, which allows the membrane to swell

predominantly in the thickness direction upon water sorption, as discussed elsewhere.[30] Note that while swelling is anisotropic, the proton conductivity for the composite film is not. Through-plane conductivity (not shown) and in-plane conductivity were found to be comparable for a composite membrane with ~70 vol% 3M660 when tested in liquid water. Isotropic conductivity is not unexpected given that the 3M660 fibers flow into a highly connected film/matrix during hot-pressing and annealing, as discussed previously.

The mechanical properties of the 3M660/PPSU composite films were also determined and are compared to a solution-cast 3M660 membrane in Figure 6.7. Several conclusions can be drawn from the stress-strain results: (i) The composite films are not brittle, with a strain at break >50%, (ii) water-swollen membranes have dramatically lower mechanical properties than dry membranes, due to the high water swelling of these films (see Table 6.2); water has negligible tensile properties and thus its presence significantly diminishes membrane strength, and (iii) surprisingly, the presence of PPSU in the nanofiber composite did not improve the mechanical properties relative to solution-cast 3M660; this observation contrasts with previous mechanical property data for PPSU-fiber reinforced Nafion[21] and requires further investigation.

Table 6.2. Membrane swelling and in-plane proton conductivity in room temperature water for a nanofiber composite membrane (72 vol% 660 EW PFSA and 28 vol% PPSU fibers), a solution-cast film of 3M660 EW polymer, and Nafion 212 (1100 EW).

Membrane	Mass Swelling [%]	Volumetric Swelling [%]	In-plane Swelling [%]	In-plane Proton Conductivity [mS/cm]
660 EW/PPSU nanofiber composite membrane	53	87	5	107
Solution-cast 660 EW film	71	137	84	132
Nafion 212	16	35	25	95

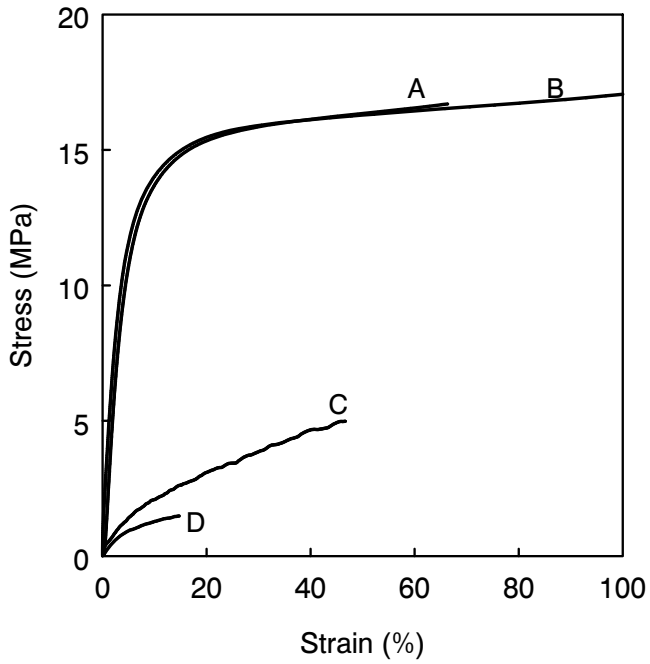

Figure 6.7. Representative stress-strain curves for dry and water-swollen membranes. (A) 3M660/PPSU nanofiber composite membrane, dry; (B) solution-cast 3M660 EW film, dry; (C) solution-cast 3M660 EW film, water-swollen; (D) 3M660/PPSU nanofiber composite membrane, water swollen. Dry membranes were tested at 30°C and 10% RH; water swollen membranes were tested at 25°C.

Hydrogen/air fuel cell performance of a 3M660/PPSU nanofiber composite membrane with 72 vol% 3M660 and a dry thickness of 51 μm is shown in Figures 6.8-6.10 for operating temperatures of 80°C, 100°C, and 120°C respectively. The binder used in this MEA (hereafter referred to as "3M MEA") was 3M's 825 EW PFSA. For comparison, data for an 1100 EW Nafion 211 membrane (25 μm dry thickness) with Nafion 1000 EW binder is also included (henceforth the "Nafion MEA"). No attempt was made to assess a 3M660/PPSU nanofiber composite membrane with Nafion binder electrodes or a commercial 1100 EW Nafion 211 membrane with 3M's 825 EW PFSA as the electrode binder. Polarization curves were obtained at 93%, 75%, 50%, and 25% RH for 80°C and 100°C. At 120°C, polarization data were collected at 50% and 25% RH

(higher humidities would have required system pressurization). The power density output at 0.6 V is shown for each temperature/humidity condition in Figure 6.11. At all operating conditions the 3M MEA outperforms the Nafion MEA. The relative improvement of the 3M MEA increases as the RH decreases. For example at 80°C and 93% RH, the 3M MEA generated 30% more power at 0.6 V than the Nafion MEA, whereas 286% more power was measured with the 3M MEA at 80°C and 25% RH. Also note that the limiting current of both MEAs was satisfactory (2.9 mA/cm^2 for the 3M MEA and 1.7 mA/cm^2 for the Nafion MEA). Figures 6.8, 6.9, and 6.11 show that the 3M MEA performs well over a wide range of relative humidities, from 50% to 93%. Thus, at 100°C, the power output at 0.6 V decreased by only 3% with the 3M MEA when the relative humidity is reduced from 93% to 50%. This compares to a 42% decrease for the Nafion MEA. The insensitivity of the 3M MEA to changes in feed gas relative humidity suggests that the ohmic overpotential is small relative to the kinetic and mass-transfer overpotentials for 50% < RH < 93%. When the relative humidity is further decreased to 25%, the ohmic overpotential is larger and there is a substantial decrease in fuel cell power output.

An important feature of the results in Figure 6.11 is the decreasing power output with increasing temperature from 80°C to 120°C when the relative humidity is held constant and the fuel cell operating pressure is fixed at 1 atm. The kinetic and ohmic overpotentials decrease with increasing temperature as the catalyst becomes more active and the conductivity of the membrane increases. This should produce an increase in fuel cell performance, but the decrease in partial pressures of hydrogen and oxygen feed gases with increasing temperatures results in lower power generation. At 80°C and 50% RH

the reactant gases have a partial pressure of ~0.75 atm, which decreases to near 0 atm at 120°C and 50% RH as the partial pressure of water approaches 1 atm. In these fuel cell systems the power loss associated with reduced fuel/oxidant pressure is greater than the improvements associated with improved catalyst kinetics and higher membrane conductivity. Adjemian et al. observed a similar decrease in power with increasing temperature due to lower reactant gas partial pressures.[31] These results clearly indicate that fuel cell pressurization is required to take full advantage of the proton conductive property of the 3M660 nanofiber composite membranes at high temperature and low RH.

The significant improvement in power output for the 3M MEA relative to the Nafion MEA is attributed to reductions in both the ohmic resistance (R_{ohm}) and the charge transfer resistance (R_{ct}). R_{ohm} and R_{ct} at 80°C are shown in Figure 6.12 as a function of RH. Similar trends were observed at 100°C and 120°C. The 3M MEA's ohmic resistance is 64 mΩ-cm^2 at 93% RH, 9% lower than that for the Nafion MEA. The reduction in ohmic resistance is more significant at 25% RH; 290 mΩ-cm^2 vs. 446 mΩ-cm^2 (a 35% decrease). The differences in R_{ohm} are primarily attributed to the higher conductivity and lower sheet resistance (conductivity divided by film thickness) of the 3M660/PPSU membrane. For example at 80°C and 25% RH, the calculated (theoretical) sheet resistance of the 3M660/PPSU nanofiber membrane is 213 mΩ-cm^2, as compared to 304 mΩ-cm^2 for Nafion 211, a similar percentage decrease to the measured R_{ohm} at those conditions.

The lower value of R_{ohm} for the 3M MEA is not associated with a higher conductivity of the 3M 825 EW binder as compared to the 1000 EW binder used in the Nafion MEA. R_{ohm} is determined at high frequencies, where the capacitive nature of the

electrodes shields the effects of catalyst layer conduction.[32, 33] Other contributions to R_{ohm} (gas diffusion layer, cell leads, current collector, etc.) were the same for both MEAs.

Values of R_{ct}, a measure of oxygen reduction reaction (ORR) kinetics, are shown in Figure 6.12B. At all humidities R_{ct} is lower for the 3M MEA than for the Nafion MEA. Also for both MEAs, R_{ct} increases as the humidity decreases, indicating a more sluggish ORR reaction at low RH. This result is consistent with previous studies which showed that the ORR proceeds more slowly with decreasing RH.[34-36] As the humidity drops, the reaction order of the ORR decreases, possibly caused by a change in the ORR reaction pathway; furthermore proton activity in the catalyst layer may be reduced at low RH.[35] The reduced ORR activity is most pronounced for Nafion-based MEAs below 60% RH.[35] The data in Figure 6.12B support this finding, as the Nafion MEA's R_{ct} did not dramatically increase until the humidity dropped from 75% to 50% RH. Conversely, R_{ct} for the 3M MEA was not strongly dependent on feed gas humidity. This result, along with the generally lower R_{ct} in the 3M MEA suggests that the low EW binder in the 3M660/PPSU MEA allows for a more humid local environment in the catalyst layer, i.e., the elevated water content reduces R_{ct} in the 3M MEA and helps improve fuel cell performance.

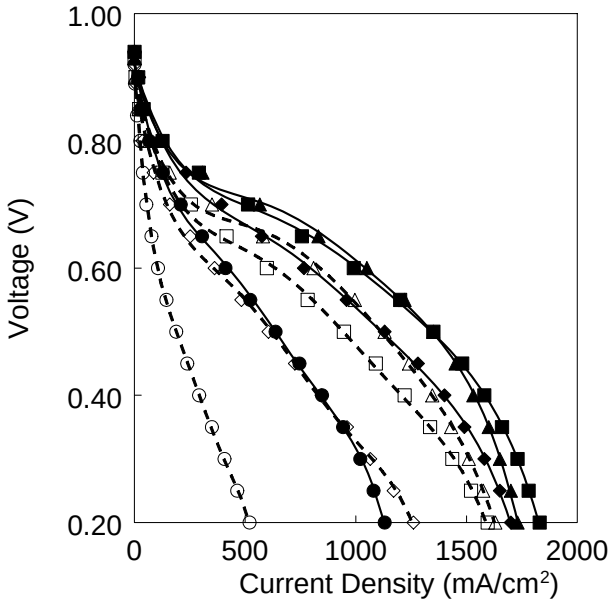

Figure 6.8. Polarization curves at 80°C for the 3M MEA (that contained a 3M660/PPSU nanofiber composite membrane) and a Nafion MEA (with a Nafion 211 membrane). (▲) 3M MEA, 93% RH; (■) 3M MEA, 75% RH; (♦) 3M MEA, 50% RH; (●) 3M MEA, 25% RH; (Δ) Nafion MEA, 93% RH; (□) Nafion MEA, 75% RH; (◊) Nafion MEA, 50% RH; (○) Nafion MEA, 25% RH.

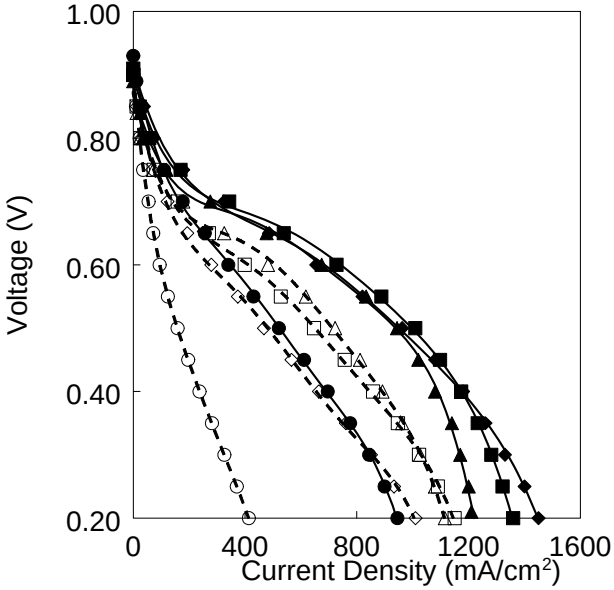

Figure 6.9. Polarization curves at 100°C for the 3M MEA (that contained a 3M660/PPSU nanofiber composite membrane) and a Nafion MEA (that contained a Nafion 211 membrane). (▲) 3M MEA, 93% RH; (■) 3M MEA, 75% RH; (♦) 3M MEA, 50% RH; (●) 3M MEA, 25% RH; (Δ) Nafion MEA, 93% RH; (□) Nafion MEA, 75% RH; (◊) Nafion MEA, 50% RH; (○) Nafion MEA, 25% RH.

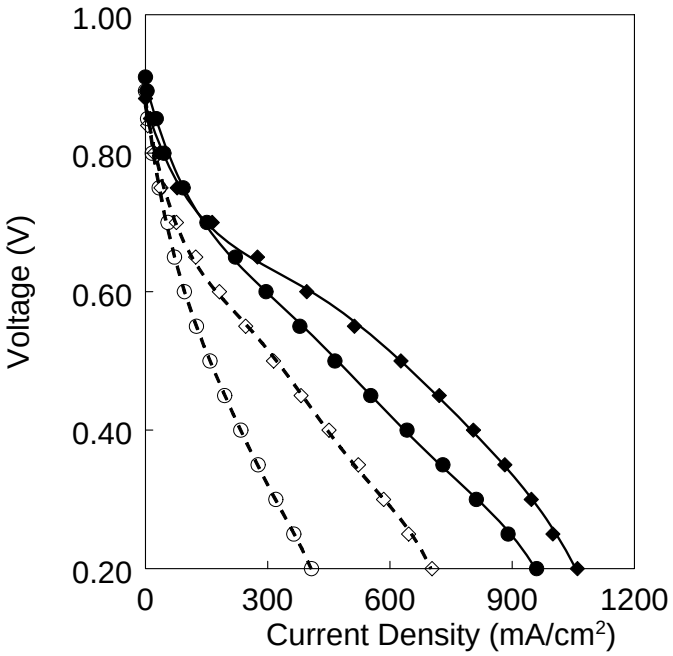

Figure 6.10. Polarization curves at 120°C for the 3M MEA (that contained a 3M660/PPSU nanofiber composite membrane) and a Nafion MEA (that contained a Nafion 211 membrane). (♦) 3M MEA, 50% RH; (●) 3M MEA, 25% RH; (◊) Nafion MEA, 50% RH; (○) Nafion MEA, 25% RH.

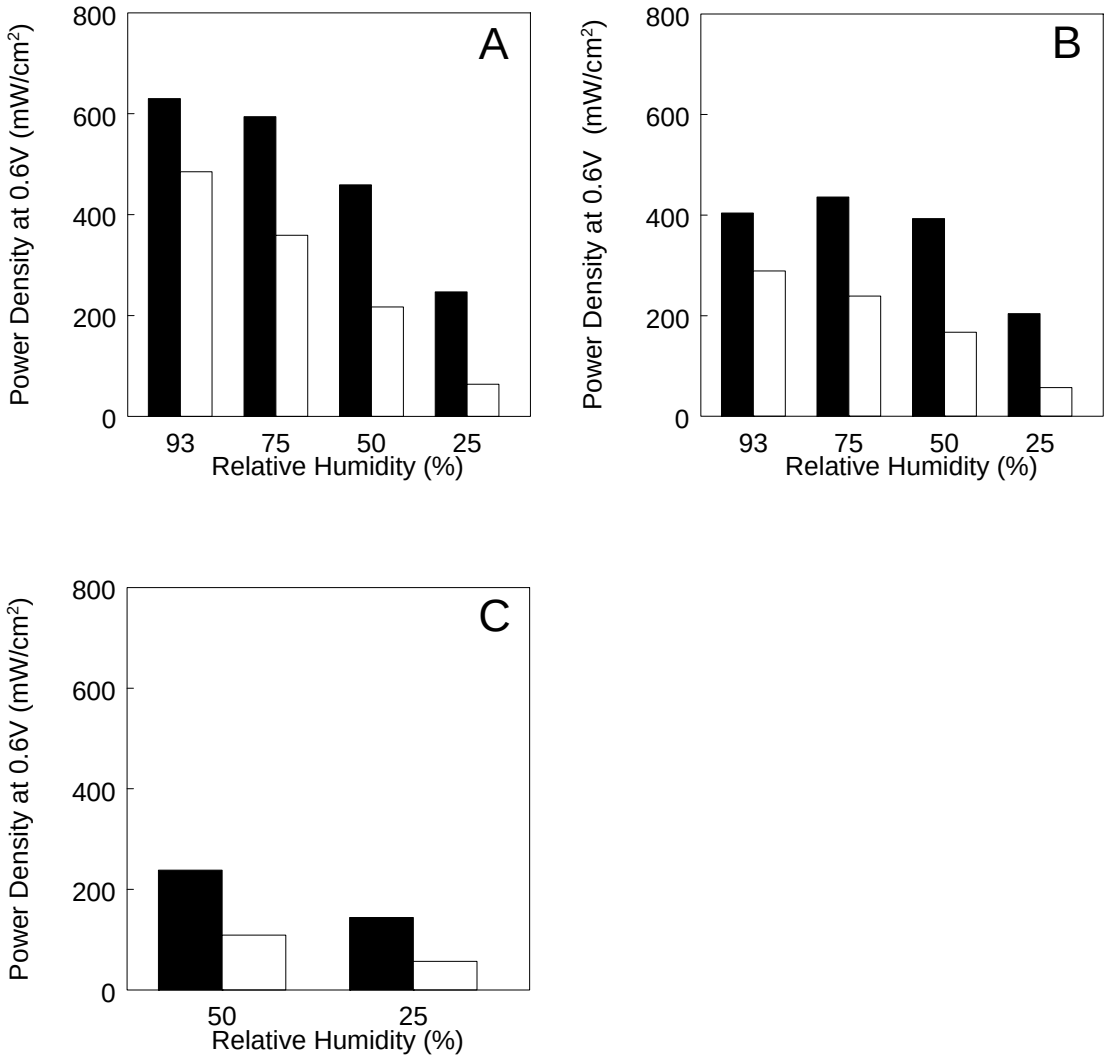

Figure 6.11. Power density output at 0.6 V at (A) 80°C, (B) 100°C, and (C) 120°C. (■) the 3M MEA (that contained a 660 EW/PPSU nanofiber composite membrane) and (□) the Nafion MEA (that contained a Nafion 211 membrane).

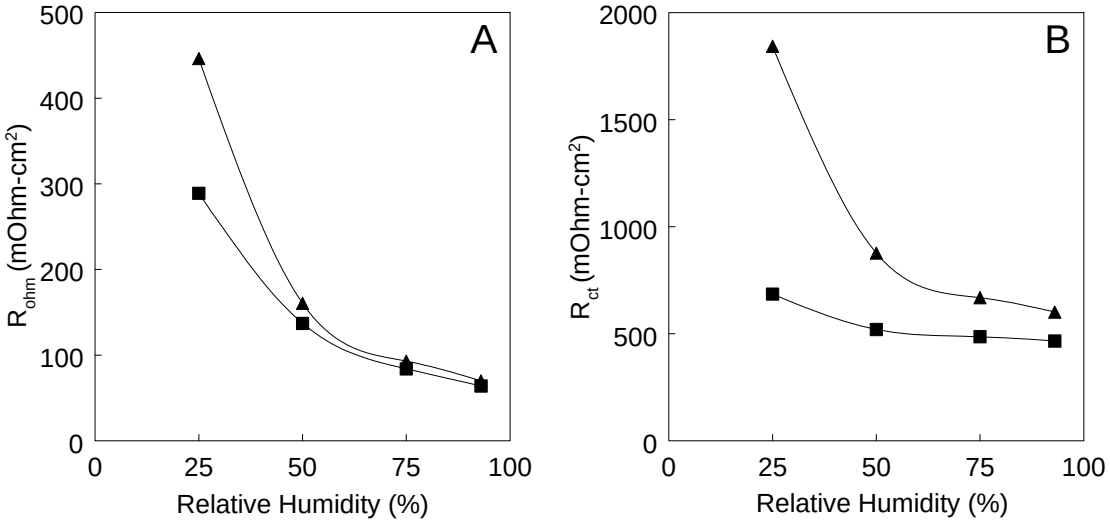

Figure 6.12. (A) Ohmic resistance and (B) charge-transfer resistance for a fuel cell operating temperature of 80°C for: (■) the 3M MEA (that contained a 3M660/PPSU nanofiber composite membrane) and (▲) a Nafion MEA (that contained a Nafion 211 membrane).

6.4 Conclusions

Composite membranes with high proton conductivity and low in-plane water swelling have been fabricated using a dual nanofiber electrospinning approach. 3M Company's 660 equivalent weight perfluorosulfonic acid (PFSA) polymer and polyphenylsulfone were simultaneously electrospun into a dual fiber mat with an average fiber diameter of 335 nm. Follow-on processing induced flow of the PFSA polymer only, resulting in a final membrane morphology where the 3M660 ionomer is reinforced by a nonwoven polyphenylsulfone nanofiber mat. The 3M660 component imparted high conductivity to the membrane; the composite film had over twice the conductivity of commercial Nafion at 120°C and 50% RH. The polyphenylsulfone nanofibers reduced the volumetric, gravimetric, and in-plane water swelling of the composite membrane

relative to a solution-cast film of 3M660 ionomer, with a lower areal swelling than Nafion 212.

Hydrogen/air fuel cell performance for a MEA with a 3M660/PPSU membrane (51 μm in dry thickness) was excellent. Power output at all tested conditions was higher than that for a Nafion-based MEA. At 100^{o}C and ambient pressure, power output was relativity insensitive to changes in the anode and cathode feed gas humidity for 50% < RH < 93%. The conductivity, dimensional stability, and fuel cell performance of the nanofiber composite membranes indicate that they are promising candidates for moderately high temperature fuel cell applications.

The remainder of this dissertation will focus on Nafion/PPSU nanofiber composites for direct methanol fuel cell applications. However, several avenues of research remain open regarding 3M660/PPSU membranes for H_2/air fuel cell applications. For instance, no optimization of membrane thickness and ionomer loading has been performed. Thinner membranes (<51 μm) with a higher ionomer loading (>72 vol% 3M660) should produce even more power when fabricated into a MEA and operated in a fuel cell. Additionally, the 3M660/PPSU membrane's and the 3M 825 EW binder's relative contributions to the 3M MEA's increased power output remain unresolved. Further studies should focus on testing both 3M660/PPSU and commercial Nafion membranes with a variety of EW binder polymers.

6.5 References

(1) Hamrock, S. J., Yandrastis, Michael A., *Polymer Reviews* **2006,** 46, 219-244.

(2) Zhu, X.; Liu, Y.; Zhu, L., In *Polymer Membranes for Fuel Cells*, Zaidi, S. M. J. M., Takeshi, Ed. Spring Science+Business Media, LLC: New York, 2009.

(3) Kreuer, K. D., *Journal of Membrane Science* **2001,** 185, (1), 29-39.

(4) Hamrock, S. J. DOE Annual Progress Report: Membranes and MEAs for Dry, Hot Operating Conditions. http://hydrogendoedev.nrel.gov/pdfs/progress09/v_d_13_hamrock.pdf

(5) de Araujo, C. C.; Kreuer, K. D.; Schuster, M.; Portale, G.; Mendil-Jakani, H.; Gebel, G.; Maier, J., *Physical Chemistry Chemical Physics* **2009,** 11, (17), 3305-3312.

(6) Schuster, M.; de Araujo, C. C.; Atanasov, V.; Andersen, H. T.; Kreuer, K. D.; Maier, J., *Macromolecules* **2009,** 42, (8), 3129-3137.

(7) Huang, X. Y.; Solasi, R.; Zou, Y.; Feshler, M.; Reifsnider, K.; Condit, D.; Burlatsky, S.; Madden, T., *Journal of Polymer Science Part B-Polymer Physics* **2006,** 44, (16), 2346-2357.

(8) Tang, H.; Peikang, S.; Jiang, S. P.; Wang, F.; Pan, M., *Journal of Power Sources* **2007,** 170, (1), 85-92.

(9) Nolte, R.; Ledjeff, K.; Bauer, M.; Mulhaupt, R., *Journal of Membrane Science* **1993,** 83, (2), 211-220.

(10) Kerres, J. A., *Fuel Cells* **2005,** 5, (2), 230-247.

(11) Ghassemi, H.; McGrath, J. E.; Zawodzinski, T. A., *Polymer* **2006,** 47, (11), 4132-4139.

(12) Gasa, J. V.; Weiss, R. A.; Shaw, M. T., *Journal of Membrane Science* **2007,** 304, (1-2), 173-180.

(13) Guan, Y. S.; Pu, H. T.; Pan, H. Y.; Chang, Z. H.; Jin, M., *Polymer* 51, (23), 5473-5481.

(14) Lee, M.; Park, J. K.; Lee, H. S.; Lane, O.; Moore, R. B.; McGrath, J. E.; Baird, D. G., *Polymer* **2009,** 50, (25), 6129-6138.

(15) Swier, S.; Ramani, V.; Fenton, J. M.; Kunz, H. R.; Shaw, M. T.; Weiss, R. A., *Journal of Membrane Science* **2005,** 256, (1-2), 122-133.

(16) Choi, J.; Lee, K. M.; Wycisk, R.; Pintauro, P. N.; Mather, P. T., *Macromolecules* **2008,** 41, (13), 4569-4572.

(17) Choi, J.; Lee, K. M.; Wycisk, R.; Pintauro, P. N.; Mather, P. T., *Journal of the Electrochemical Society* **2010,** 157, (6), B914-B919.

(18) Choi, J.; Lee, K. M.; Wycisk, R.; Pintauro, P. N.; Mather, P. T., *Journal of Materials Chemistry* **2010,** 20, (30), 6282-6290.

(19) Choi, J.; Wycisk, R.; Zhang, W. J.; Pintauro, P. N.; Lee, K. M.; Mather, P. T., *ChemSusChem* **2010,** 3, (11), 1245-1248.

(20) Lee, K. M.; Choi, J.; Wycisk, R.; Pintauro, P. N.; Mather, P., *ECS Transactions* **2009,** 25, (1), 1451-1458.

(21) Ballengee, J. B.; Pintauro, P. N., *Macromolecules* **2011,** 44, (18), 7307-7314.

(22) Loppinet, B.; Gebel, G.; Williams, C. E., *The Journal of Physical Chemistry B* **1997,** 101, (10), 1884-1892.

(23) Ballengee, J. B.; Pintauro, P. N., *Journal of the Electrochemical Society* **2011,** 158, (5), B568-B572.

(24) Chen, H.; Snyder, J. D.; Elabd, Y. A., *Macromolecules* **2008,** 41, (1), 128-135.

(25) Osborn, S. J.; Hassan, M. K.; Divoux, G. M.; Rhoades, D. W.; Mauritz, K. A.; Moore, R. B., *Macromolecules* **2007,** 40, (10), 3886-3890.

(26) Page, K. A.; Landis, F. A.; Phillips, A. K.; Moore, R. B., *Macromolecules* **2006,** 39, (11), 3939-3946.

(27) Garland, N. L.; Kopasz, J. P., *Journal of Power Sources* **2007,** 172, (1), 94-99.

(28) Kusoglu, A.; Karlsson, A. M.; Santare, M. H.; Cleghorn, S.; Johnson, W. B., *Journal of Power Sources* **2007,** 170, (2), 345-358.

(29) Kusoglu, A.; Karlsson, A. M.; Santare, M. H.; Cleghorn, S.; Johnson, W. B., *Journal of Power Sources* **2006,** 161, (2), 987-996.

(30) Ballengee, J. B.; Pintauro, P. N., *Submitted* **2011**.

(31) Adjemian, K. T.; Lee, S. J.; Srinivasan, S.; Benziger, J.; Bocarsly, A. B., *Journal of the Electrochemical Society* **2002,** 149, (3), A256-A261.

(32) Boyer, C.; Gamburzev, S.; Velev, O.; Srinivasan, S.; Appleby, A. J., *Electrochimica Acta* **1998,** 43, (24), 3703-3709.

(33) Cooper, K. R.; Ramani, V.; Fenton, J. M.; Kunz, H. R., *Experimental Methods and Data Analysis for Polymer Electrolyte Fuel Cells*; Scibner Associates, Inc.: Southern Pines, NC, 2009.

(34) Uribe, F. A.; Springer, T. E.; Gottesfeld, S., *Journal of the Electrochemical Society* **1992,** 139, (3), 765-773.

(35) Xu, H.; Song, Y.; Kunz, H. R.; Fenton, J. M., *Journal of the Electrochemical Society* **2006,** 153, (1), L1-L1.

(36) Zhang, J.; Tang, Y.; Song, C.; Xia, Z.; Li, H.; Wang, H.; Zhang, J., *Electrochimica Acta* **2008,** 53, (16), 5315-5321.

CHAPTER VII

MULTI-LAYER NAFION/PPSU ELECTROSPUN COMPOSITE MEMBRANES

7.1 Introduction

Direct methanol fuel cells (DMFCs) are an attractive energy conversion device. DMFCs have high energy densities and compared to hydrogen fuel cells, the methanol fuel is easier to store and transport.[1] However, DMFC membranes, most notably the benchmark material Nafion, are plagued by high methanol crossover from the fuel cell's anode to the cathode.[2] Methanol crossover reduces DMFC performance due to chemical oxidation of methanol at the air cathode. Oxidation at the cathode results in power loss via cell depolarization, consumption of oxygen without the generation of power, excessive water generation at the cathode that could lead to electrode flooding, and cathode catalyst poisoning from CO (an intermediate of methanol oxidation). Furthermore, a high transmembrane methanol flux results in inefficient consumption of the fuel at the anode, i.e., methanol must be over-supplied to account for losses through the membrane. Crossover can be reduced by diluting methanol with water and using thicker membranes, thus reducing the concentration-gradient/driving-force for methanol transport. Unfortunately dilution with water results in excess system weight/volume and the use of a thick membrane reduces power output due to higher membrane ohmic resistance. A more desirable solution is to develop new membranes with reduced methanol permeability and low ohmic resistance. One approach to prepare such membrane is through blending.

Nafion has been blended with a number of different materials in order to reduce its methanol permeability. For example, Si et al.[3] prepared solution-cast blends of Nafion with polyvinylidene fluoride (PVDF). The presence of the methanol blocking PVDF dramatically reduced methanol permeability; however proton conductivity was also reduced far in excess of the PVDF volume fraction. Thus, films with 55 wt% PVDF had a methanol permeability of 1.1 $x10^{-8}$ cm^2/s, but a proton conductivity of only 6 mS/cm, as compared to $1.1x10^{-6}$ cm^2/s and ~100 mS/cm for 1100 EW Nafion. In order to take advantage of the methanol blocking abilities of this blend without sacrificing too much conductivity, Si and co-workers sandwiched a 10 μm Nafion/PVDF film between two 20 μm Nafion films, such that the final membrane construct had an effective conductivity of 33 mS/cm and a permeability of 3.6 x 10^{-7} cm^2/sec. A membrane-electrode-assembly with this membrane generated ~28% higher maximum power output than Nafion 117 for a fuel cell operated at 60°C with 1 M methanol. A number of other Nafion-blends have been fabricated, including thermally blended/extruded films of Nafion and fluorinated ethylene-propylene (FEP) and solution-cast blends of Nafion and poly(benzimidazole) (PBI).[4,5] In the latter, a portion of the sulfonic acid groups present in Nafion were ionically crosslinked with the PBI's imidazole nitrogens. Both Nafion-FEP and Nafion-PBI composite membranes had reduced proton conductivity (undesirable) and reduced methanol permeability (desirable) when the hydrophobic/methanol-blocking component of the composite was present. Fortunately, the reduction in methanol permeability with increasing membrane hydrophobicity (i.e., as the amount of uncharged polymer increased) occurred more dramatically/rapidly than the decrease in proton conductivity. Thus, composite membranes with high loadings of hydrophobic polymer had a high

selectivity (selectivity here is defined as the ratio of proton conductivity to methanol permeability). A Nafion-FEP film with 70 wt% FEP had a selectivity 20 times higher than that of Nafion 117 and a Nafion-PBI film with 8 wt% PBI had a selectivity 4 times greater than that of Nafion 117. Unfortunately, these films had a low proton conductivity in water (~1.5 mS/cm for Nafion-FEP and 20 mS/cm for Nafion-PBI) which necessitated the need for very thin films in a DMFC membrane-electrode-assembly (<3 μm and <20 μm for Nafion-FEP and Nafion–PBI, respectively). Membranes this thin typically cannot withstand the mechanical processing of membrane-electrode-assembly fabrication. Composite films suitable for fuel cell testing (i.e., those with less FEP or PBI, higher conductivity, and higher thickness) were found to perform similarly to Nafion 117 in a DMFC when 1 M methanol was used as a feed, but outperformed Nafion when higher feed concentrations (5 M and 10 M methanol) were used.

In 2008 electrospinning was introduced as an alternative polymer-blending technique for fuel cell membrane preparation.[6] The first membranes were fabricated by electrospinning an ionomer fiber mat and then impregnating a hydrophobic polymer into the ionomer's interfiber void space.[6-9] In Chapter IV, this electrospinning technique was refined/improved to eliminate the need for an impregnation step.[10] In the so-called dual-fiber electrospinning technique, ionomer and hydrophobic polymer fibers are spun separately but simultaneously into a single mat. Follow-on processing of the mat results in one of two distinct membrane structures: i) ionomer fibers encapsulated in hydrophobic (uncharged) polymer, or ii) an ionomer film reinforced by hydrophobic polymer nanofibers. Composite films fabricated in this way were found to have a number of desirable properties including: reduced membrane swelling in water, in-plane

proton conductivity that was a linear function of ionomer volume fraction with no observed percolation threshold, and enhanced mechanical properties as compared to neat ionomer films. These properties translated into excellent hydrogen/air fuel cell performance. For example, an electrospun Nafion film reinforced by polyphenylsulfone (PPSU) nanofibers had the same fuel cell power output as commercial Nafion 212, but lasted 54% longer in an accelerated durability test.[10]

A yet unexplored potential advantage of the dual-fiber technique is the ability to easily control the spatial variation of the polymer components' volume fraction in the direction perpendicular to the membrane surface. Thus, membranes with layered structures can be easily manufactured by sequentially changing the relative amounts of ionomer and uncharged polymer fibers that are spun into a fiber mat. For example, a membrane with three layers may be constructed: two 20 μm outer layers containing 60 vol% Nafion and 40 vol% PPSU and an inner layer only 5 μm thick and containing 10 vol% Nafion and 90 vol% PPSU.

This ability to vary the polymer volume fraction within a single film has potential applications for methanol fuel cell membranes in which a thin, methanol-barrier layer is incorporated into a thicker nanofiber composite film. Such an approach takes advantage of the methanol-barrier properties of composites with high hydrophobic polymer loading, but whose low conductivity necessitates that they be very thin (to minimize ohmic resistance). The thick, conductive outer layers allow the membrane to be made into a thick film which is easy to handle and can withstand the processing required to prepare membrane-electrode-assemblies.

In this chapter, relevant methanol fuel cell properties are presented for single-layer and multi-layered Nafion/PPSU dual-fiber electrospun composite membranes. Proton conductivity, water swelling, methanol permeability, and membrane selectivity are presented as a function of Nafion volume fraction. Additionally, the fabrication procedure and properties of layered membrane structures with an inner methanol barrier are described and discussed. Finally, methanol fuel cell performance for the electrospun films is shown.

7.2 Experimental

7.2.1 Electrospinning

Fiber mats were electrospun using the dual-fiber electrospinning technique as discussed in Chapter IV. Note that Nafion nanofibers require the addition of a carrier polymer such as poly(ethylene oxide) (PEO).[11] Nafion lacks polymer chain entanglements and forms a micellar dispersion in solvent.[12] Thus, it cannot be electrospun without the addition of a carrier polymer to provide the entanglement necessary for electrospinning. In these electrospinning experiments, PEO with MW=400,000 Da was used in a 99:1 wt. ratio of Nafion:PEO. PEO was extracted after membrane fabrication by boiling the final films in acid and then water. PPSU fibers were electrospun without the addition of a carrier polymer.

Multi-layer membranes, which will be referred to as trilayers, were fabricated by varying the relative flow rates of the Nafion/PEO and PPSU spinning solutions over the course of an electrospinning experiment. The electrospinning flow rates for the different trilayer membranes prepared for this Chapter are given in Tables 7.1-7.3.

Table 7.1. Electrospinning flow rates for a trilayer membrane to produce a membrane with 60 vol% Nafion outer layers and a 15 vol% Nafion inner/barrier layer.

Layer	Nafion Flow Rate (mL/hr)	PPSU Flow Rate (mL/hr)
1st layer (60% Nafion, 40% PPSU)	0.20	0.038
2nd layer (15% Nafion, 85% PPSU)	0.20	0.35
3rd layer (60% Nafion, 40% PPSU)	0.20	0.038

Table 7.2 Electrospinning flow rates for a trilayer membrane to produce a membrane with 55 vol% Nafion outer layers and a 15 vol% Nafion inner/barrier layer.

Layer	Nafion Flow Rate (mL/hr)	PPSU Flow Rate (mL/hr)
1st layer (55% Nafion, 45% PPSU)	0.20	0.04
2nd layer (15% Nafion, 85% PPSU)	0.20	0.35
3rd layer (55% Nafion, 45% PPSU)	0.20	0.04

Table 7.3. Electrospinning flow rates for a trilayer membrane to produce a membrane with 60 vol% Nafion outer layers and a 8 vol% Nafion inner/barrier layer.

Layer	Nafion Flow Rate (mL/hr)	PPSU Flow Rate (mL/hr)
1st layer (60% Nafion, 40% PPSU)	0.20	0.038
2nd layer (8% Nafion, 92% PPSU)	0.10	0.40
3rd layer (60% Nafion, 40% PPSU)	0.20	0.038

7.2.2 Membrane fabrication

Single layer mats, i.e., those with a uniform distribution of Nafion and PPSU, and trilayer dual fiber mats were processed into either i) membranes with Nafion fibers

encapsulated in PPSU (Structure 1) or ii) Nafion films reinforced by PPSU fibers (Structure 2) as discussed in Chapter IV and Reference 10.

Structure 1 (*Nafion nanofibers encapsulated in PPSU)*: Both single layer and trilayer composite membranes with Nafion fibers encapsulated in PPSU polymer were fabricated by compressing dual-fiber mats to 70 psi, then exposed to chloroform vapor for 16 minutes at 25^{o}C. Membranes were then dried at 70^{o}C for 1 hour and 140^{o}C for 10 minutes and later annealed for 2 hours at 150^{o}C. After annealing, the membranes were boiled in 1 M H_2SO_4 and H_2O to ensure full protonation of Nafion's sulfonic acid sites as well as to extract the PEO carrier polymer from the membrane. PEO dramatically reduces Nafion's conductivity and thus its extraction is an important step.

Structure 2 (Nafion films reinforced by PPSU nanofibers): Both single layer and trilayer composite membranes were prepared by hot pressing a dual-fiber mat at 15,000 psi and ~127^{o}C for ~40 seconds and then immediately annealing 2 hours at 150^{o}C. After annealing, the membranes were boiled in 1 M H_2SO_4 and H_2O.

7.2.3 Scanning electron micrographs

Scanning electron micrographs were imaged as discussed in Chapter IV, section 4.2.3.

7.2.4 In-plane proton conductivity

In-plane proton conductivity of water-equilibrated films was measured as in Chapter IV. Proton conductivity was also measured for membranes equilibrated in 1 M methanol, but the conductivity did not significantly deviate from that in liquid water.

7.2.5 Through-plane proton conductivity

Through-plane conductivity for samples immersed in liquid water at 25°C was determined with a custom-built cell (see Figure 7.1). Membrane samples were clamped between two polished copper electrodes with an active area of only 0.0507 cm^2; the area was kept small in order to reduce the interfacial/contact impedance. The clamping pressure was fixed at 310 psi with a Hookean spring (Gardner GC480-038-0875). The pressure was chosen based on the work of Cooper et. al[13] who previously found 310 psi to be a suitable compression pressure for through-plane testing of Nafion films. A two-electrode AC impedance technique was then used to determine the ohmic resistance of the membrane.

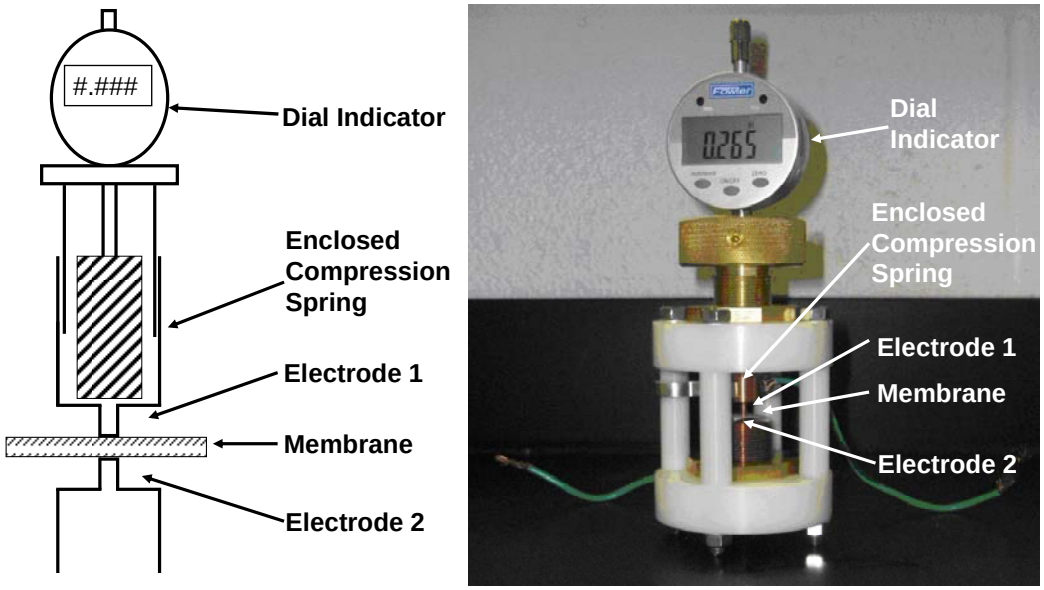

(a) (b)

Figure 7.1. a) Schematic of through-plane conductivity apparatus, and (b) photo of through-plane conductivity apparatus.

The new through-plane conductivity cell was first tested using commercial Nafion films and nanofiber composite films with a uniform composition (i.e., trilayer films were evaluated only after fully testing the apparatus on films with a well-characterized composition/structure). In order to minimize the effects of interfacial/contact impedance, membranes of different thickness were tested either by i) fabricating the same membrane material with different thickness or ii) by stacking sheets of membranes on top of each other. Both methods gave the same result, indicating no measurable membrane-membrane contact resistance. Measured resistances, taken from a Nyquist plot like that in Figure 7.2, were extrapolated to zero-thickness (as shown in Figure 7.3) to determine the interfacial/contact impedance. The through-plane conductivity was then calculated from Equation 7.1. Further details about through-plane conductivity testing are included in Appendix E.

$$\sigma_{through-plane} = \frac{\delta}{(R_{measure} - R_{interfacial})A} \tag{7.1}$$

where $\sigma_{through\text{-}plane}$ [S/cm] is through-plane proton conductivity, δ is the sample's thickness, $R_{measure}$ [Ω] is the measured resistance between the electrodes, $R_{interfacial}$ [Ω] is the calculated surface impedance, and A [cm^2] is the electrode area.

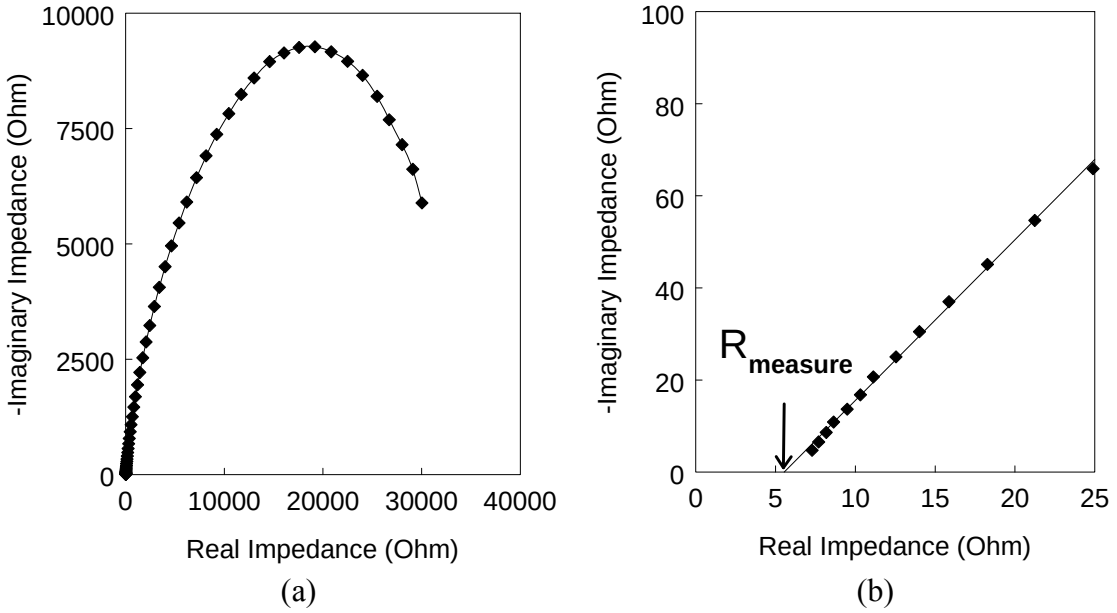

Figure 7.2. (a) Example Nyquist plot, and (b) high-frequency region of the same Nyquist plot. The measured resistance is the real resistance when the imaginary resistance is zero. If necessary the high frequency region of the curve was extrapolated until the imaginary resistance was zero, as shown above.

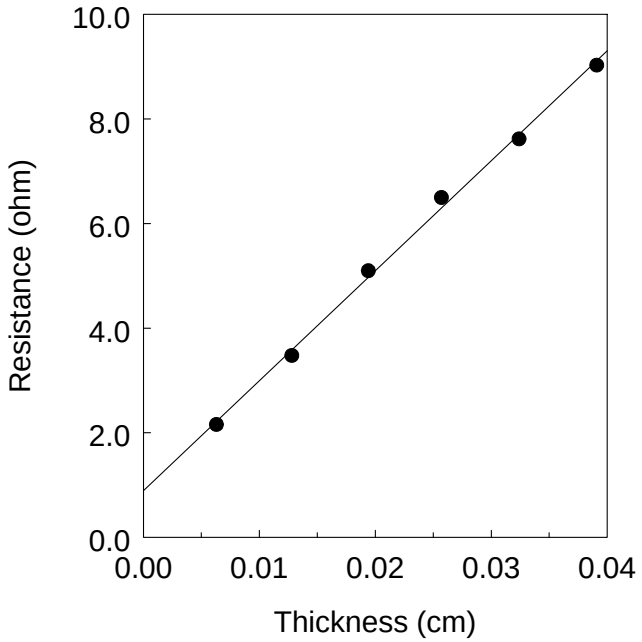

Figure 7.3. Representative plot of resistance as a function of membrane thickness for water-equilibrated Nafion 212. Resistance measurements were made in water at 25°C. The resistance at thickness = 0 (i.e., the interfacial/contact impedance) in this example is 0.89 ohms.

7.2.6 Methanol/water swelling

Gravimetric swelling was measured after soaking membrane samples in an appropriate methanol/water mixture for 12 hours. Excess solution on the membrane's surface was removed with filter paper immediately prior to the mass measurement. Swelling was determined by Equation 7.2.

$$\%\,Swelling = \frac{Mass_{wet} - Mass_{dry}}{Mass_{dry}} x100 \tag{7.2}$$

7.2.7 Methanol permeability

Methanol permeability was measured in a two-compartment diffusion cell at 25°C, as also used elsewhere.[4, 5, 14, 15] The membrane was clamped between the two glass compartments. One compartment was filled with 1 M methanol and the other (receiving) compartment was filled with DI water. As methanol permeated through the membrane, the methanol concentration in the receiving compartment was constantly monitored by circulating the liquid through a differential refractometer. The refractive index of the solution was linearly proportional to the methanol concentration as determined from calibration experiments. The fluid was circulated with an HPLC pump.

Methanol permeability was determined from the slope of a linear methanol concentration vs. time plot, using Equation 7.3.[16]

$$P = \frac{slope \times V \times \delta}{A \times \Delta C} \tag{7.3}$$

where P is permeability [cm^2/s], slope is the experimentally determined slope of the concentration vs. time curve [mol/L-s], V is the volume of the receiving chamber (34.8 cm^3), A is the membrane area (5.62 cm^2), and ΔC is the concentration gradient across the membrane at time = 0 (1 M methanol).

7.2.8 Membrane-electrode-assembly preparation

Direct methanol fuel cell membrane-electrode-assemblies (MEAs) were fabricated using electrodes prepared similarly to those described elsehwhere.[4, 5, 14] Anodes were composed of two catalyst layers. The first layer had a Pt:Ru black (Alfa Aesar #41171) loading of 3.0 mg/cm^2 and a Nafion binder content of 7 wt%. The second layer (that nearest the membrane) had a Pt:Ru black loading of 1.0 mg/cm^2 and a Nafion binder content of 23 wt%. Cathodes were also prepared as two-layer catalyst structures. The first layer had a Pt-black (Alfa Aesar #12755) loading of 3.0 mg/cm^2 and 7 wt% Nafion binder. The second layer, closest to the membrane, had a Pt-black loading of 1.0 mg/cm^2 and 29 wt% Nafion binder. Overall, both the anode and cathode each had a catalyst loading of 4.0 mg/cm^2.

Membrane-electrode-assemblies were prepared by hot pressing gas diffusion electrodes onto a membrane for 5 minutes at 140^oC and 55 psi using a Carver heated press. Gas diffusion electrodes (GDEs) were prepared by painting layers of catalyst ink onto carbon cloth until the desired catalyst loading was achieved. After each catalyst layer was painted the GDEs were dried at 70^oC for 30 minutes and the mass was recorded. Once the desired catalyst loading was achieved the electrodes were annealed at 140^oC for 10 minutes in vacuum and stored until ready for use.

After hot-pressing the anode and cathode onto the membrane the MEA was soaked in 1 M H_2SO_4 for several hours and H_2O for several hours prior to fuel cell testing.

7.2.9 Fuel cell testing

MEAs were tested in a 5 cm^2 fuel cell test fixture connected to an 850e Scribner Fuel Cell Test System. The MEAs were conditioned with air and 1 M methanol fuel at 25^oC and a constant current of 40 mA/cm^2 for two hours and then further conditioned for one hour at 60^oC and 40 mA/cm^2. Methanol was supplied by a LMI Milton Roy metering pump at a flow rate of 2 ml/min.

Polarization curves were obtained for methanol feed concentrations of 1 M, 5 M, and 10 M methanol at a flow rate of 2 ml/min. Air was supplied to the cathode at 500 sccm. The polarization curves were obtained by varying the fuel cell voltage in 0.05 V increments and measuring the current output. The fuel cell was equilibrated for 30 seconds at each voltage condition prior to recording the current.

The high-frequency resistance (or ohmic resistance) in an MEA was determined using the 850e's electrochemical impedance spectroscopy (EIS) capabilities. EIS data were collected at 100 mA/cm^2 with a 5% oscillation in the DC current.

The methanol crossover limiting current was determined by a linear sweep voltammetry method[17] using a Gamry Reference 3000 potentiostat, where the cathode voltage was scanned from 0 to 0.9 V. A schematic of the limiting current experimental setup is shown in Figure 7.4. During the limiting current experiment a methanol solution was supplied to the cathode at 5 mL/min and fully humidified nitrogen was pumped through the anode chamber at 200 sccm. An example voltammetric curve from a limiting

current experiment is shown in Figure 7.5. Limiting current can be related to permeability by Equation 7.4 and 7.5; note that Equation 7.4 corrects the limiting current for electro-osmotic drag effects in the fuel cell.[18]

$$\frac{J_{crossover}}{J_{\lim}} = \frac{6\xi\chi_o}{\ln[1+6\xi\chi_o]} \tag{7.4}$$

$$P = \frac{J_{crossover}\delta}{6FC} \tag{7.5}$$

where $J_{crossover}$ is the methanol crossover current, J_{lim} is the measured limiting current, ξ is the electro-osmotic drag coefficient (2.9 CH_3OH/H^+ at 60°C for Nafion),[19] χ_o is the molar fraction of methanol in the feed, F is Faraday's constant (96,485 C/mol), C is the methanol concentration in the feed, δ is the membrane thickness, and P is the membrane's methanol permeability.

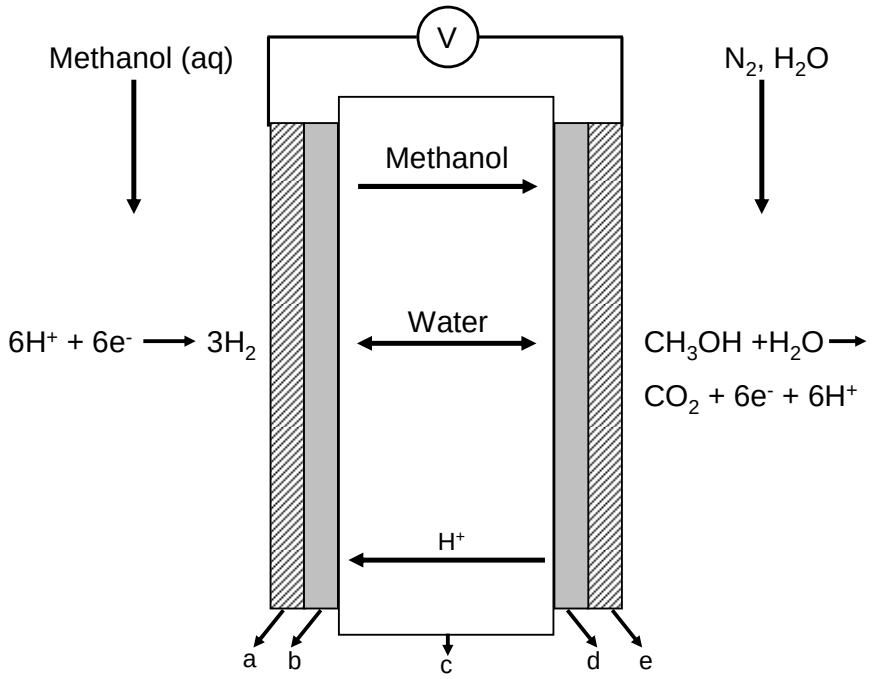

Figure 7.4. Experimental setup for a limiting current experiment. Figure adapted from Reference 17. (a) Carbon cloth on methanol feed side, (b) Pt:Ru electrode with Nafion binder, (c) membrane, (d) Pt electrode with Nafion binder, (e) carbon cloth on nitrogen side.

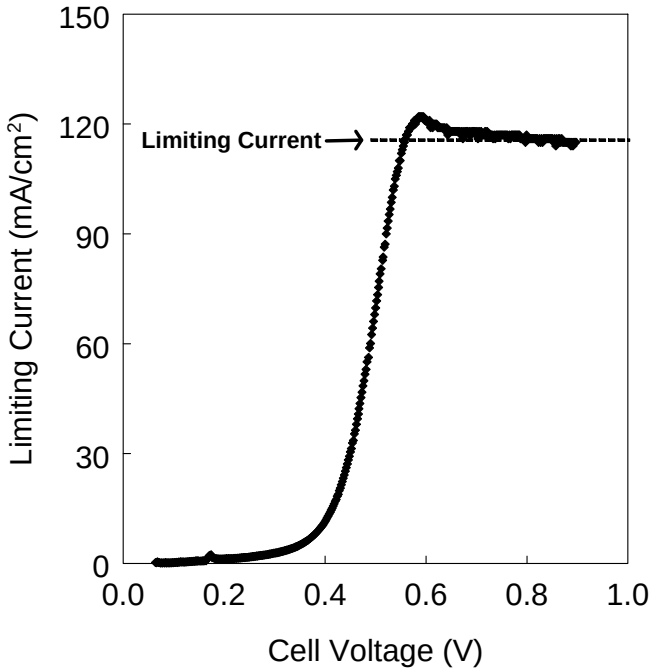

Figure 7.5. Voltametric curve resulting from a limiting current experiment with a Nafion 117 membrane using a 1 M methanol feed and at 60^{o}C.

7.3 Results and discussion

7.3.1 Structure 1: Nafion fibers encapsulated in PPSU

7.3.1.1 Single layer membranes (composite membranes with a uniform composition)

Composite membranes with Nafion fibers encapsulated in PPSU were prepared from mats of Nafion and PPSU, as shown in Figure 7.6a. The Nafion and PPSU fibers are both present, but indistinguishable in this scanning electron micrograph (SEM). Follow-on processing of the fiber mat (exposure to chloroform vapor, drying, annealing, and boiling in acid and water) resulted in a defect-free, dense membrane where Nafion nanofibers were surrounded by PPSU polymer. The surface of a dense membrane with this morphology is shown in Figure 7.6b and a freeze-fracture cross-section of a membrane is shown in Figure 7.6c. It is difficult to clearly see the Nafion fibers and PPSU-matrix in these images. However, the underlying Nafion-fiber structure was confirmed by extracting the PPSU component in a processed membrane, by soaking the membrane in liquid chloroform, a solvent for PPSU only. The underlying Nafion structure (top-down view) is shown in Figure 7.6d and a freeze-fracture cross-section image is shown in Figure 7.6e. The underlying PPSU structure was imaged by soaking a dense, but un-annealed composite film in alcohol:water solution, thus washing out the Nafion fibers. A cross-sectional image of the remaining PPSU is shown in Figure 7.6f. The "holes" in this picture are locations where Nafion fibers resided before extraction.

After membrane fabrication, membranes were tested for proton conductivity in liquid water. Proton conductivity as a function of Nafion volume fraction is shown in Figure 7.7a. The conductivity of Nafion fibers encapsulated in PPSU is anisotropic, i.e.,

the conductivity in the through-plane direction is lower than that in the in-plane direction. This is attributed to Nafion fibers higher connectivity in the in-plane direction as compared to that in the through-plane direction. While in-plane conductivity is the property most commonly reported in the fuel cell literature, through-plane conductivity is more relevant since ions migrate in the through-plane direction during fuel cell operation. This study highlights the importance of not relying on in-plane conductivity measurements alone for the characterization of composite fuel cell membranes.

The methanol permeability (in the through-plane direction) of composite membranes where Nafion nanofibers are embedded in PPSU is presented in Figure 7.7b. Like through-plane conductivity, the permeability is lower than that predicted by a simple mixing rule. PPSU is impermeable to methanol and thus its addition to the membrane affects methanol transport in two ways, it blocks methanol passage and creates a more tortuous pathway for methanol crossover through/in the Nafion fibers.

Selectivity (the ratio of proton conductivity to methanol permeability) is shown as a function of through-plane conductivity in Figure 7.8a (in absolute terms) and in Figure 7.8b (relative to that of commercial Nafion 117). The dashed line represents the selectivity that is calculated from curves fit to the through-plane conductivity and permeability data. For the most conductive membranes, i.e., those with the highest Nafion loading, the relative selectivity is lower than that of Nafion 117. However, as through-plane conductivity and Nafion volume fraction decrease, there is an increase in membrane selectivity, particularly at low Nafion loadings (<15 vol%). Normally membranes with such low conductivity would necessitate films so thin (<10 μm) as to make them impractical for fuel cell use (such films would be prone to defect pinholes and

would not have the requisite mechanical strength for MEA fabrication). However, by electrospinning multi-layered membranes, these selective materials can be incorporated as thin barriers within a thicker trilayer film where the total membrane thickness is reasonably high, e.g., 40 μm. Thus, the barrier layer's ohmic resistance is minimized while the thicker/overall film has sufficient mechanical strength to withstand fabrication into a MEA and fuel cell testing.

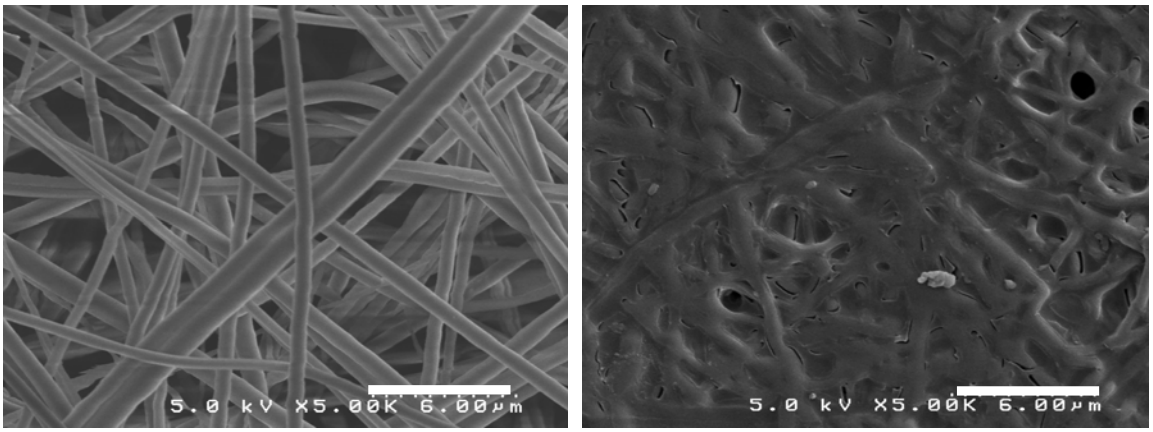

(a) (b)

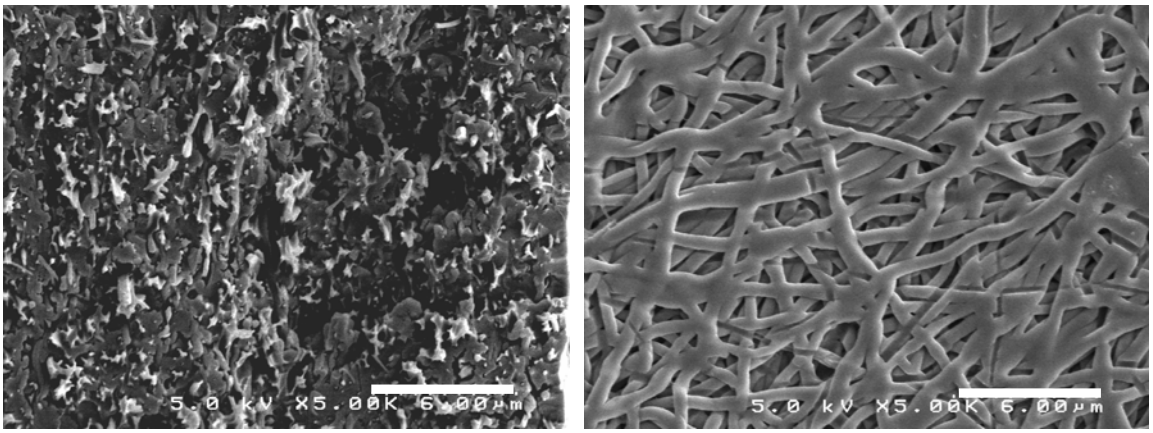

(c) (d)

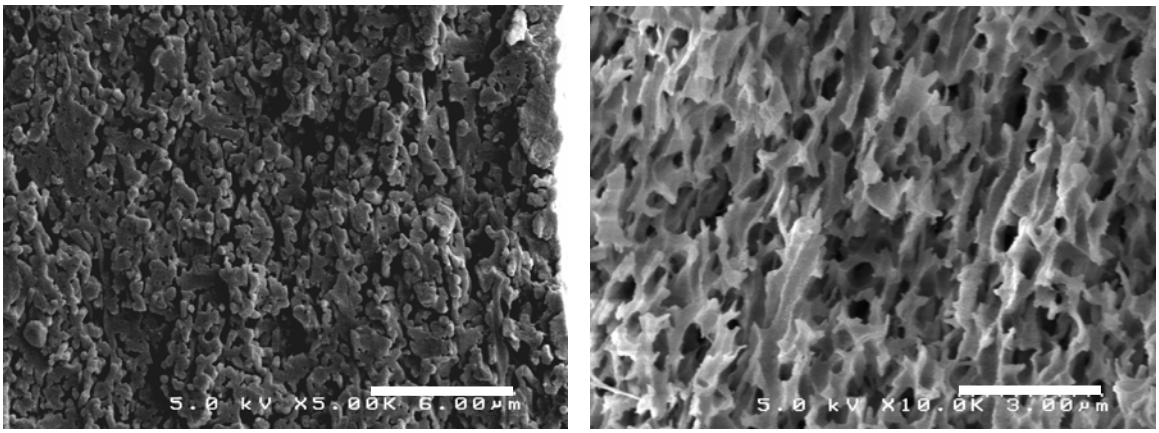

(e) (f)

Figure 7.6. SEMs of a membrane with Nafion fiber encapsulated in PPSU (~50 vol% Nafion): a) electrospun mat, b) densified membrane surface, c) membrane cross-section, d) surface of dense membrane with PPSU extracted e) cross-section of dense membrane with PPSU extracted f) cross-section of dense membrane with Nafion extracted. Scale bar for image a-e is 6 μm; scale bar for image f is 3 μm.

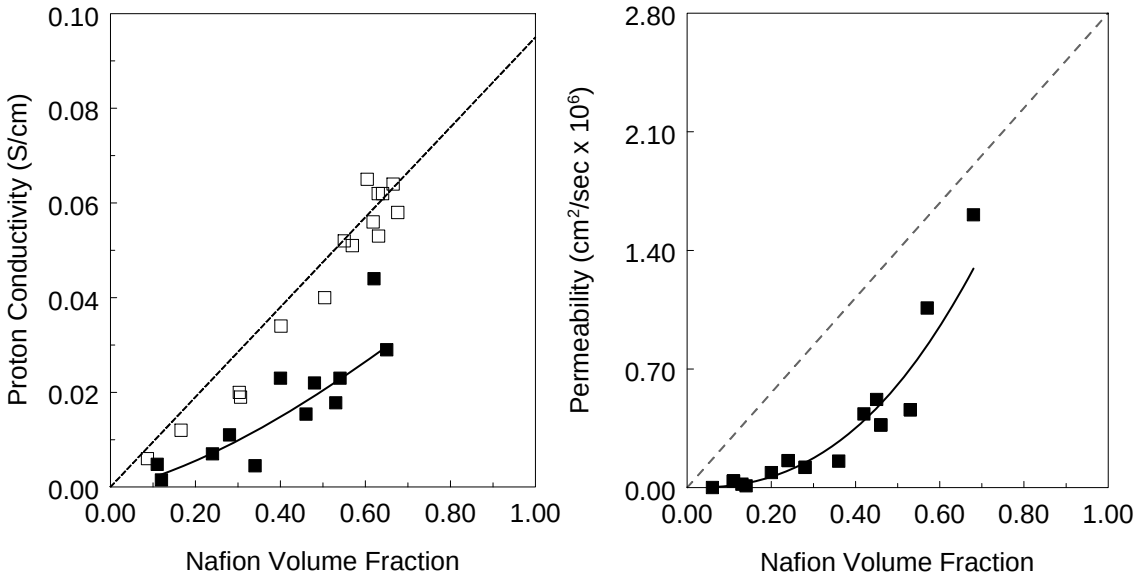

(a) (b)

Figure 7.7. (a) (□) In-plane and (■) through-plane conductivity as a function volume fraction for Nafion fibers encapsulated in PPSU. In-plane conductivity data was taken from Reference 10. (b) Methanol permeability (through-plane direction) for the same structure.

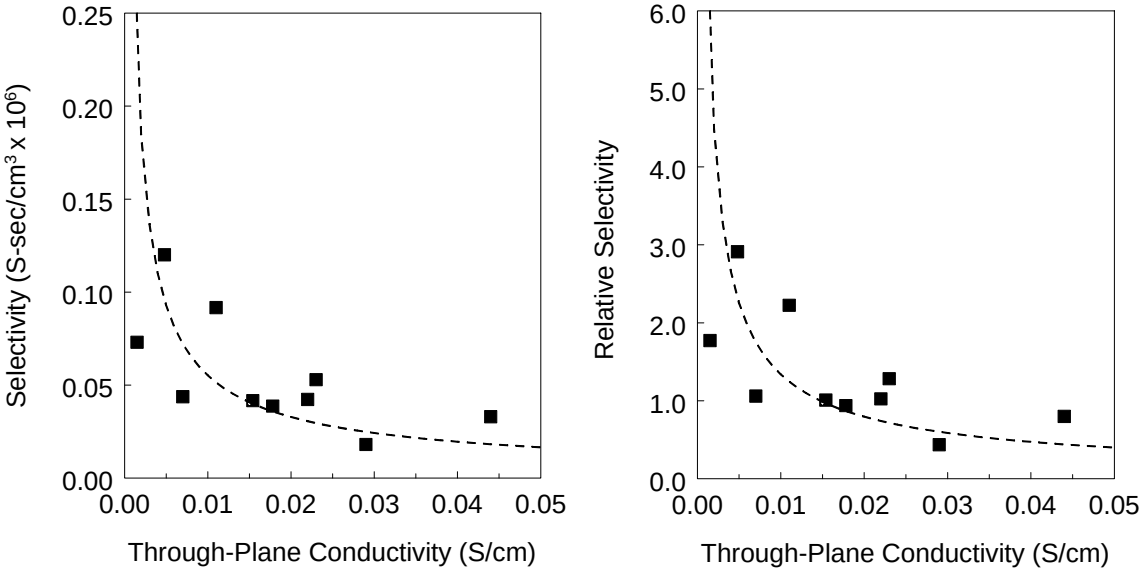

(a) (b)

Figure 7.8. (a) Selectivity as a function of through-plane conductivity for Nafion fibers encapsulated in PPSU. (b) Relative selectivity as a function of through-plane conductivity for Nafion fibers encapsulated in PPSU. Dashed line reflects the selectivity calculated from trendlines fit to proton conductivity and permeability data.

7.3.1.2 Trilayer membranes

Several trilayer membranes with Nafion fibers encapsulated in PPSU were fabricated by the dual fiber electrospinning process, as listed in Tables 7.1-7.3. For example, one membrane with 19 μm thick outer layers of ~55 vol% Nafion and having an inner layer, 8 μm thick of only 15 vol% Nafion, was fabricated by changing the relative flow rates of Nafion and PPSU during the electrospinning process. A SEM cross-section of this trilayer membrane is shown in Figure 7.9a. Figure 7.9b shows only the Nafion fiber component of the membrane (the PPSU was extracted by soaking the membrane in liquid chloroform). There is minimal connectivity of the Nafion fibers in the center (low Nafion content) layer which is anticipated to reduce transmembrane flux of both methanol and ions.

The properties of the layered membranes can be predicted from the properties of neat Nafion and PPSU membranes and the thickness and composition of each layer. Transport (i.e., proton conductivity and methanol permeability) in the trilayer membrane can be modeled as three resistors in series (for through-plane conductivity and permeability) or as three resistors in parallel (for in-plane proton conductivity). See Figure 7.10 for a schematic of the two resistance models and Equation 7.6-7.13 for relationships that describe the in-plane and through-plane conductivity and through-plane permeability of the trilayer films. The ionic resistances of the individual layers (R_1-R_3) are given by Equation 7.7 for conductivity and by Equation 7.8 for the methanol permeation resistances.[20] The final through-plane conductivity and methanol permeability of the layered membrane can be calculated by Equations 7.9 and 7.10, respectively.

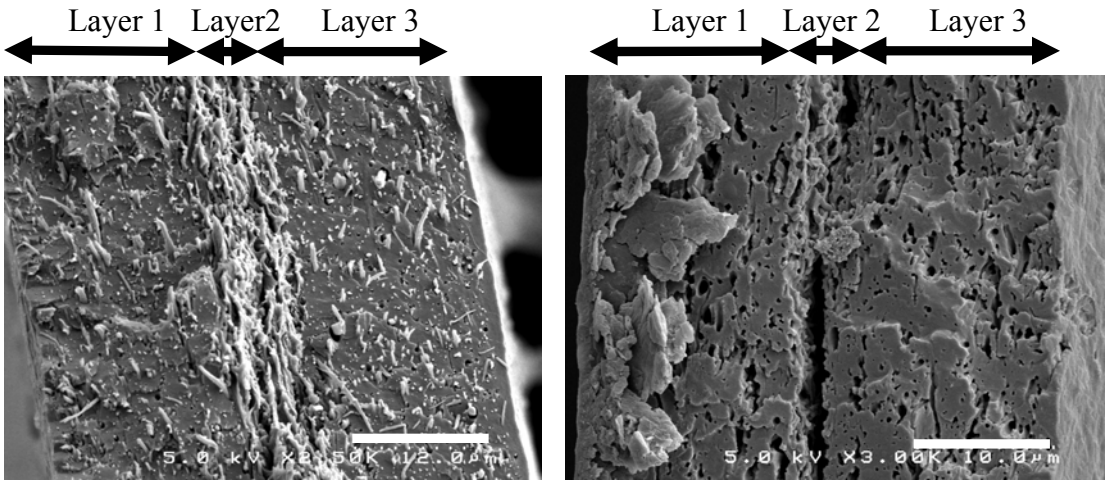

(a) (b)

Figure 7.9. (a) SEM cross-section of a trilayer membrane with Nafion fibers encapsulated by PPSU. Outer layers are ~55 vol% Nafion and 19 µm thick and the inner layer is ~15 vol% Nafion and 8 µm thick. Scale bar is 12 µm. (b) Image of same cross-section after extracting PPSU with chloroform solvent. Scale bar is 10 µm.

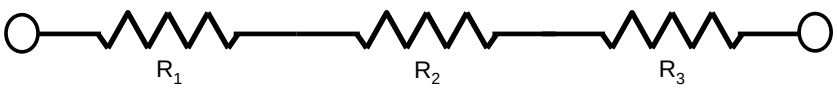

(a)

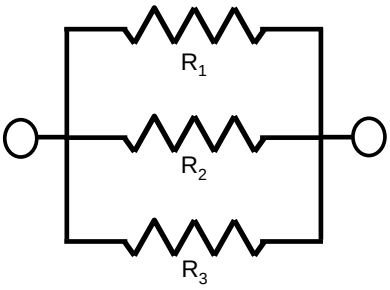

(b)

Figure 7.10. Resistor models for the prediction of trilayer membrane properties. (a) Resistors in series, used to predict through-plane conductivity and permeability, (b) resistors in parallel, used to predict in-plane conductivity

$$R_{lay,t.p.} = R_1 + R_2 + R_3 \tag{7.6}$$

$$R_{n,\Omega,t.p.} = \frac{\delta_n}{\sigma_n} \tag{7.7}$$

$$R_{n,P} = \frac{\delta_n}{P_n} \tag{7.8}$$

$$\sigma_{lay,t.p.} = \frac{\delta_{lay}}{R_{lay,\Omega,t.p}} \tag{7.9}$$

$$P_{lay} = \frac{\delta_{lay}}{R_{lay,P}} \tag{7.10}$$

where $R_{lay,t.p.}$ is the resistance of the layered membrane; R_1, R_2, and R_3 are the resistance of the three individual layers; $R_{n,\Omega,t.p}$ is the ohmic resistance of the n^{th} layer; and δ_n and σ_n are the thickness and conductivity of the n^{th} layers, respectively. $R_{n,P}$ is the permeation resistance (i.e., resistance to methanol flux) of the n^{th} layer; $\delta_{lay,t.p}$ and $\sigma_{lay,t.p.}$ are the thickness and conductivity of the entire layered membrane. $R_{lay,p}$ is the permeation resistance of the layered membrane. $\sigma_{lay,\ t.p,}$ and P_{lay} are the through-plane conductivity and permeability of the layered membrane. Note that no membrane area term appears in Equations 7.5-7.9 (conductivity and permeability are membrane area independent).

In-plane conductivity is calculated using Equations 7.11 - 7.13. This is the same conductivity that would be predicted by using a simple mixing rule, e.g., Nafion's bulk conductivity multiplied by the overall Nafion volume fraction.

$$\frac{1}{R_{lay,i.p.}} = \frac{1}{R_1} + \frac{1}{R_2} + \frac{1}{R_3} \tag{7.11}$$

$$R_{n,\Omega,i.p.} = \frac{1}{\sigma_n \delta_n} \tag{7.12}$$

$$\sigma_{lay,i.p.} = \frac{1}{R_{lay,i.p.}\delta_{lay}} \tag{7.13}$$

where $R_{lay,i.p.}$ is the resistance of the layered membrane; R_1, R_2, and R_3 are the resistance of the three individual layers; $R_{n,\Omega,i.p}$ is the ohmic resistance of the n^{th} layer; δ_n and σ_n are the thickness and conductivity of the n^{th} layers respectively. $\sigma_{lay,\ i.p,}$ is the final in-plane conductivity of the composite film.

The properties of the layered membrane shown in Figure 7.9 (Trilayer A) are presented in Table 7.4 along with two other trilayer membranes (Trilayer B and Trilayer C). Proton conductivity and methanol permeability were both measured experimentally and calculated using Equations 7.6-7.13, along with the estimated composition and thickness of the three layers. The selectivity of "Trilayer A" was 7.52 x 10^{-8} S-sec/cm^3, which translates into a relative selectivity (relative to commercial Nafion) of 1.83. The relative selectivity of "Trilayer B" and "Trilayer C" were 1.1 and 0.6 respectively.

The measured conductivities and permeabilities in Table 7.4 were somewhat different than expected/calculated. Reasons for this deviation may include: i) variability of electrospinning experiments, described in more detail in section 4.3.2 of Chapter IV, ii) difficulty in accurately determining the barrier layer thickness, which was estimated from SEM cross-sectional images, and iii) experimental errors inherent to the conductivity and permeability measurements, which may be on the order of 5-10%. In spite of these difficulties, the simple resistance model does allow for an approximate calculation of the measured conductivity and permeability.

No systematic attempt was made to determine the minimum barrier layer thickness, though membranes with barriers as thin as 2 μm were prepared. In principle the middle barrier layer can be made as thin as a single fiber, though in practice we expect that a small multiple of the fiber diameter is necessary to form a continuous barrier layer of uniform Nafion volume fraction.

Table 7.4 Methanol permeability and conductivity of several trilayer membranes (Trilayer A-C) with Nafion fibers encapsulated in PPSU. Calculated conductivity and permeability are based on Equations 7.6-7.13 and the composition/thickness of each trilayer film. All compositions are given in volume percent.

	Trilayer A	**Trilayer B**	**Trilayer C**
Outer layer thickness/ composition (% Nafion)	19 μm / (~55%)	19 μm / (~60%)	18 μm / (~60%)
Barrier layer thickness/ composition (% Nafion)	8 μm / (~15%)	5 μm / (~15%)	2.2 μm / (~8%)
Measured in-plane conductivity (mS/cm)	48	42	58
Calculated in-plane conductivity (mS/cm)	46	52	54
Measured through-plane conductivity (mS/cm)	7.6	4.4	7
Calculated through-plane conductivity (mS/cm)	12	15	13
Measured permeability (cm^2/s) x 10^6	0.10	0.10	0.28
Calculated permeability (cm^2/s) x 10^6	0.15	0.22	0.11

Gravimetric swelling in methanol/water mixtures was measured for one trilayer membrane and compared to Nafion 117 (see Figure 7.11). The trilayer composite swells considerably less than Nafion at all methanol concentrations tested. Furthermore, the swelling reduction effect is more pronounced at higher methanol concentrations, i.e., the

trilayer has 36% lower swelling than Nafion at 1 M methanol, but 43% lower swelling at 10 M methanol. The reduced swelling is attributed to the confining/constricting presence of PPSU in the membrane and may also contribute to the reduced methanol permeability observed for these films.

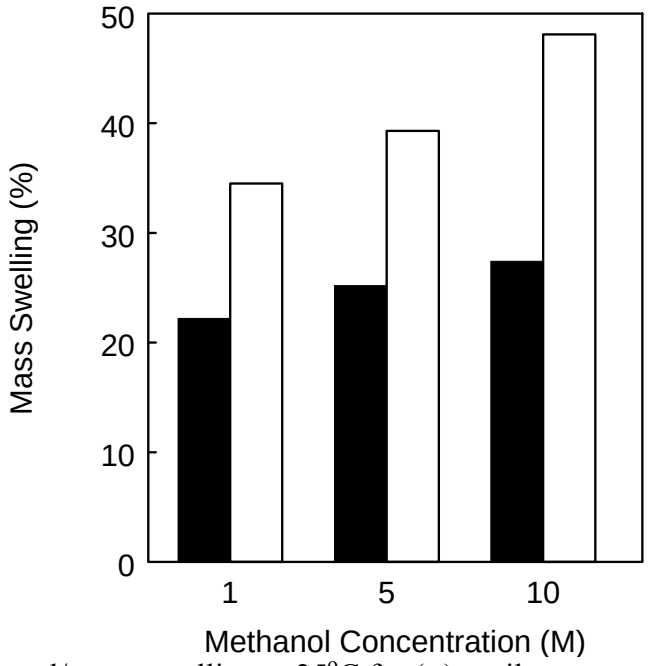

Figure 7.11. Methanol/water swelling at 25°C for (■) a trilayer nanofiber membrane and (□) Nafion 117. The trilayer membrane has 19 μm outer layers (~60 vol% Nafion) and a 5 μm inner/barrier layer (~15 vol% Nafion).

7.3.1.3 Direct methanol fuel cell experiments

In order to determine if the reduced methanol permeability of the layered membranes had any benefit on fuel cell performance, a membrane with 19 μm outer layers (~60 vol% Nafion) and a 5 μm inner/barrier layer (~15 vol% Nafion) was fabricated into a membrane-electrode assembly (MEA) and tested in a direct methanol fuel cell. Polarization curves for the trilayer membrane MEA with 1 M, 5 M, and 10 M

methanol feeds are compared to those for a Nafion 117 MEA in Figure 7.12. Fuel cell power densities at an operating voltage of 0.4 V are shown in Figure 7.13. Methanol limiting current and ohmic resistance for each MEA is presented in Table 7.5 and Table 7.6 respectively.

As can be seen in Figures 7.12 and 7.13, the trilayer membrane (50 μm in total thickness) did not perform as well as Nafion 117 (200 μm in thickness) when the methanol concentration was 1 M. This is primarily attributed to the high ohmic resistance of the layered membrane relative to that of Nafion 117. At low methanol concentrations, ohmic resistance is the dominant membrane property determining power output; crossover is relatively low and of secondary concern.[21] However, as the methanol feed concentration increases, the performance of the trilayer composite membrane relative to that of Nafion improved. When operating at 0.4 V with 10 M methanol, the layered composite has a power density of 23 mW/cm^2, nearly 3 times higher than that of Nafion 117 (8 mW/cm^2). At higher methanol feed concentrations, methanol crossover significantly lowers fuel cell power output and thus the layered membrane's lower methanol crossover outweighs the detrimental effect of the higher ohmic resistance of the trilayer membrane (ohmic resistance was not a strong function of methanol concentration for either membrane). The layered composite's methanol limiting current was significantly lower than Nafion 117's at both 5 M and 10 M methanol. Thus, at 10 M methanol the methanol limiting current was 506 mA/cm^2, 39% lower than Nafion.

High methanol concentrations, such as 10 M, are desirable for fuel applications because a high methanol concentration feed means the methanol fuel tank will be smaller. Thus, layered composite membranes show promise for use in DMFCs with concentrated

methanol supplies, particularly after further optimization of both layer thickness and composition.

Table 7.7 shows the methanol permeability (calculated from Equation 7.4 and 7.5) for both Nafion 117 and the trilayer membrane. A comparison of Table 7.7 to Table 7.8 indicates that the calculated permeability for Nafion 117 is relatively close to the values for permeability measured in a diffusion cell (also note the differences in operating temperature, 25^{o}C for the diffusion cell vs. 60^{o}C for the permeability cell). Table 7.7 and 7.8 also show that Nafion's permeability does not dramatically change with the methanol feed concentration, similar to Ren et. al's observation of methanol transport's weak dependence on methanol solution concentration.[22] On the other hand, the trilayer membrane has considerably higher permeability calculated inside the fuel cell when compared to that measured in a diffusion cell (1.1 x 10^-6 cm^2/s vs. 1.0 x 10^-7 cm^2/s at 1 M methanol). Surprisingly, the methanol permeability in the fuel cell decreases considerably as the methanol feed concentration increases even though permeability was not a strong function of methanol concentration when measured inside a diffusivity cell. The reason for this requires further investigation, but may be related to one of several factors. For one, the electro-osmotic drag coefficient is not known for trilayer membrane, but was assumed to be the same as neat Nafion (2.9 CH_3OH/H^+) for the permeability calculation. Additionally, the effects of differential swelling in different composite layers, interfacial effects within the trilayer, and membrane confinement within the fuel cell fixture remain unknown and may contribute to the discrepancy between permeability measured in the fuel cell and permeability measured in a diffusion cell.

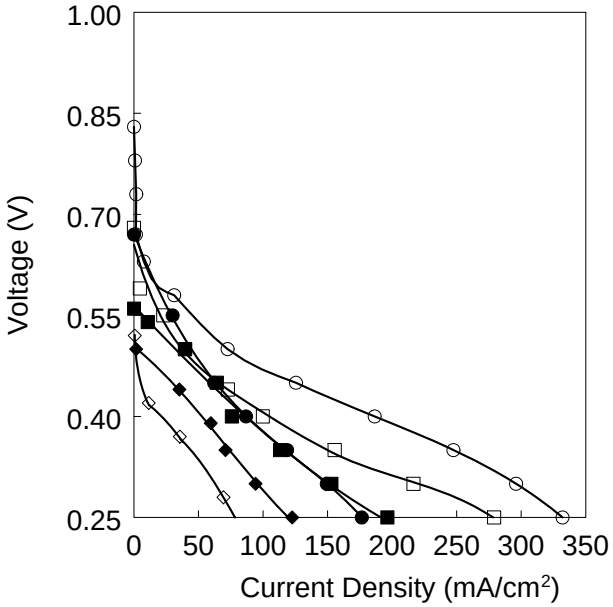

Figure 7.12. Polarization curves for a trilayer nanofiber composite at (●) 1 M methanol, (■) 5 M methanol, and (♦) 10 M methanol compared to Nafion 117 at (○) 1 M methanol, (□) 5 M methanol, and (◊) 10 M methanol. Each curve is the average of two tests conducted at 60°C. The trilayer membrane has 19 μm outer layers (~60 vol% Nafion) and a 5 μm inner/barrier layer (~15 vol% Nafion).

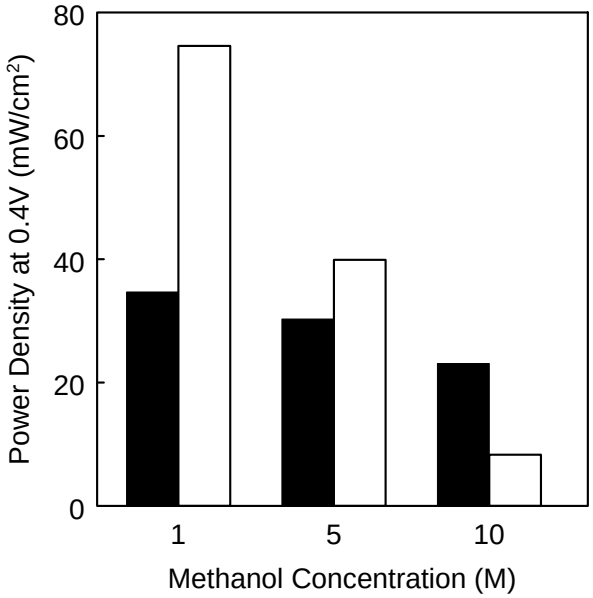

Figure 7.13. Power densities at 0.4 V for (■) a trilayer nanofiber membrane and (□) Nafion 117. The trilayer membrane has 19 μm outer layers (~60 vol% Nafion) and a 5 μm inner/barrier layer (~15 vol% Nafion).

Table 7.5. Methanol limiting current data for a layered nanofiber composite membrane and for Nafion 117. All data were collected at 60°C. The trilayer membrane has 19 μm outer layers (~60 vol% Nafion) and a 5 μm inner/barrier layer (~15 vol% Nafion).

Membrane	Limiting Current, 1 M Methanol (mA/cm^2)	Limiting Current, 5 M Methanol (mA/cm^2)	Limiting Current, 10 M Methanol (mA/cm^2)
Trilayer Nanofiber Composite	123	309	311
Nafion 117	115	415	506

Table 7.6. Ohmic resistance for a layered nanofiber composite membrane and for Nafion 117. All data were collected at 60°C. The trilayer membrane has 19 μm outer layers (~60 vol% Nafion) and a 5 μm inner/barrier layer (~15 vol% Nafion).

Membrane	Ohmic Resistance, 1 M Methanol (mΩ)	Ohmic Resistance, 5 M Methanol (mΩ)	Ohmic Resistance, 10 M Methanol (mΩ)
Trilayer Nanofiber Composite	58	61	63
Nafion 117	37	38	40

Table 7.7. Permeability calculated from methanol limiting current data and Equations 7.4-7.5 for a layered nanofiber composite membrane and for Nafion 117. All data were collected at 60°C. The trilayer membrane has 19 μm outer layers (~60 vol% Nafion) and a 5 μm inner/barrier layer (~15 vol% Nafion).

Membrane	Permeability, 1 M Methanol ($cm^2/s \times 10^6$)	Permeability, 5 M Methanol ($cm^2/s \times 10^6$)	Permeability, 10 M Methanol ($cm^2/s \times 10^6$)
Trilayer Nanofiber Composite	4.77	5.23	4.49
Nafion 117	1.09	0.83	0.59

Table 7.8. Methanol permeability determined from diffusion cell experiments at 25°C for Nafion 117 and a trilayer nanofiber composite. The trilayer membrane has 19 μm outer layers (~60 vol% Nafion) and a 5 μm inner/barrier layer (~15 vol% Nafion).

Membrane	Permeability, 1 M Methanol ($cm^2/s \times 10^6$)	Permeability, 15 M Methanol ($cm^2/s \times 10^6$)
Trilayer Nanofiber Composite	0.100	0.105
Nafion 117	2.40	2.53

7.3.2 Structure 2: Nafion films reinforced by PPSU nanofibers

7.3.2.1 Single-layer membranes (composites with a uniform composition)

Nafion films reinforced by PPSU fibers were prepared from electrospun fiber mats of Nafion and PPSU (i.e., the same starting fiber mat as shown in Figure 7.6a for Structure 1). Follow-on processing of the fiber mat (hot-pressing, annealing, and boiling in acid and water) resulted in a defect-free, dense membrane structure in which a Nafion film was reinforced by PPSU fibers (the inverse morphology of Structure 1). The surface of a dense membrane is displayed in Figure 7.14, a cross-section in Figure 7.14b, and a cross-section with only the Nafion component (after PPSU was leached out by soaking in chloroform) is shown in Figure 7.14c.

The proton conductivity (both through-plane and in-plane) for Nafion films reinforced by PPSU fibers is shown in Figure 7.15a. All samples were tested while immersed in DI water at 25^{o}C. The results show that proton conductivity is isotropic for these membranes, which contrasts with the divergence between the in-plane and through plane conductivity observed for the Structure 1 membranes. Furthermore, both in-plane and through-plane conductivity follow the same simple mixing rule, as has been discussed elsewhere (see Chapter IV and Reference 10).[10] No percolation threshold in ionomer content is observed for Nafion volume fractions as low as 15%, indicating that the Nafion component of the membrane is highly connected in all three dimensions regardless of its net volume in a given film.

Methanol permeability (in the through-plane direction) of Nafion films reinforced by PPSU fibers is shown in Figure 7.15b. Like proton conductivity, the permeability of these films is higher than that of Structure 1. The permeability is approximated by the

rule of mixtures, however, the permeability may subtly deviate from this simple mixing rule around 50 vol% Nafion. Further permeability studies are required to determine if this departure is an anomaly, though discontinuity in methanol permeability as a function of Nafion loading has been previously observed for composite membranes.[4, 23] Note that the permeability of a dense membrane fabricated from a Nafion nanofiber mat without PPSU (2.8×10^{-6} cm^2/s) is higher than that of commercial Nafion 212 and Nafion 117 (2.4×10^{-6} cm^2/s). This may be due to the higher swelling of electrospun Nafion when compared to commercial Nafion, a phenomenon observed by Laforgue et al.[24] Likewise, Nafion fibers densified into a homogeneous Nafion film also swell more in water. For example, a dense film prepared from Nafion fibers swells 43% in 100°C water, while a commercial Nafion membrane swells only 35%. A similar trend is anticipated for swelling in 1 M methanol (the concentration used to determine methanol permeability in these experiments) which may contribute to the higher measured methanol permeability.

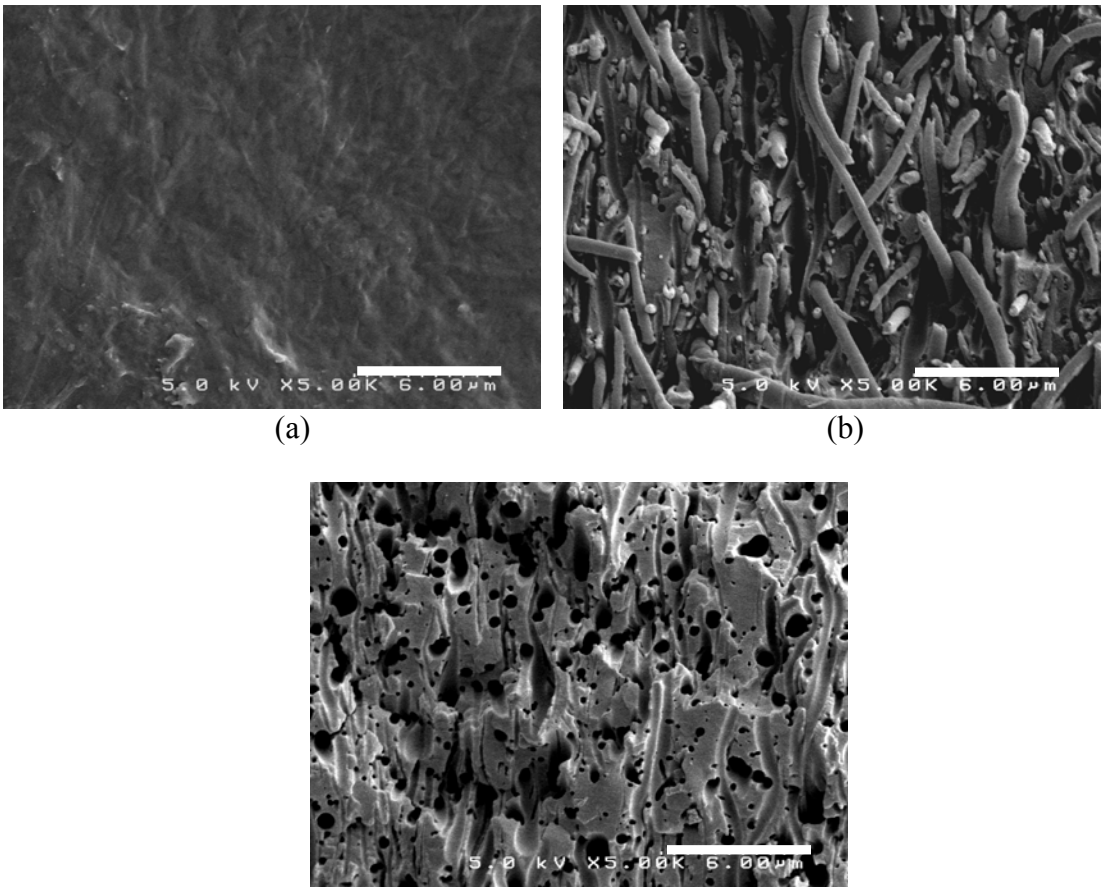

(a) (b)

(c)

Figure 7.14. SEMs of homogenous Nafion-PPSU composites (~50 vol% Nafion): a) membrane surface after densification, b) membrane cross-section, c) cross-section of dense membrane with PPSU extracted. Scale bars are 6 μm.

Permeability and proton conductivity decrease with decreasing Nafion volume fraction at a similar rate. Thus, for all Nafion loadings, the selectivity (the ratio of proton conductivity with units of S/cm to methanol permeability with units of cm^2/s) is approximately the same at 3.78×10^{-8} S-sec/cm^3. Nafion 117's selectivity is 4.12×10^{-8} S-sec/cm^3, thus the relative selectivity of Nafion films reinforced by electrospun PPSU fibers is ~0.92 (a lower selectivity is undesirable and shows that the membrane is less suitable for use in a DMFC, as compared to commercial Nafion).

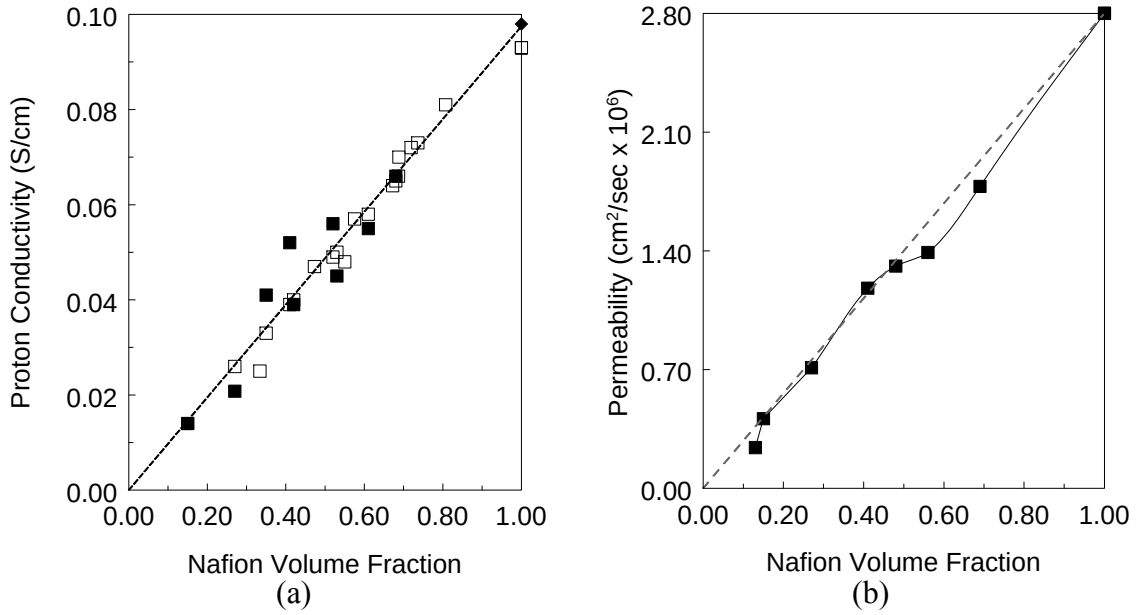

Figure 7.15. (a) (□) In-plane and (■) through-plane conductivity as a function of volume fraction for Nafion films reinforced by PPSU fibers. (♦) represents the in-plane and through-plane conductivity for Nafion 212. In-plane conductivity data was taken from Reference 10. (b) Methanol permeability for the same structure.

7.3.2.2 Trilayer membrane

For completeness, a trilayer membrane with Nafion films reinforced by PPSU fibers was fabricated by the dual fiber electrospinning process. A layered membrane with 21 μm thick outer layers of ~55 vol% Nafion and an inner layer, 6 μm thick, of only ~15 vol% Nafion was fabricated by changing the relative flow rates of Nafion and PPSU during the electrospinning process. A SEM cross-section of such a membrane is shown in Figure 7.16a. Figure 7.16b shows only the Nafion component of the membrane (the PPSU fibers were extracted by soaking in liquid chloroform). There is a high degree of Nafion connectivity in all three layers of the membrane, in strong contrast to the low degree of connectivity of the Nafion component in the Structure 1 trilayer films described above.

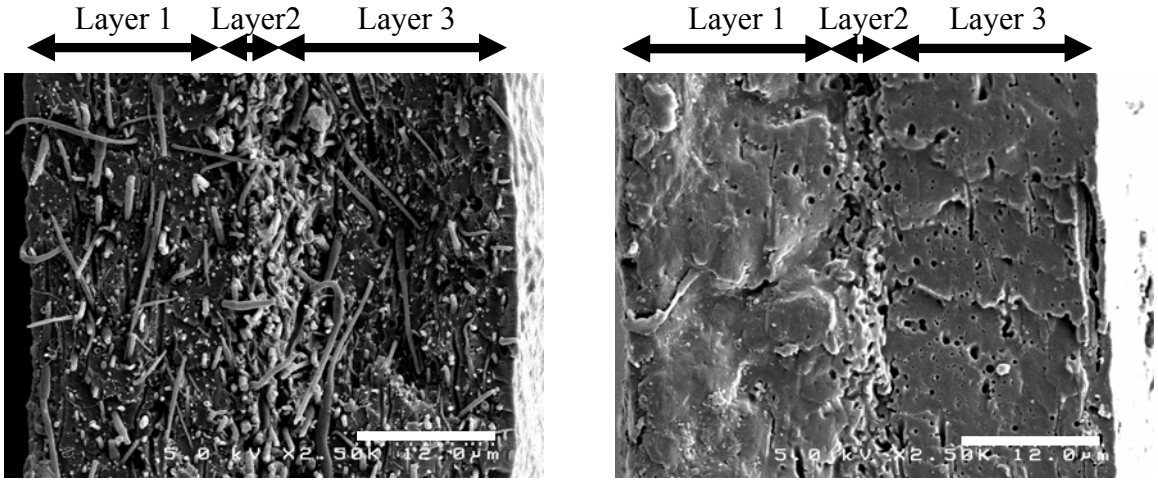

Figure 7.16. (a) SEM cross-section of layered membrane with Nafion reinforced by PPSU nanofibers. Outer layers are ~55 vol% Nafion and 21 μm thick, the inner layer is ~15 vol% Nafion and 6 μm thick. (b) Image of same cross-section after extracting PPSU nanofibers with chloroform solvent. Scale bars are 12 μm.

Measured and calculated proton conductivity and permeability are reported in Table 7.9 for the membrane shown in Figure 7.16. The measured selectivity of this particular tri-layer membrane was 3.43 x 10^{-8} S-sec/cm^3 (or a relative selectivity of 0.83), close to the selectivity of the single-layer composite films, i.e., those having a uniform Nafion/PPSU volume ratio. The calculated conductivity and permeability were obtained from Equations 7.6– 7.13 and the estimated composition and thickness of each layer. The measured transport properties were all slightly higher than predicted, most likely due experimental variations/errors discussed previously in section 7.3.1.2.

The permeability of Nafion films reinforced by PPSU fibers was not dramatically reduced relative to commercial Nafion's permeability and the selectivity of Nafion films reinforced by PPSU fibers is ~0.9 for all membranes, regardless of the volume fraction of

Nafion and the presence/absence of layering. Therefore such membranes were not chosen for testing in a direct methanol fuel cell.

Table 7.9. Actual and predicted performance of a trilayer membrane (Nafion film reinforced by PPSU nanofibers).

Property	Measured	Calculated*
Conductivity (mS/cm), in-plane	53	47
Conductivity (mS/cm), through-plane	49	41
Permeability (cm^2/s) x 10^6	1.5	1.1

*Based on Equations 7.6-7.13 and the compositions/thicknesses of each layer of the trilayer film. In the present example those compositions and thicknesses are: Outer layers are ~60 vol% Nafion and 21 μm thick, the inner layer is ~15 vol% Nafion and 6 μm thick

7.4 Conclusions

For the first time, layered nanofiber composite membranes were prepared. The dual-fiber electrospinning method was used to prepare trilayer composite films composed of Nafion and polyphenylsulfone (PPSU). Nafion and PPSU were electrospun from separate syringes onto a common collecting surface. A trilayer film was created by the flow rates of Nafion and PPSU during electrospinning, where one composition of Nafion/PPSU fibers was deposited directly on another to build a trilayer membrane morphology. Two different trilayer membrane structures were prepared from dual-fiber mats of Nafion and PPSU. One, in which Nafion nanofibers were surrounded by PPSU and a second structure where a Nafion film was reinforced by PPSU fibers. In the latter case, the measured proton conductivity at 25°C was isotropic (i.e., the same conductivity was measured in the in-plane and through-plane directions). Both conductivities followed a simple linear mixing rule based on the volume fraction of Nafion in the membrane. The through-plane methanol permeability also followed a Nafion volume fraction mixing

rule. The inverse structure of Nafion fibers encapsulated in PPSU exhibited anisotropic proton conductivity, where through-plane conductivity was lower than in-plane conductivity. Both the through-plane conductivity and permeability were lower than would be predicted by a simple mixing rule due to the tortuous pathway for methanol/proton transport (i.e., inter-fiber connectivity was low for this structure). At low Nafion volume fractions, these membranes were more selective than commercial Nafion (i.e., the ratio of proton conductivity to methanol permeability was greater than that for Nafion membranes) and thus were good candidates for incorporation as a thin methanol barrier layer in a trilayer composite membrane. One trilayer membrane with 55 vol% Nafion, 19 μm thick outer layers and an inner layer of ~15 vol% Nafion and 8 μm thick had a measured selectivity 83% higher than Nafion 117. A second layered membrane (with 19 μm outer layers, ~60 vol% Nafion and a 5 μm inner/barrier layer with ~15 vol% Nafion) was tested in a fuel cell and had nearly three times higher power output relative to Nafion 117 when 10 M methanol was used as the fuel, though this power output remained below Nafion 117's 1 M methanol power output.

Incorporation of thin barrier layers or gradient composite structures into a dense and defect-free membrane may have applications beyond blocking methanol in a DMFC. For example, a gas-tight polymer layer or reactive barrier could by introduced into a membrane to reduce gas permeability in a hydrogen/air fuel cell. Alternatively, the hydrophilicity of the membrane (the relative amount of ionomer) could be varied in the membrane thickness direction, from the anode to the cathode, to improve fuel cell water management. Additionally, it is envisioned that electrospinning of multilayered fiber structures can be easily carried out using standard roll-to-roll fabrication methods and

that such methods could be expanded to add the anode, cathode, and gas diffusion layers to a multilayer nanofiber composite membrane.

7.5 References

(1) Ren, X.; Zelenay, P.; Thomas, S.; Davey, J.; Gottesfeld, S., *Journal of Power Sources* **2000,** 86, (1-2), 111-116.

(2) Kreuer, K. D., *Journal of Membrane Science* **2001,** 185, (1), 29-39.

(3) Si, Y. C.; Lin, J. C.; Kunz, H. R.; Fenton, J. M., *Journal of the Electrochemical Society* **2004,** 151, (3), A463-A469.

(4) Lin, J.; Lee, J. K.; Kellner, M.; Wycisk, R.; Pintauro, P. N., *Journal of the Electrochemical Society* **2006,** 153, (7), A1325-A1331.

(5) Wycisk, R.; Chisholm, J.; Lee, J.; Lin, J.; Pintauro, P. N., *Journal of Power Sources* **2006,** 163, (1), 9-17.

(6) Choi, J.; Lee, K. M.; Wycisk, R.; Pintauro, P. N.; Mather, P. T., *Macromolecules* **2008,** 41, (13), 4569-4572.

(7) Choi, J.; Lee, K. M.; Wycisk, R.; Pintauro, P. N.; Mather, P. T., *Journal of the Electrochemical Society* **2010,** 157, (6), B914-B919.

(8) Choi, J.; Lee, K. M.; Wycisk, R.; Pintauro, P. N.; Mather, P. T., *Journal of Materials Chemistry* **2010,** 20, (30), 6282-6290.

(9) Choi, J.; Wycisk, R.; Zhang, W. J.; Pintauro, P. N.; Lee, K. M.; Mather, P. T., *ChemSusChem* **2010,** 3, (11), 1245-1248.

(10) Ballengee, J. B.; Pintauro, P. N., *Macromolecules* **2011,** 44, (18), 7307-7314.

(11) Ballengee, J. B.; Pintauro, P. N., *Journal of the Electrochemical Society* **2011,** 158, (5), B568-B572.

(12) Loppinet, B.; Gebel, G.; Williams, C. E., *The Journal of Physical Chemistry B* **1997,** 101, (10), 1884-1892.

(13) Cooper, K. R., *Journal of the Electrochemical Society* **2010,** 157, (11), B1731-B1739.

(14) Lin, J.; Wu, P. H.; Wycisk, R.; Trivisonno, A.; Pintauro, P. N., *Journal of Power Sources* **2008,** 183, (2), 491-497.

(15) Wycisk, R.; Lee, J. K.; Pintauro, P. N., *Journal of the Electrochemical Society* **2005,** 152, (5), A892-A898.

(16) Lee, C. H.; Park, H. B.; Chung, Y. S.; Lee, Y. M.; Freeman, B. D., *Macromolecules* **2005,** 39, (2), 755-764.

(17) Ren, X.; Springer, T. E.; Zawodzinski, T. A.; Gottesfeld, S., *Journal of the Electrochemical Society* **2000,** 147, (2), 466-474.

(18) Ren, X.; Springer, T. E.; Gottesfeld, S., *Journal of the Electrochemical Society* **2000,** 147, (1), 92-98.

(19) Ren, X. M.; Henderson, W.; Gottesfeld, S., *Journal of the Electrochemical Society* **1997,** 144, (9), L267-L270.

(20) Chung, T.-S.; Swee Phin Loh, E.; Shieh, J.-J., *Chemical Engineering Science* **2000,** 55, (6), 1093-1099.

(21) Zhang, J.; Wang, Y., *Fuel Cells* **2004,** 4, (1-2), 90-95.

(22) Ren, X. M.; Springer, T. E.; Zawodzinski, T. A.; Gottesfeld, S., *Journal of the Electrochemical Society* **2000,** 147, (2), 466-474.

(23) Park, J. W.; Pintauro, P., *ECS Transactions*, In Press.

(24) Laforgue, A.; Robitaille, L.; Mokrini, A.; Ajji, A., *Macromolecular Materials and Engineering* **2007,** 292, (12), 1229-1236.

CHAPTER VIII

CONCLUSIONS

(1) The first comprehensive electrospinning study of a common ionomer, DuPont's perfluorosulfonic acid (PFSA) known as Nafion®, was performed. Electrospinning conditions were identified for the preparation of well-formed Nafion nanofiber mats where the average fiber diameter could be set between 300 and 900 nm, as desired by the user. See Table 8.1 for these electrospinning conditions.

Table 8.1. Solution properties and electrospinning conditions to produce Nafion nanofiber mats with different average fiber diameters. For solution properties, a 2:1 wt. ratio alcohol:water solvent was always used and the PEO carrier polymer loading was always 1 wt% (on a total polymer weight basis). Under electrospinning conditions, SCD denotes the spinneret-to-collector distance.

Average Nanofiber Diameter	**Solution Properties**	**Electrospinning Conditions**
300 nm	Total polymer concentration: 15 wt% Solvent: 2-propanol/water PEO MW: 300 kDa	Applied voltage: 4.5 kV Flow rate: 0.2 mL/hr SCD: 5 cm Relative humidity: 20%
500 nm	Total polymer concentration: 20 wt% Solvent: 2-propanol/water PEO MW: 300 kDa	Applied voltage: 4 kV Flow rate: 0.2 mL/hr SCD: 6 cm Relative humidity: 40%
700 nm	Total polymer concentration: 25 wt% Solvent: 1-propanol/water PEO MW: 400 kDa	Applied voltage: 4 kV Flow rate: 0.4 mL/hr SCD: 5 cm Relative humidity: 30%
900 nm	Total polymer concentration: 25 wt% Solvent: 1-propanol/water PEO MW: 400 kDA	Applied voltage: 4 kV Flow rate: 0.6 mL/hr SCD: 5 cm Relative humidity: 30%

(2) A new dual-fiber electrospinning manufacturing method was introduced as a technique for the fabrication of proton exchange membranes (PEMs). Two distinct polymers, an ionomer and an uncharged material, were electrospun from separate syringes onto a common collecting surface. Follow-on processing allowed for the fabrication of two distinct structures, either i) an ionomer film reinforced by uncharged fibers or ii) ionomer fibers encapsulated in uncharged polymer. See Figure 8.1 for a schematic of the two membrane structures. Such structures could not be fabricated by a traditional solution-casting blending method. A variety of dual-fiber electrospun systems were studied in this work, and are listed in Table 8.2.

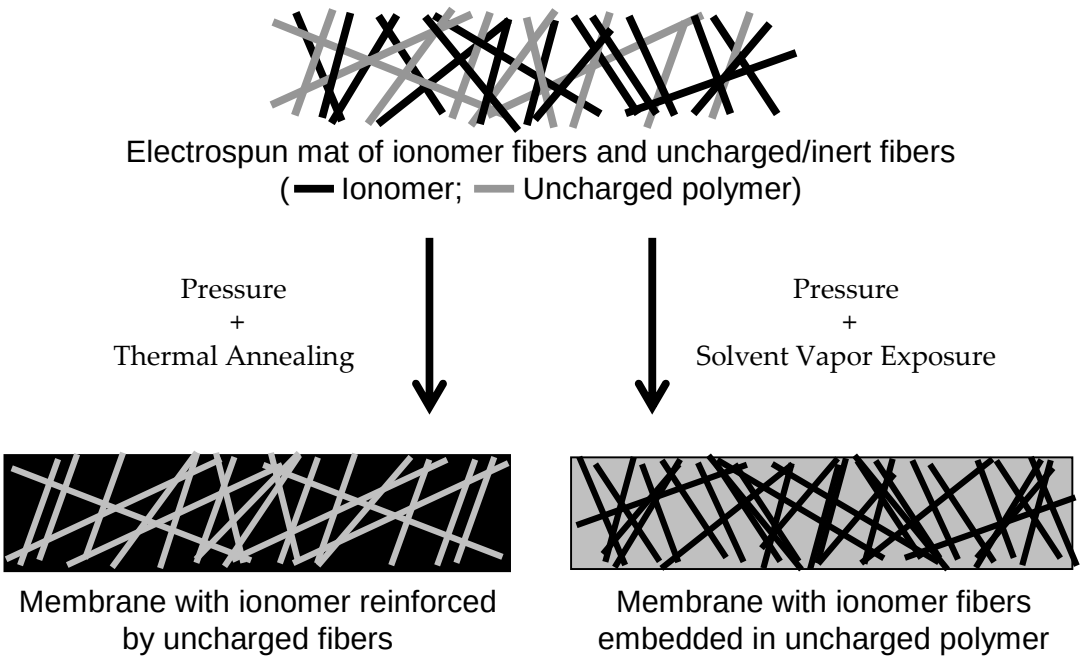

Figure 8.1. Schematic of dual-fiber mat and processing into two distinct membrane structures.

Table 8.2. Electrospun nanofiber composite membranes studied in this dissertation.

Ionomer	Uncharged Polymer	Structure(s)
Nafion PFSA (1100 EW)	PPSU	i) Ionomer film reinforced by uncharged nanofibers ii) Ionomer fibers encapsulated by uncharged polymer iii) Trilayer membranes with structure (i) iv) Trilayer membranes with structure (ii)
Nafion PFSA (1100 EW)	PVDF	i) Ionomer film reinforced by uncharged nanofibers
Nafion PFSA (1100 EW)	PBI-OO	i) Ionomer film reinforced by uncharged nanofibers
3M 660 EW PFSA	PPSU	i) Ionomer film reinforced by uncharged nanofibers
3M 825 EW PFSA	PPSU	i) Ionomer film reinforced by uncharged nanofibers

(3) Nafion films reinforced by one of three different uncharged fibers were fabricated: i) polyphenylsulfone (PPSU), ii) polyvinylidene fluoride (PVDF), or iii) poly-[(1-(4,4′-diphenylether)-5-oxybenzimidazole)-benzimidazole (PBI-OO). Of the three composite systems, those with Nafion and PPSU had the best combination of high proton conductivity and low water swelling (e.g., conductivity of 0.081 S/cm in water and 8% planar water swelling for a membrane with 81 vol% Nafion). Thus, this dissertation focused on using PPSU as the uncharged/reinforcing polymer.

(4) The Nafion and PPSU nanofiber composite membranes were the most well-studied. These materials exhibited several properties:

(a) In-plane proton conductivity (conductivity parallel to the membrane surface) was a product of the Nafion volume fraction and the bulk Nafion conductivity, thus obeying a simple linear mixing rule where proton conductivity was the product of the membrane's Nafion volume fraction and neat Nafion's proton conductivity. This rule was followed by both membrane structures (i.e., Nafion films reinforced by PPSU fibers and Nafion fibers encapsulated in PPSU). Thus,

a membrane that was 81 vol% Nafion had a conductivity of 0.081 S/cm in liquid water, which was ~81% the conductivity of neat Nafion (0.095 S/cm). Likewise a membrane that was 9 vol% Nafion had a conductivity equal to ~9% of Nafion's .

(b) Through-plane conductivity (conductivity perpendicular to the membrane surface) followed the same mixing rule for membranes with a Nafion film reinforced by PPSU fibers. However, when Nafion fibers were embedded in PPSU polymer the through-plane conductivity was below that predicted by the mixing rule, i.e., a through-plane conductivity of 0.023 S/cm was measured when the mixing rule predicted 0.051 S/cm for a nanofiber membrane with 54 vol% Nafion.

(c) The volumetric and mass water swelling were the same for both membrane structures and were below that predicted by the mixing rule. Thus, swelling was *not* the product of neat Nafion swelling and the composite's Nafion volume fraction. For example, membranes with 50 vol% Nafion had a volumetric swelling of ~20%, as compared to 45% if the mixing rule was followed.

(d) In-plane water swelling, a critical property for the mechanical durability of PEMs,[1, 2] was lower than that of commercial Nafion. Swelling was particularly low when a Nafion film was reinforced by PPSU nanofibers, e.g., only ~5% when the Nafion volume fraction in the membrane was 65 vol%. This compares to an in-plane swelling of ~15% for a membrane with the same Nafion volume fraction,

but with Nafion fibers encapsulated in PPSU. In-plane water swelling was 37% for Nafion 212. The low swelling of Nafion films reinforced by PPSU fibers was attributed to the low through-plane connectivity of PPSU fibers, thus favoring high swelling in the thickness direction and low swelling in the in-plane/areal direction.

(e) Nanofiber composite membranes had excellent properties with a mechanical strength higher than that of commercial Nafion 212 (measured at 30^{o}C, 20% RH). Additionally, Nafion fibers encapsulated in PPSU had higher strength than Nafion films reinforced by PPSU fibers (a proportional limit stress (PLS) of 21.1 MPa vs. 15.9 MPa for membrane with 61 vol% Nafion; this compares to a PLS of 11.9 MPa for Nafion 212). The difference between the two structures was attributed to the three dimensional connectivity of the PPSU when it encapsulated Nafion fibers versus the two dimensional connectivity of PPSU in the fiber form.

(f) Methanol permeability for Nafion films reinforced by PPSU fibers decreased linearly with decreasing Nafion volume fraction. Methanol permeability was lower for Nafion fibers encapsulated by PPSU and decreased non-linearly with reductions in Nafion volume fraction. Thus, for composites with a Nafion volume fraction of 42 vol%, the permeability of a membrane with Nafion reinforced by PPSU fibers was 1.2 cm^2/sec and was 0.4 cm^2/sec for a membrane with Nafion fibers encapsulated by PPSU. This compares to commercial Nafion's methanol

permeability of 2.4 cm^2/sec. (All permeability measurements were conducted at 25^oC with a membrane placed between 1 M methanol and water).

(g) Selectivity (through-plane proton conductivity in water divided by methanol permeability with 1 M methanol) was approximately 3.78 x 10^{-8} S-sec/cm^3 for all membranes in which a Nafion film was reinforced by PPSU fibers, as compared to 4.17 x 10^{-8} S-sec/cm^3 for commercial Nafion. However, selectivity increased with decreasing Nafion loading for membranes with Nafion fibers encapsulated in PPSU. Selectivity was high at low Nafion loading (≤ 15 vol%), e.g., 12.6 x 10^{-8} S-sec/cm^3 for a membrane with 11 vol% Nafion. This selectivity was 2.9 times higher than commercial Nafion's.

(5) A Nafion film reinforced with PPSU fibers (~65 vol% Nafion) was found to have an excellent combination of high proton conductivity (0.066 S/cm) and low water swelling, (particularly in the planar direction, 5%). Thus, this membrane (30 μm dry thickness) was selected for fabrication into a membrane-electrode-assembly (MEA) and hydrogen/air fuel cell testing (with 0.4 mg/cm^2 platinum electrodes). The MEA's power output at 80^oC, 100% RH and 0.6 V was 570 mW/cm^2, the same power output measured for a Nafion 212 MEA. In an accelerated durability/humidity-cycling test the nanofiber membrane MEA lasted over 54% longer than the Nafion 212 MEA, as determined by open circuit voltage and hydrogen limiting current experiments.

(6) Nafion and PPSU nanofiber mats could be fabricated into dense membranes within 15-18 minutes. The processing conditions are listed in Table 8.3.

Table 8.3. Summary of membrane processing conditions and membrane properties. Conductivity was measured at 80°C, 80% RH; mass swelling in 100°C water; and proportional limit stress was determined at 30°C for dry membranes. Both membranes were 56 vol% Nafion.

	Processing Conditions	**Conductivity (mS/cm)**	**Mass Swelling (%)**	**Proportional Limit Stress (MPa)**
Rapid Processing of Nafion-films reinforced by PPSU	1. Hot-press fiber mat ~40 seconds at 127°C 2. Anneal 5 min., 210°C 3. Boil 5 min. in 1 M H_2SO_4 and 5 min. in H_2O	48	18	23.5
Rapid Processing of Nafion fibers encapsulated in PPSU	1. Compact mat ~10 seconds at 25°C 2. Expose to 50°C chloroform vapor, 3min. 3 Anneal 5 min., 210°C 4. Boil 5 min. in 1 M H_2SO_4 and 5 min. in H_2O	48	23	21.9

(7) Nanofiber membranes were fabricated where a film of 3M Company's 825 EW PFSA was reinforced with PPSU fibers. These composite membranes had a desirable combination of high proton conductivity and low water swelling. One 825 EW-containing composite had similar proton conductivity as commercial Nafion in liquid water (0.096 S/cm) while also having lower planar swelling than Nafion (25% vs. 5%).

(8) A nanofiber membrane was prepared with 3M Company's 660 EW PFSA reinforced by PPSU fibers that was 72 vol% 3M 660 EW and had a dry thickness of 51 μm. The 660 EW-containing membrane had higher conductivity than Nafion in the water-swollen state (0.107 S/cm vs. 0.095 S/cm) and also had low planar water swelling (5% vs. 25%). The proton conductivity was especially high at elevated temperatures and low humidity; e.g., an in-plane conductivity of 0.093 S/cm at 120°C and 50% RH (2.5 times higher than commercial Nafion). This conductivity closely approached the U.S. Department of Energy's conductivity target of 0.1 S/cm at 120°C and 50% RH.[3] The excellent conductivity of these membranes was attributed to the high concentration of fixed-charge sulfonic acid groups and high water uptake in the 660 EW polymer.

(9) The same 3M 660 EW PFSA film reinforced by PPSU fibers as in (8) had excellent fuel cell performance (at 80-120°C, 25-93% RH) after fabrication into a MEA, particularly compared to a MEA with commercial Nafion 211. For example at 100°C and 50% RH, the nanofiber MEA (with 0.25 mg/cm^2 platinum electrodes) produced 135% more power than a Nafion MEA (393 mW/cm^2 vs. 167 mW/cm^2 at 0.6 V).

(10) Nafion and PPSU nanofiber composite trilayer membranes (like that shown in Figure 8.2) could be fabricated by varying the relative flow rates of Nafion and PPSU during electrospinning. The resulting mats were then processed into dense membranes using the same techniques as for a non-layered composite. A dense trilayer membrane with 19 μm thick outer layers of ~60 vol% Nafion and having an inner layer, 8 μm thick

of only ~15 vol% Nafion, had a selectivity 83% higher than commercial Nafion 117. High selectivity is desirable for direct methanol fuel cell (DMFC) operation.

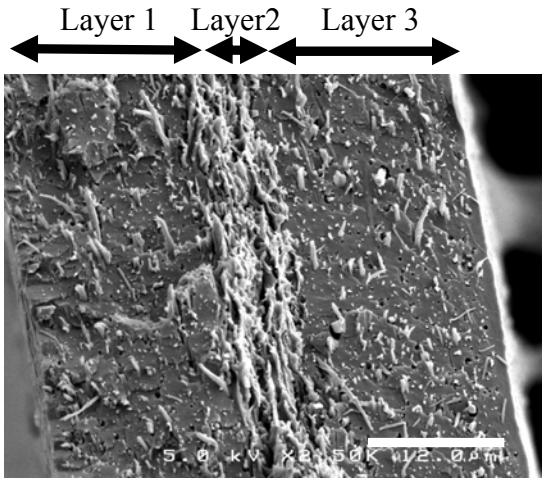

Figure 8.2. SEM cross-section of a trilayer membrane with Nafion fibers encapsulated by PPSU. Outer layers are ~55 vol% Nafion and 19 μm thick and the inner layer is ~15 vol% Nafion and 8μm thick. Scale bar is 12 μm.

(11) A trilayer membrane with 19 μm outer layers (~60 vol% Nafion) and a 5 μm inner/barrier layer (~15 vol% Nafion) was fabricated into a MEA with a 4.0 mg/cm^2 platinum:ruthenium anode and a 4.0 mg/cm^2 platinum cathode. This MEA had ~3 times higher power output than a Nafion 117 MEA when tested in a DMFC at 60^{o}C with 10 M methanol fuel (23 mW/cm^2 vs. 8 mW/cm^2).

8.1 References

(1) Kusoglu, A.; Karlsson, A. M.; Santare, M. H.; Cleghorn, S.; Johnson, W. B., *Journal of Power Sources* 2006, 161, (2), 987-996.

(2) Kusoglu, A.; Karlsson, A. M.; Santare, M. H.; Cleghorn, S.; Johnson, W. B., *Journal of Power Sources* 2007, 170, (2), 345-358.

(3) Garland, N. L.; Kopasz, J. P., *Journal of Power Sources* 2007, 172, (1), 94-99.

CHAPTER IX

SUGGESTIONS FOR FUTURE WORK

(1) Sulfonated polyphenylenes have been shown to have very high proton conductivity (e.g., 0.10 S/cm at 120^{o}C and 30% RH).[1] However, these ionomers are brittle in the dry state and swell excessively with water.[1-5] Therefore, these materials are excellent candidates for use in nanofiber composite membranes where their high conductivity can be exploited and where their poor mechanical and swelling properties can be ameliorated by reinforcement with uncharged polymer.

(2) Thinner membranes have lower ohmic resistance and thus result in higher fuel cell power output (provided the fuel/oxidant crossover does not become too high). The thinnest membranes subjected to fuel cell testing in this dissertation were 30 μm. Future work should focus on evaluating fuel cell performance of even thinner membranes (<30 μm).

(3) The optimum combination of i) PFSA volume fraction, ii) PFSA equivalent weight (EW), iii) membrane thickness, and iv) membrane structure (PFSA fibers vs. uncharged fibers) remain undetermined as it relates to both hydrogen/air fuel cell short-term and long-term performance (i.e., high initial power output and durability). This dissertation only tested the hydrogen/air power output of three membranes: i) a 30 μm, 65 vol% Nafion film reinforced by PPSU fibers, ii) a 30 μm membrane with Nafion fibers

encapsulated in PPSU that was 65 vol% Nafion, and iii) a 30 μm, 72 vol% 3M 660 EW film reinforced by PPSU fibers. The durability of only one membrane was tested: a 30 μm, 65 vol% Nafion film reinforced by PPSU fibers. More fuel cell studies (power output and durability) should be performed to determine the best combination of the 4 parameters listed above.

(4) The optimum morphology and composition of trilayer membranes for direct methanol fuel cell performance remains unknown. Membranes should be prepared with different: i) barrier layer and outer layer thicknesses, ii) barrier layer and outer layer compositions, iii) positions of the barrier layers within the membrane (e.g., closer to the anode), and iv) numbers of barrier layers. Such membranes should be fabricated into MEAs and tested for power output, ohmic resistance, and methanol crossover in DMFCs (25-80^{o}C, 1 M – 15 M methanol feed concentration).

(5) Watanbe et al.[6, 7] have shown that uniformly dispersing platinum nanoparticles throughout a PEM reduces gas crossover and provides membrane humidification in hydrogen/air fuel cells. However, it may be beneficial/cost-effective to incorporate a thin platinum particle layer into a PEM's interior, thus reducing the overall use of expensive platinum. Such particles could be included in a nanofiber PEM by a 3-step electrospinning process: i) begin by simultaneously electrospinning PFSA and PPSU as discussed throughout this dissertation, ii) second, simultaneously electrospin PFSA, PPSU, and a third fiber loaded with platinum nanoparticles on top of the original Nafion/PPSU fiber layer, and iii) electrospin PFSA and PPSU as in step (i). After

processing this electrospun mat into a dense membrane, the composite PEM should have the excellent properties of a nanofiber composite membrane supplemented by the crossover/humidification benefits provided by the platinum particles.

(6) The effects of nanofiber diameter on membrane properties and fuel cell performance remain unknown and should be investigated. The typical fiber diameters reported in this dissertation are ~350 nm; future research efforts should focus on varying this diameter and evaluating the properties of such membranes. In particular, it would be worthwhile to investigate the effect of low fiber diameters (<10 nm), where nano-effects may result in unique material properties.[8]

(7) No attempt was made to optimize MEA fabrication procedures in this dissertation. When Nafion-based nanofiber membranes were used, the MEA fabrication technique for commercial Nafion was utilized. Similarly, when 3M Company's 660 EW PFSA was incorporated into nanofiber membranes, 3M's proprietary technique for solution-cast 3M 660 EW MEA fabrication was used. Thus the effects of i) binder type and content ii) hot-pressing conditions, and iii) catalyst loading, remain unknown for nanofiber membranes. Optimization of the MEA fabrication procedure for nanofiber membranes could result in improved fuel cell performance.

(8) This dissertation has focused on electrospun membranes, however, electrospun electrodes have been prepared by other Pintauro group members and have been shown to perform well in fuel cells.[9] Thus, a fully electrospun membrane-electrode-assembly could

be prepared to benefit from the advantageous properties of both electrospun membranes and electrospun electrodes. Using this technique, it is easy to envision electrospun MEA fabrication being a roll-to-roll process at the industrial scale.

(9) PEM electrolyzers can be used for the production of hydrogen gas streams.[10] In PEM electrolysis, the membrane may be subjected to high pressures (e.g., 5,000 -10,000 psi).[11, 12] Thus, nanofiber membranes, with their high mechanical strength may find a useful application in these systems. Still, for this demanding application, the mechanical properties of nanofiber membranes may require even further improvements. For example by: i) replacing PPSU with a stronger polymer such as Torlon® (a polyamide-imide),[13] or ii) adding a strengthening particle to the uncharged polymer, for example particles of nanodiamond.[14]

(10) Vanadium redox-flow batteries (VRBs) are a promising energy storage technology. VRBs use an ion-exchange membrane, ideally with: i) low iR drop, i.e. low ohmic resistance, ii) low vanadium ion permeability, and iii) high chemical stability.[15, 16] Nanofiber composite membranes could fulfill these requirements. First, this dissertation showed the fabrication of highly conductive membranes of reasonably low thickness, i.e. low iR drop. Secondly, the reduced PFSA swelling in nanofiber membranes is expected to reduce vanadium ion permeability.[17] Finally, nanofiber composite membranes containing PFSA[16] and an appropriately selected uncharged/reinforcing polymer (e.g., PVDF)[18] are expected to be chemically stable in the VRB environment. Thus, VRB performance with nanofiber composite membranes should be evaluated.

9.1 References

(1) Si, K.; Wycisk, R.; Dong, D.; Cooper, K.; Rodgers, M.; Brooker, P.; Slattery, D.; Litt, M., *Macromolecules* **2013,** 46, (2), 422-433.

(2) Kreuer, K. D.; Schuster, M.; Obliers, B.; Diat, O.; Traub, U.; Fuchs, A.; Klock, U.; Paddison, S. J.; Maier, J., *Journal of Power Sources* **2008,** 178, (2), 499-509.

(3) Schuster, M.; de Araujo, C. C.; Atanasov, V.; Andersen, H. T.; Kreuer, K. D.; Maier, J., *Macromolecules* **2009,** 42, (8), 3129-3137.

(4) de Araujo, C. C.; Kreuer, K. D.; Schuster, M.; Portale, G.; Mendil-Jakani, H.; Gebel, G.; Maier, J., *Physical Chemistry Chemical Physics* **2009,** 11, (17), 3305-3312.

(5) Litt, M.; Granados-Focil, S.; Kang, J.; Si, K.; Wycisk, R., *ECS Transactions* **2010,** 33, (1), 695-710.

(6) Watanabe, M.; Uchida, H.; Emori, M., **1998,** 145, (4), 1137-1141.

(7) Watanabe, M.; Uchida, H.; Seki, Y.; Emori, M.; Stonehart, P., **1996,** 143, (12), 3847-3852.

(8) Martin, C. R., *Science* **1994,** 266, (5193), 1961-1966.

(9) Zhang, W. J.; Pintauro, P. N., *ChemSusChem* **2011,** 4, (12), 1753-1757.

(10) Grigoriev, S. A.; Porembsky, V. I.; Fateev, V. N., *International Journal of Hydrogen Energy* **2006,** 31, (2), 171-175.

(11) OnSite, P. Proton Energy Sysemts Acheives Breakthrough in High Pressure Hydrogen Technology. Available at http://www.fuelcellmarkets.com/Proton_OnSite_Hydrogen_Electrolysers_Fuelling/news_and_information/3,1,427,1,28022.html, (2/26/2013)

(12) Jackson, T. *High-Efficiency, Ultra-High Pressure Electrolysis with Direct Linkage to Photovoltaic Arrays (Phase II Project)*; 2005.

(13) Solvay, Torlon 4203L: Polyamide-imide. 2012.

(14) Branson, B. T.; Seif, M. A.; Davidson, J. L.; Lukehart, C. M., *Journal of Materials Chemistry* 21, (46), 18832-18839.

(15) Hwang, G.-J.; Ohya, H., *Journal of Membrane Science* **1996,** 120, (1), 55-67.

(16) Wang, W.; Luo, Q.; Li, B.; Wei, X.; Li, L.; Yang, Z., *Advanced Functional Materials* **2012,** 23, (8), 970-986.

(17) Mai, Z. S.; Zhang, H. M.; Li, X. F.; Xiao, S. H.; Zhang, H. Z., *Journal of Power Sources* **2011,** 196, (13), 5737-5741.

(18) Wei, W.; Zhang, H.; Li, X.; Zhangab, H.; Liab, Y.; Vankelecomc, I., *Physical Chemistry Chemical Physics* **2013,** 15, 1766-1771.

APPENDIX A

POLY(AMPS) AS A NAFION ELECTROSPINNING CARRIER

While Chapter III focused on using polyethylene oxide as a carrier for Nafion electrospinning, poly(2-acrylamido-2-methyl-1-propanesulfonic acid) (known as poly(AMPS)) was also used as a carrier. As discussed in Chapter III section 3.1, Nafion polymer electrospinning is notoriously difficult; it does not dissolve completely in alcohol/water solutions and in common organic solvents like dimethylacetamide or dimethylformamide, but rather forms a micellar dispersion.[1] Thus, a carrier such as the poly(AMPS) polymer discussed here, must be added to Nafion to allow electrospinning. The electrospinning conditions for Nafion/poly(AMPS) are listed in Table A.1 and a SEM micrograph of a fiber mat is shown in Figure A.1. Poly(AMPS) is a highly charged polymer with high proton conductivity (0.3 S/cm at 70^{o}C and 98% RH).[2] Thus, its addition to the mat is not expected to reduce the conductivity of Nafion in the same fashion as polyethylene oxide (as discussed in Chapter III section 3.1 and Chapter V section 5.3.1.2). However, no proton conductivity measurements were performed on the Nafion/poly(AMPS) nanofiber mat. Also, note that no attempt was made to minimize the amount of poly(AMPS) used as carrier polymer.

Table A.1. Electrospinning conditions and solution properties for Nafion/poly(AMPS) electrospinning

Electrospinning Conditions:	**Value**
Electrospinning voltage	12 kV
Polymer solution flow rate	0.40 mL/hr
Spinneret-to-collector distance	6 cm
Relative humidity of the air	35%
Solution Properties:	
Total polymer concentration	25 wt%
Solvent system	2:1 wt. ratio of n-propanol:water
Poly(AMPS) molecular weight*	2,000 kDa
Nafion:Poly(AMPS) ratio	80:20 wt. ratio

*from SigmaAldrich, Product #191973

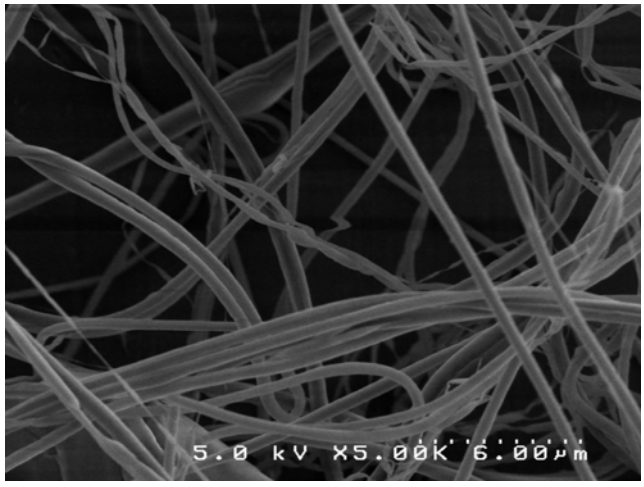

Figure A.1. SEM micrograph of a Nafion/poly(AMPS) fiber mat. The fibers are 80 wt% Nafion and 20 wt% poly(AMPS). The average fiber diameter is 415 nm.

A.1 References

(1) Loppinet, B.; Gebel, G.; Williams, C. E., *The Journal of Physical Chemistry B* **1997,** 101, (10), 1884-1892.

(2) Karlsson, L. E.; Wesslen, B.; Jannasch, P.. *Electrochimica Acta* **2002**, 47, (20), 3269-3275.

APPENDIX B

NAFION FILMS REINFORCED BY PVDF AND PBI

B.1 Description of membrane preparation and material properties

The focus of Chapter IV was on preparing nanofiber composite membranes with Nafion as the ionomer and using polyphenylsulfone (PPSU) as the uncharged/reinforcing polymer. However, two nanofiber membranes were prepared with alternative reinforcing polymers: a membrane with Nafion that was reinforced by polyvinylidene fluoride (PVDF) and another membrane with Nafion that was reinforced by poly-[(1-(4,4′-diphenylether)-5-oxybenzimidazole)-benzimidazole (PBI-OO). Both PVDF and PBI-OO are uncharged polymers with excellent mechanical properties, low water sorption, and chemical stability.[1, 2] Additionally, it was hypothesized that PBI-OO's basic imidazole nitrogen moieties may form ionic crosslinks with Nafion's sulfonic acid groups and thus enhance the interaction between the two polymer components.[3]

Prior to electrospinning dual-fiber mats, PBI-OO solutions were prepared by dissolving polymer powder (provided by FuMA-Tech) in dimethylsulfoxide solution. The solution was electrospun at a flow rate of 0.20 mL/hr and a concentration of 15 wt%. The electrospinning voltage was 6.25 kV and the spinneret-to-collector-distance (SCD) was 8 cm. PVDF solutions were prepared by dissolving polymer pellets (Kynar 760 from Arkema) in a 70:30 wt. ratio of dimethylacetamide:acetone. The PVDF solution was electrospun at a flow rate of 0.20 mL/hr and a concentration of 20 wt%. The

electrospinning voltage was 6 kV and the SCD was 8.5 cm. Nafion solutions were prepared and electrospun with the conditions discussed in section 4.2.1 of Chapter IV.

Dual-fiber mats of Nafion and PVDF were prepared by simultaneously electrospinning the Nafion and PVDF solutions from separate syringes, as described for the production of Nafion and PPSU fiber mats in Chapter IV section 4.2.1 and depicted in Figure 4.2. Nafion and PBI-OO dual-fiber mats were prepared in the same fashion.

After electrospinning dual-fiber mats of either Nafion and PVDF (Nafion/PVDF), or Nafion and PBI-OO (Nafion/PBI-OO), the mats were processed into dense films using the procedures described in section 4.2.2 of Chapter IV (i.e., the mats were hot pressed at 260^{o}F, annealed 2 hours at 150^{o}C in vacuum, and boiled one hour each in 1 M H_2SO_4 and H_2O). The only structure studied for Nafion/PVDF and Nafion/PBI-OO membranes was a Nafion film reinforced by uncharged fibers. Cross-sectional SEMs of fully-processed Nafion/PVDF and Nafion/PBI-OO membranes are shown in Figure B.1. The images show flow of Nafion during hot-pressing while the PVDF or PBI-OO remains in the fiber form. It should be noted in Figure B.1a that there appears to be a Nafion-enriched domain in the upper right-hand corner of the image. The reason for this enrichment is not well understood at this time

A summary of the material properties of Nafion/PVDF and Nafion/PBI-OO membranes is presented in Table B.1 and compared to two Nafion/PPSU membranes (where each membrane was a fiber-reinforced Nafion film). While electrospinning conditions were not optimized for direct comparison of these three composites (i.e., one property, such as proton conductivity, is not held constant for all three), it is clear that Nafion/PPSU composites outperform Nafion/PVDF and Nafion/PBI-OO composites.

Nafion/PPSU membranes have a superior combination of high proton conductivity and low water swelling.

Additionally, there is no evidence to suggest that an ionic crosslink formed between Nafion and PBI-OO. The SEM cross-section of the Nafion/PBI-OO membrane has small gaps between the Nafion and PBI-OO domains. Furthermore, the swelling properties of the Nafion/PBI-OO membrane are not improved relative to the Nafion/PPSU system as might be expected were there enhanced interaction between the two domains.

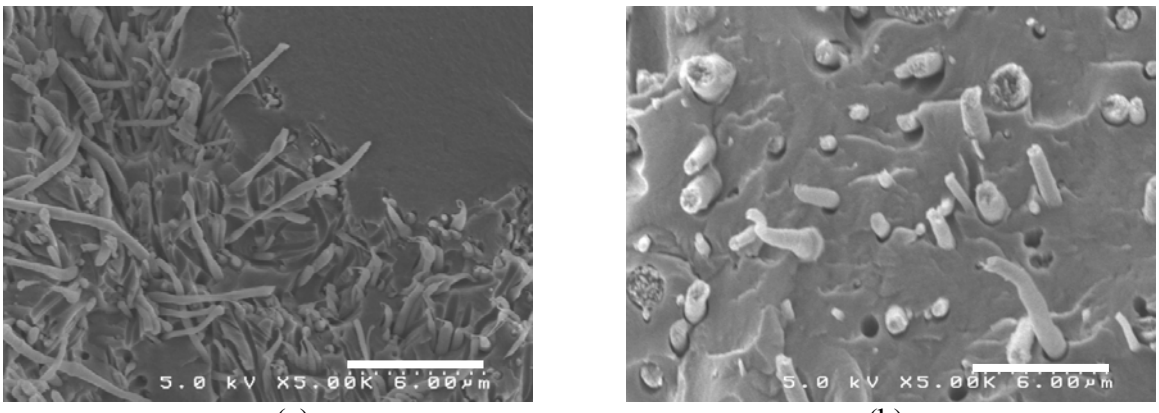

(a) (b)

Figure B.1. SEM cross-section of (a) a Nafion film reinforced by PVDF fibers, 56 vol% Nafion, and (b) and a Nafion film reinforced by PBI-OO fibers, 75 vol% Nafion. Scale bars are 6 μm.

Table B.1. Properties of Nafion films reinforced with different inert fibers. Conductivity data was collected in water at 22°C. In-plane and volumetric swelling data was collected in 100°C.

	Nafion	**Nafion/PPSU (70 vol% Nafion)**	**Nafion/PPSU (81 vol% Nafion)**	**Nafion/PVDF (56 vol% Nafion)**	**Nafion/PBI-OO (75 vol% Nafion)**
Conductivity (S/cm)	0.095	0.066	0.081	0.053	0.071
In-plane swelling (%)	37	6	8	10	13
Volumetric swelling (%)	75	42	55	62	52

B.2 References

(1) Peron, J.; Ruiz, E.; Jones, D. J.; Roziere, J., *Journal of Membrane Science* **2008,** 314, (1-2), 247-256.

(2) Arkema *KYNAR® & KYNAR FLEX® PVDF: Performance Characteristics & Data*; 2007.

(3) Wycisk, R.; Chisholm, J.; Lee, J.; Lin, J.; Pintauro, P. N., *Journal of Power Sources* **2006,** 163, (1), 9-17.

APPENDIX C

ADDITIONAL FUEL CELL TESTING OF NAFION/PPSU COMPOSITES

C.1 Vanderbilt fuel cell testing of Nafion fibers encapsulated in PPSU

Membranes with Nafion-fibers encapsulated in polyphenylsulfone (PPSU) (see membrane fabrication description in Chapter IV section 4.2.2) were fabricated into membrane-electrode-assemblies (MEAs) using the procedure described in section 4.2.8 of the main text. MEAs with these membranes (30 μm thick and 60 vol% Nafion) had excellent fuel cell performance that was comparable to a MEA with a Nafion 212 membrane at 80^{o}C and a relative humidity of either 100% or 50%, as seen in Figure C.1. This result is similar to that obtained for MEAs with a Nafion film reinforced by PPSU fibers (that had similar Nafion loading in the membrane) which is discussed in more detail in section 4.3.4 of Chapter IV.

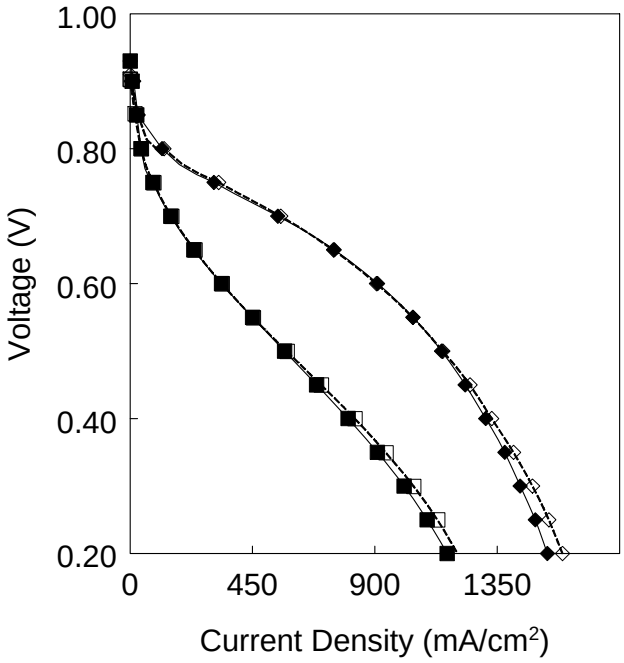

Figure C.1. Polarization curves for membranes with Nafion nanofibers encapsulated in PPSU and Nafion 212 at 80°C. The nanofiber membrane was 30 μm thick and 60 vol% Nafion. (♦) Nafion fibers encapsulated in PPSU at 100% RH (◊) Nafion 212 at 100% RH (■) Nafion fibers encapsulated in PPSU at 50% RH (□) Nafion 212 at 50% RH.

C.2 General Motors fuel cell testing of Nafion films reinforced by PPSU fibers

Nanofiber membrane fuel cell polarization and durability experiments were conducted at Vanderbilt as discussed in section 4.3.4 of Chapter IV. Similar fuel cell tests were also performed by General Motors (GM). The membrane GM tested was a Nafion film reinforced by PPSU fibers with 65 vol% Nafion and had a thickness of 30 μm. The conductivity and swelling properties of the composite membrane are shown in Table C.1. GM fabricated the membrane into a MEA using their proprietary procedures. The MEA was then tested for power output at 80°C and 85% RH. Furthermore, the high-frequency resistance (HFR) was measured during the polarization experiment. HFR is a measure of the membrane's ohmic resistance and is discussed in more detail in section

6.2.9 of Chapter VI. As can be seen in Figure C.2a, the MEA with the nanofiber membrane has similar power output and HFR when compared to a MEA with a 24 μm neat Nafion film, though the neat Nafion MEA does have slightly higher power output (higher current density for a given voltage). The difference in performance is attributed to the neat Nafion film's lower sheet resistance, i.e., the Nafion film is thinner and more conductive than the nanofiber composite.

The MEA with the nanofiber membrane was also subjected to an accelerated durability test in which the humidity was cycled from 0% RH to 150% RH in two minute intervals while passing air at 2 slpm to both the anode and cathode-side of the MEA.[1] Since no hydrogen gas was supplied to the MEA, this particular test does not capture any effect from chemical degradation that might occur in a normally operating fuel cell.[1] Air crossover was periodically measured by determining the air flow passing through the membrane when a 21 kPa pressure was applied to one side of the MEA.[1] When the crossover exceeded 10 sccm, the membrane was considered to have failed. The results of the durability test are shown in Figure C.2b and compared to several other MEAs. The electrospun nanofiber MEA lasted 87% longer than commercial Nafion 211 (25 μm thick). This result corroborates the increased durability of a MEA with a Nafion film reinforced by PPSU fibers that was discussed in section 4.3.4 of Chapter IV, where a nanofiber membrane MEA lasted 54% longer than a MEA with a Nafion 212 membrane (51 μm thick). The differences in the relative improvement between the Chapter IV result and that obtained by GM are primarily attributed to the difference in thickness of the Nafion membrane used in Chapter IV (51 μm) and the Nafion membrane used by GM

(25 μm), but could also be related to the use of hydrogen gas in the Chapter IV durability study (versus only air in the GM study).

The MEA with the nanofiber membrane also performed well compared to W.L. Gore's Primea® MEA, lasting 22% longer. The Primea® MEA is a commercial product which contains a GORE-SELECT membrane (perfluorosulfonic acid reinforced by expanded polytetrafluoroethylene, discussed more in section 2.3.4 of Chapter II). Two other MEAs, being developed by W.L. Gore and Ion Power had higher durability than the nanofiber composite, though the details of fabrication, composition, and structure remain unknown for these materials.

Table C.1. Properties of the Nafion film reinforced with PPSU fibers that was sent to GM for fuel cell testing. The membrane was 65 vol% Nafion and had a thickness of 30 μm.

Property	Nanofiber membrane tested at GM	Nafion 212
Conductivity in water at 22°C (S/cm)	0.063	0.095
In-plane areal swelling in 100°C water (%)	4	37
Volumetric swelling in 100°C water (%)	38	75
Mass swelling in 100°C water (%)	27	36

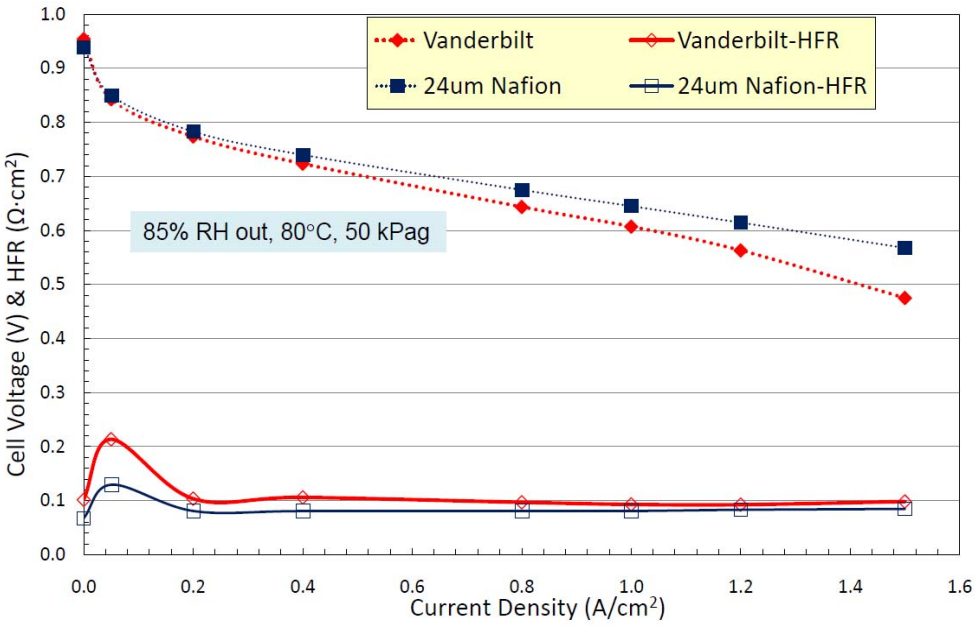

(a)

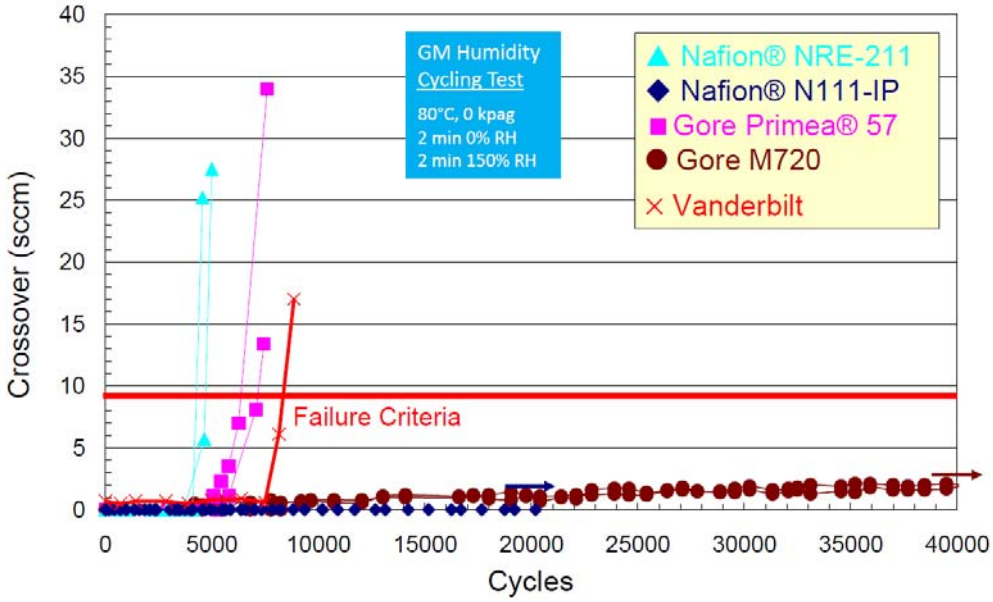

(b)

Figure C.2. (a) Polarization curves and high frequency resistance for a 30 µm 65 vol% Nafion film reinforced by PPSU fibers which is referred to as "Vanderbilt" in the figures. A polarization curve for a 24 µm neat Nafion film is included for comparison. Note that "RH out" refers to the RH of the exiting gas streams from the fuel cell. (b) Accelerated durability tests for several proton exchange membranes.

C.3 References

(1) Yeh-Hung, L.; Cortney, K. M.; Craig, S. G.; David, A. D., *Journal of Fuel Cell Science and Technology* **2009,** 6, (2), 021002.

APPENDIX D

NANOFIBER COMPOSITE MEMBRANES WITH 3M'S 825 EW PERFLUOROSULFONIC ACID

Nanofiber composite membranes composed of polyphenylsulfone and 3M Company's 660 EW perfluorosulfonic acid were fabricated and discussed in Chapter VI. Additionally, two nanofiber composite membranes were also prepared from 3M Company's 825 equivalent weight perfluorosulfonic acid ionomer (3M 825 EW) and polyphenylsulfone (PPSU). PEO (400 kDa MW) was used as the carrier polymer during 3M 825 EW electrospinning, as was also required for other PFSA polymers electrospun in this dissertation (see sections 4.2.1. and 6.2.1 of the main text). Electrospinning conditions for 3M 825 EW and PPSU dual-fiber mats are presented in Table D.1. Mats were densified into 3M 825 EW films reinforced by PPSU fibers using similar processing conditions to those described in Chapter VI section 6.2.2. Specifically, the mats were hot pressed at 15,000 psi and 127^{o}C, annealed for 5 minutes at 140^{o}C, and then soaked in 1 M H_2SO_4 for 6 hours and H_2O for 16 hours at room temperature. As discussed in section 6.2.2, this soaking procedure may not be sufficient for the extraction of the PEO carrier polymer. SEMs of an electrospun mat and dense 3M 825 EW and PPSU membrane are shown in Figure D.1.

The conductivity and water swelling of 3M 825 EW and PPSU nanofiber membranes is presented in Table D.2. The properties of these composite membranes are quite attractive. Specifically, the nanofiber membrane is able to achieve the same conductivity as commercial Nafion, but with dramatically lower planar swelling. Note

that the conductivity of the nanofiber composite membranes with 3M 825 EW and PPSU is higher than those of Nafion and PPSU (see section 4.3.3 of Chapter IV), due to 3M 825 EW's high concentration of sulfonic acid groups relative to that of Nafion. On the other hand, the conductivity of 3M 825 EW and PPSU composites is lower than those of 3M 660 EW and PPSU since 3M 825 EW has fewer fixed sulfonic acid sites than 3M 660 EW (see Chapter VI section 6.3).

While no fuel cell testing of 3M 825 EW and PPSU nanofiber membranes has been performed, it is recommended that such tests be conducted as a part of future studies.

Table D.1. Electrospinning conditions for a 3M 825 EW and PPSU dual-fiber mat.

Parameter	**3M 825 EW**	**PPSU**
Polymer Comp.	99:1 wt. ratio, 3M825:PEO (17 wt% total polymer in solution)	25 wt%
Solvent	n-propanol:water in a 2:1 wt. ratio	NMP:acetone in a 8:2 wt. ratio
Voltage	7.0 kV	7.5 kV
SCD	6 cm	9 cm
Flow Rate	0.60 mL/hr (x 2 syringes)	0.09-0.12 mL/hr

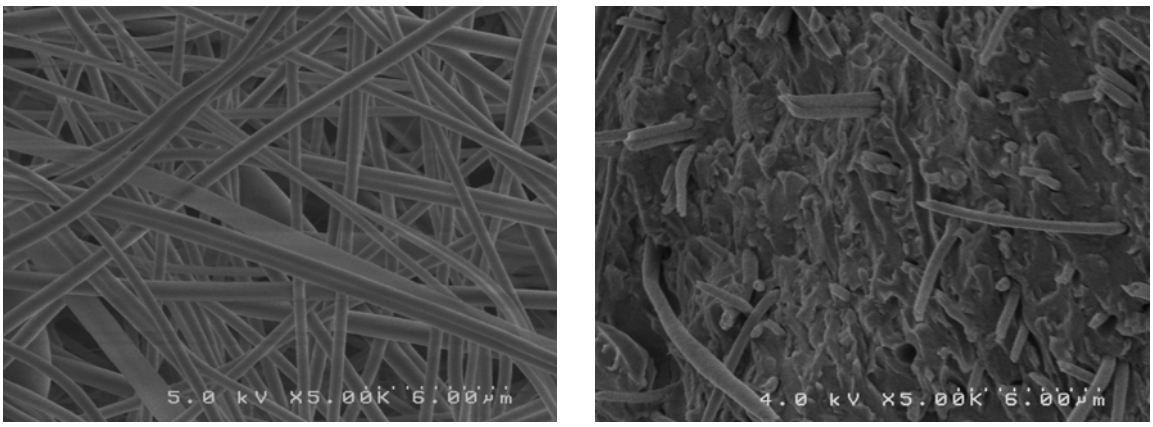

(a) (b)

Figure D.1 (a) a SEM of the surface of a 3M 825 EW and PPSU dual-fiber mat and (b) a SEM of the cross-section of a 3M 825 EW and PPSU membrane.

Table D.2. Properties of two 3M 825 EW film reinforced by PPSU fibers compared to a solution-cast 3M 825 EW membrane and a commercial Nafion 212 membrane. The volume fractions of the composite membranes were not determined.

Material	Conductivity in Water at 23°C [S/cm]	In-Plane Water Swelling at 23°C [%]	Volumetric Water Swelling at 23°C [%]	Membrane Thickness, dry state [µm]
Nanofiber Composite (3M 825 EW:PPSU) - Membrane #1	0.096	5	40	30
Nanofiber Composite (3M 825 EW:PPSU) - Membrane #2	0.086	3	34	28
Cast 3M 825 EW	0.115	25	85	116
Nafion 212	0.095	19	35	51

APPENDIX E

THROUGH-PLANE CONDUCTIVITY MEASUREMENTS

E.1 Motivation and experimental details

The proton exchange membrane (PEM) community typically measures ionic/proton conductivity in the in-plane direction, i.e., the conductivity parallel to a membrane's surface.[1-11] The geometry of in-plane conductivity measurements allows easy implementation of a 4-electrode cell for electrochemical impedance spectroscopy. Such a cell separates the effects of the membrane and interfacial impedances, and thus is superior to a simpler 2-electrode cell.[12-14] Furthermore, in-plane conductivity measurements involve large measured resistances (>500 Ω) since the distance between the electrodes is substantial, usually 1 cm or more. Larger resistances make for easier measurements and reduce errors resulting from nonmembrane resistances (since the nonmembrane resistance is small relative to the membrane resistance). While in-plane conductivity measurements may be facile, protons do not migrate in the in-plane direction during proton exchange membrane fuel cell (PEMFC) operation. In actuality protons move in the through-plane direction, perpendicular to the membrane surface (see Figure E.1). Thus, accurate through-plane conductivity measurements would be useful to researchers.

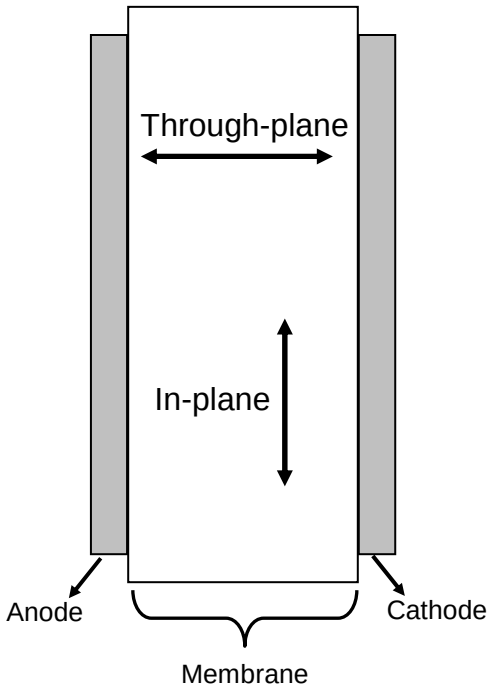

Figure E.1. Schematic showing the difference between the in-plane and through-plane directions.

Unfortunately, through-plane conductivity measurements are difficult to perform accurately. It is not easy to implement a 4-electrode setup since it is impractical to locate electrodes inside the membrane. Consequently a 2-electrode method must be used. PEMs are thin (typically <100 μm), thus measured resistances are small and nonmembrane resistances (e.g., surface/contact impedances) cannot be ignored. Still, one suitable through-plane conductivity measurement apparatus and technique was recently published by Cooper.[15] This method allowed for through-plane conductivity measurement at a variety of temperature and humidity combinations. However, the apparatus was prohibitively expensive ($32,000),[16] did not permit measurements in liquid water, and required the use of carbon paint and two gas diffusion electrodes for each membrane sample tested. Thus, a new through-plane conductivity measurement apparatus and

technique was developed as part of this Ph.D. dissertation. The apparatus was designed to measure proton conductivity in liquid water, be constructed for a reasonable price, and to not require carbon paint nor gas diffusion electrodes. The apparatus that was built to meet these requirements is shown in Figure 7.1 of Chapter VII. The total cost (parts and labor) for the apparatus was ~$1,000.

The apparatus is composed of copper electrodes, a compression spring, dial indicator, and casing (plastic and copper casing was used where appropriate). Copper lead wires were attached to both electrodes to facilitate connection to a potentiostat. The active area of each electrode was small (0.0507 cm^2) so as to minimize the effect of interfacial/contact resistance. The compression spring (Gardner GC480-038-0875) and dial indicator served to maintain a constant contact pressure of the electrodes on the membrane. For example, to achieve a pressure of 310 psi (the most commonly used pressure in this dissertation and that used by Cooper)[15] the spring was compressed 0.265 in. Note that the pressure can be calculated by Equation E.1.

$$P = \frac{kX}{A} \tag{E.1}$$

where P is the pressure applied to the membrane [psi], k is the spring constant (9.12 lb_f/in), X is the amount of spring compression [in], and A is the area (0.0078585 in^2) over which the pressure is applied.

Resistance measurements were made by connecting the apparatus' lead wires to a Gamry Reference 3000 potentiostat. An EIS experiment was then performed where the frequency was scanned from 1 MHz to 1 Hz with a voltage amplitude of 10 mV RMS.

An example of the resulting Nyquist plot is shown in Chapter VII, Figure 7.2. The measured ohmic resistance is the high frequency real resistance when the imaginary resistance is zero, i.e., the high-frequency x-intercept. If the impedance curve did not intercept the x-axis, the curve was extrapolated to the intercept, as shown in Figure 7.2b of Chapter VII and as has been done elsewhere.[17]

Nonmembrane resistances were corrected for by measuring samples of a variety of thicknesses (typically by stacking individual membranes, but also by fabricating membranes of different thickness). The EIS-determined resistances were then extrapolated to zero thickness. The resistance at zero thickness was taken as the nonmembrane resistance, which was primarily attributed to interfacial/contact resistance (see Figure 7.3b of Chapter VII). Conductivity was subsequently calculated by Equation 7.1 of Chapter VII.

E.2 Effects of applied pressure

One concern with conductivity measurements is the effect of the applied pressure on the membrane. In particular, if the pressure is too high, the membrane could be compressed. Were the amount of membrane compression unknown this could introduce errors in the conductivity measurement. On the other hand, if the pressure is too low, the electrodes and the membrane may not make good electrochemical contact. In this work, the pressure applied on the membrane was chosen based on the work of Cooper.[15] However, the effect of applied pressure on the through-plane conductivity of a Nafion 212 membrane was also determined and is shown in Figure E.2. For the pressures tested, 60 psi to 310 psi, there is no effect of pressure on conductivity – indicating good

electrochemical contact and minimal effects of membrane compression (if any membrane compression occurs at all).

Note that the conductivity of this particular Nafion 212 sample is slightly lower than is typically measured. The in-plane and through-plane conductivity of this sample are 88 mS/cm and 85 mS/cm respectively, while most Nafion 212 conductivity data in the literature range from 95-100 mS/cm in the in-plane and through-plane directions.[18]

While there was no effect of applied pressure on through-plane conductivity measurements for a Nafion membrane, there was a pressure effect on through-plane conductivity of a nanofiber composite membrane composed of 3M's 660 EW PFSA (3M660) and reinforced by PPSU fibers (see Chapter VI section 6.2 for membrane fabrication details). The 3M660 and PPSU composite swells more in water than Nafion and thus is expected to have inferior mechanical properties in the wet state (see Chapter VI section 6.3 for more details about water swelling and mechanical properties of the 3M660 and PPSU composite membrane). The nanofiber membrane tested here had a 3M660 volume fraction of 70 vol% and an in-plane conductivity of 106 mS/cm in 25^{o}C liquid water. The 3M660 and PPSU composite membrane preparation is discussed in detail in section 6.2 of Chapter VI.

As can be seen in Figure E.3 at high pressure (> 116 psi) there is a dramatic increase in the calculated through-plane conductivity (see Equation 7.1 of Chapter VII). This is largely attributed to membrane compression at these elevated pressures, which was not accounted for in the conductivity calculation (the nominal, micrometer-determined thickness was used for the calculation). Furthermore, at very low pressure (29 psi) there was a small drop-off in conductivity, perhaps due to poor electrochemical

contact between the electrodes and the membrane. Between the pressures of 58 psi and 116 psi, the conductivity was independent of pressure. Thus, when determining through-plane conductivity of 3M660/PPSU membranes the pressure should between 58 psi and 116 psi to reduce errors associated with membrane compression and electrode-membrane contact.

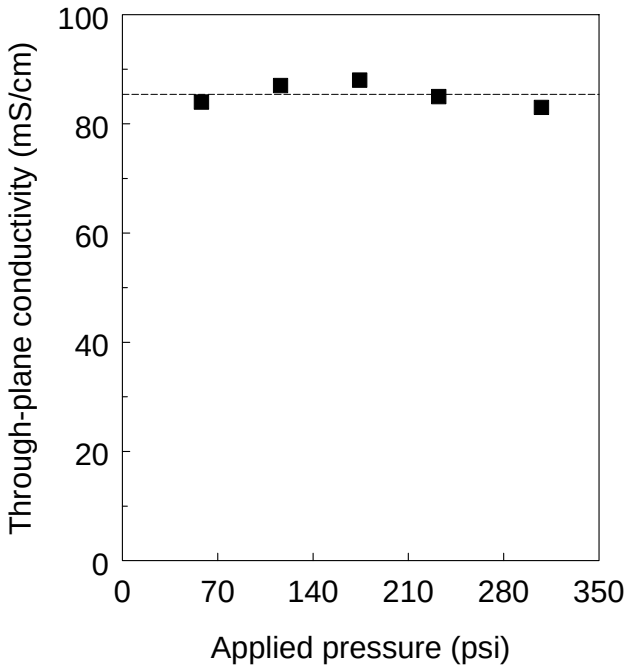

Figure E.2. Effect of pressure on through-plane conductivity of a Nafion 212 film. All measurements taken while membranes were immersed in 25^{o}C water

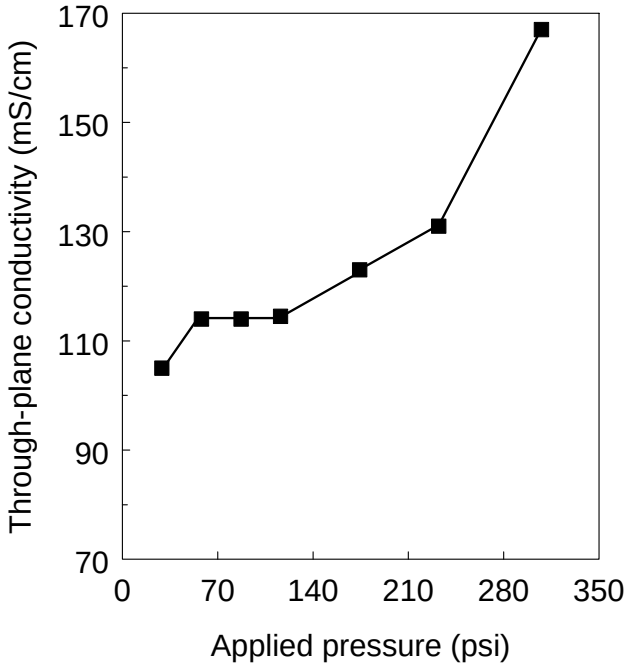

Figure E.3. Effect of pressure on through-plane conductivity of a 3M660/PPSU nanofiber composite with 70 vol% 3M660. The membrane's thickness was ~70 μm in the wet state. All measurements taken while membranes were immersed in 25°C water.

E.3 Effects of stacking membranes

Through-plane conductivity is shown as a function of membrane thickness in Figure E.4. All the films in Figure E.4 are composite membranes with Nafion fibers encapsulated in PPSU, where the Nafion volume fraction is ~0.24. Film thickness is varied in two different ways: i) by preparing membranes of different thickness and ii) by stacking individual membranes on top of each other. Regardless of which method is used, the through-plane conductivity was approximately the same, 16 mS/cm. Note that of the 27 total measurements, there are 3 outliers with elevated through-plane conductivity. These 3 samples have the lowest measured resistance of the 27 samples, thus they are most susceptible to any error in the nonmembrane ohmic resistance determination, membrane thickness measurement, and membrane ohmic resistance measurement.

Normally, these resistances can be discarded. They are included here to demonstrate the limitations of the measurement apparatus and experimental method.

The data in Figure E.4 indicate there is no measurable resistance between individual membrane films. In other words, stacking individual films is the same as testing individual films with different intrinsic thickness (see Figure E.5 for a graphic representation).

Also note that even after discarding the three thin membrane outliers, there is still some scatter in the measured through-plane conductivity, ranging from 9 mS/cm to 20 mS/cm. This variability is attributed to differences in the membrane sample composition and errors associated with extrapolating the impedance curve to the x-intercept. However, it should be noted that the membrane structures discussed here (Nafion fibers encased in PPSU) had the largest scatter of all membranes tested. Nafion films reinforced by PPSU fibers and commercial Nafion films did not have as high a variation in through-plane conductivity measurements, as is shown in Figure E.6.

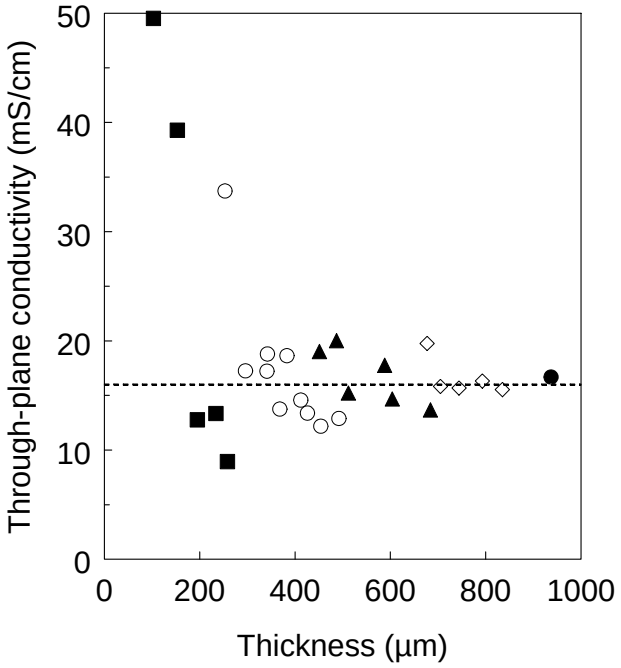

Figure E.4. Through-plane conductivity as a function of membrane thickness. All measurements taken while membranes were immersed in 25°C water using an applied pressure of 310 psi**.** (■) Individual film, (○) stacked two individual films, (▲) stacked three individual films, (◊) stacked four individual films, (●) stacked five individual films.

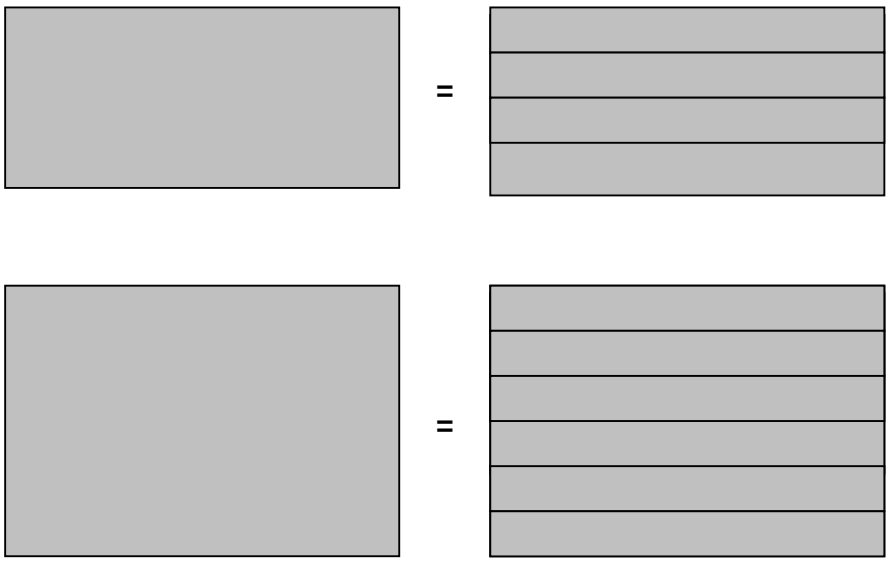

Figure E.5. Schematic depicting equality of a single thick membrane and several, thinner stacked membranes (for the purposes of determining through-plane conductivity). Each enclosed rectangle represents a single, individual membrane.

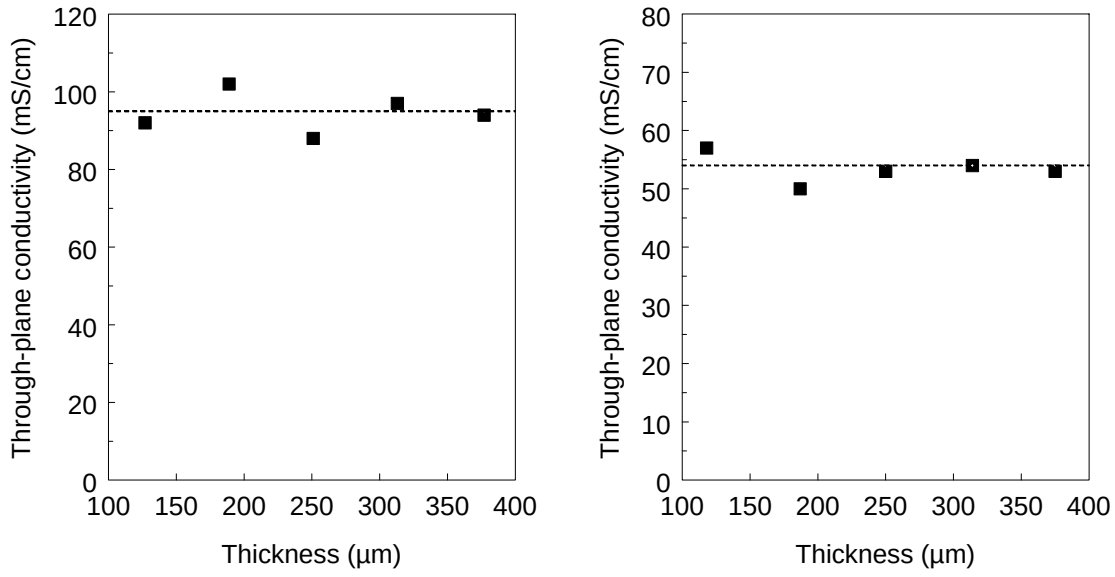

(a) (b)

Figure E.6. Through-plane conductivity as a function of membrane thickness for (a) Nafion 212 with an in-plane conductivity of 95 mS/cm and (b) a Nafion film reinforced by PPSU fibers with an in-plane conductivity of 49 mS/cm. All measurements taken while membranes were immersed in 25^{o}C water using an applied pressure of 310 psi**.**

E.4 References

(1) Li, H.; Kirk, N. J.; Mauritz, K. A.; Storey, R. F., *Polymer* 52, (16), 3550-3559.

(2) Xu, H.; Wu, M.; Liu, Y.; Mittal, V.; Kassim, F.; Vieth, B.; Bonville, L.; Kunz, H. R.; Fenton, J. M., *ECS Transactions* **2006,** 3, (1), 561-568.

(3) Ye, X.; Bai, H.; Ho, W. S. W., *Journal of Membrane Science* **2006,** 279, (1-2), 570-577.

(4) Choi, J.; Wycisk, R.; Zhang, W. J.; Pintauro, P. N.; Lee, K. M.; Mather, P. T., *ChemSusChem* **2010,** 3, (11), 1245-1248.

(5) Emery, M.; Frey, M.; Guerra, M.; Haugen, G.; Hintzer, K.; Lochhaas, K. H.; Pham, P.; Pierpont, D.; Schaberg, M.; Thaler, A.; Yandrasits, M.; Hamrock, S., *ECS Transactions* **2007,** 11, (1), 3-14.

(6) Vernon, D. R.; Meng, F.; Dec, S. F.; Williamson, D. L.; Turner, J. A.; Herring, A. M., *Journal of Power Sources* **2005,** 139, (1-2), 141-151.

(7) Robeson, L. M.; Hwu, H. H.; McGrath, J. E., *Journal of Membrane Science* **2007,** 302, (1-2), 70-77.

(8) Si, K.; Wycisk, R.; Dong, D.; Cooper, K.; Rodgers, M.; Brooker, P.; Slattery, D.; Litt, M., *Macromolecules* 46, (2), 422-433.

(9) Park, M. J.; Downing, K. H.; Jackson, A.; Gomez, E. D.; Minor, A. M.; Cookson, D.; Weber, A. Z.; Balsara, N. P., *Nano Letters* **2007,** 7, (11), 3547-3552.

(10) Chang, Y.; Brunello, G. F.; Fuller, J.; Hawley, M.; Kim, Y. S.; Disabb-Miller, M.; Hickner, M. A.; Jang, S. S.; Bae, C., *Macromolecules* 44, (21), 8458-8469.

(11) Kienitz, B.; Zawodzinski, T.; Pivovar, B.; Garzon, F. H., *ECS Transactions* **2008,** 16, (2), 1069-1078.

(12) Cahan, B. D.; Wainright, J. S., *Journal of the Electrochemical Society* **1993,** 140, (12), L185-L186.

(13) Sone, Y.; Ekdunge, P.; Simonsson, D., *Journal of the Electrochemical Society* **1996,** 143, (4), 1254-1259.

(14) Lee, C. H.; Park, H. B.; Lee, Y. M.; Lee, R. D., *Industrial & Engineering Chemistry Research* **2005,** 44, (20), 7617-7626.

(15) Cooper, K. R., *Journal of the Electrochemical Society* **2010,** 157, (11), B1731-B1739.

(16) Scribner, J., Personal Communication. In 2011.

(17) Alberti, G.; Casciola, M.; Massinelli, L.; Bauer, B., *Journal of Membrane Science* **2001,** 185, (1), 73-81.

(18) Ballengee, J. B.; Pintauro, P. N., *Macromolecules* **2011,** 44, (18), 7307-7314.